

Flexible variable selection in the presence of missing data

Brian D. Williamson^{1,2} and Ying Huang^{2,3}

¹Biostatistics Division, Kaiser Permanente Washington Health Research
Institute

²Vaccine and Infectious Disease Division, Fred Hutchinson Cancer Research
Center

³Department of Biostatistics, University of Washington

May 11, 2022

Abstract

In many applications, it is of interest to identify a parsimonious set of features, or panel, from multiple candidates that achieves a desired level of performance in predicting a response. This task is often complicated in practice by missing data arising from the sampling design or other random mechanisms. Most recent work on variable selection in missing data contexts relies in some part on a finite-dimensional statistical model, e.g., a generalized or penalized linear model. In cases where this model is misspecified, the selected variables may not all be truly scientifically relevant and can result in panels with suboptimal classification performance. To address this limitation, we propose several nonparametric variable selection algorithms combined with multiple imputation to develop flexible panels in the presence of missing-at-random data. We outline strategies based on the proposed algorithms that achieve control of commonly used error rates. Through simulations, we show that our proposals have good operating characteristics and result in panels with higher classification performance compared to several existing penalized regression approaches in cases where a generalized linear model is misspecified. Finally, we use the proposed methods to develop biomarker panels for separating pancreatic cysts with differing malignancy potential in a setting where complicated missingness in the biomarkers arose due to limited specimen volumes.

Keywords: variable selection; missing data; machine learning; nonparametric statistics; multiple imputation; stability selection; variable importance.

1 Introduction

Missing data present a common challenge in many scientific domains. This challenge is compounded if a goal of the analysis is to identify a parsimonious set of features that are related to

the response, a notion that has been referred to as variable selection. Regardless of the method used to account for missing data, many existing approaches to variable selection in missing-data contexts rely in some part on a finite-dimensional statistical model, including generalized linear models (see, e.g., [Little and Schluchter, 1985](#); [Garcia et al., 2010](#); [Long and Johnson, 2015](#); [Liu et al., 2019](#)). While variable selection based on generalized linear models has been shown to perform well in many cases, recovering the true set of important variables and selecting a small number of unimportant variables, performance of these methods is less clear when the model is misspecified or when the features are correlated (see, e.g., [Bang and Robins, 2005](#); [Johnson et al., 2008](#)). This motivates the consideration of approaches to variable selection with missing data that are more robust to model misspecification. These approaches should incorporate flexible algorithms, ensuring that complex relationships between the features and the outcome can be captured reliably.

Traditional approaches to variable selection with missing data can be broadly categorized into two groups. In the first, complete-case variable selection methods are adapted to the missing-data paradigm using either likelihood-based methods (see, e.g., [Garcia et al., 2010](#)) or inverse probability weighting methods (see, e.g., [Tsiatis, 2007](#); [Bang and Robins, 2005](#); [Johnson et al., 2008](#)). These approaches, while useful in many contexts, often are tailored to a specific data-generating distribution or missing data process. Additionally, inverse probability weighting is challenging in cases with non-monotone missing data (see, e.g., [Sun and Tchetgen Tchetgen, 2018](#)), limiting its more widespread adoption. The second group of approaches is based on multiple imputation ([Rubin, 1987](#)), and is widely used in missing-data settings (see, e.g., [Long and Johnson, 2015](#); [Zhao and Long, 2017](#); [Liu et al., 2019](#)). Among its advantages over other approaches are that imputation is easily done with existing software (see, e.g., [van Buuren and Groothuis-Oudshoorn, 2010](#)) and the imputation process is disentangled from the variable selection procedure. The imputation process must be specified with care, because methods that rely too heavily on modelling assumptions may still be subject to bias in cases with misspecification. Multiple imputation by chained equations, also referred to as fully conditional specification (see, e.g., [Raghuathan et al., 2001](#); [van Buuren, 2007](#)), allows flexible imputation

models to be used in an effort to reduce the risk of misspecification. Once an imputation procedure has been specified, variable selection methods developed for complete-case data can be used on the imputed datasets.

Widely-used methods for complete-case variable selection include the lasso (Tibshirani, 1996), smoothly clipped absolute deviation (Fan and Li, 2001), and extensions thereof (see, e.g., Bach, 2008; Meinshausen and Bühlmann, 2010; Fan and Lv, 2010). The knockoff procedure (Barber and Candès, 2015) has been a focus of recent developments; these have been aimed towards making the procedure more robust to model misspecification (see, e.g., Candès et al., 2018), but often some level of assumptions are necessary for valid error control or inference (see, e.g., Barber et al., 2020). Stability selection (Meinshausen and Bühlmann, 2010; Shah and Samworth, 2013; Hofner et al., 2015) has also been shown to provide error control for lasso-based procedures. However, as noted above, in some contexts model misspecification may result in poor performance of these procedures (see, e.g., Leng et al., 2006), motivating the consideration of alternatives that are not based upon generalized linear models. Additionally, in settings with missing data, the results from complete-case variable selection methods must be combined after being applied to each imputed dataset separately. Often, variables that are selected in some proportion of the imputed datasets are designated in the final set (see, e.g. Heymans et al., 2007; Long and Johnson, 2015).

In this article, we propose two approaches to more flexible variable selection in contexts with missing data. To allow for flexible modeling of the missing data process, we propose that missing data be imputed using multiple imputation by chained equations. Both of our proposed approaches to variable selection are based upon algorithm-agnostic definitions of variable importance. We distinguish between the extrinsic importance of a variable, which quantifies the extent to which a given algorithm makes use of the variable (see, e.g., Murdoch et al., 2019); and the intrinsic importance of a variable, which quantifies the population-level prediction potential of features (see, e.g., Williamson et al., 2021). In both cases, we propose to use ensembles of flexible algorithms to estimate the variable importance, and to use this estimated importance for variable selection. Interactions between variables can be taken into account either explic-

itly or implicitly through the choice of algorithms. Because both the extrinsic and intrinsic approaches studied here allow for the use of a wide array of candidate prediction algorithms, they are potentially more robust to model misspecification than procedures that are tied to a single algorithm or rely on a posited data-generating mechanism.

Our proposed extrinsic approach to variable selection builds upon the Super Learner ([van der Laan et al., 2007](#)), which incorporates potentially complex algorithms, e.g., boosted trees ([Friedman, 2001](#)), random forests, or neural networks ([Barron, 1989](#)). The Super Learner uses cross-validation to determine the final ensemble of the individual algorithms; we use these cross-validated ensemble weights to take a weighted average of the ranked variable importance from each algorithm, and variable selection is done using a cutoff for this ranked importance. While other approaches to ensemble variable selection have been proposed in the literature ([Breiman, 2001](#); [Xin and Zhu, 2012](#); [Saeys et al., 2008](#); [Guan et al., 2014](#); [Pes, 2020](#); [Shin et al., 2020](#)), none use cross-validation to determine the final ensemble ranking. We further show how to embed this procedure within stability selection. Finally, the resulting sets of selected variables on multiply-imputed datasets can be combined using a stability selection-type procedure ([Heymans et al., 2007](#); [Long and Johnson, 2015](#)).

Our proposed intrinsic approach to variable selection builds on the Shapley population variable importance measure ([Williamson and Feng, 2020](#)), and explicitly selects variables based on estimated population importance. We provide theoretical results guaranteeing control over several commonly-used error rates, including the generalized family-wise error rate and the false discovery rate. Further, we provide an approach based on Rubin’s rules ([Rubin, 1987](#)) that formally incorporates variability from the imputation process into the variable selection procedure and results in a single set of selected variables, removing the need for post-hoc combination of variable sets selected on different imputed datasets. Importantly, though recent theoretical developments have led to a procedure for doing inference on intrinsic variable importance, using this importance as part of a variable selection procedure has not been studied. Using intrinsic variable importance for variable selection should protect against model misspecification as long as a sufficiently flexible set of algorithms is used to estimate importance.

2 Variable selection using algorithm-agnostic importance

2.1 Data structure and notation

Suppose that observations Z_1, \dots, Z_n are drawn independently from data-generating distribution P_0 known only to belong to a rich class of distributions \mathcal{M} . Suppose further that $Z_i := (Y_i, X_i)$, where $X_i := (X_{i1}, \dots, X_{ip}) \in \mathcal{X} \subseteq \mathbb{R}^p$ is a vector of covariates and $Y_i \in \mathbb{R}$ is the outcome of interest. However, we do not observe the entire vector Z on all participants: let $\Delta := (\Delta_0, \dots, \Delta_p) \in \{0, 1\}^{p+1}$ denote a pattern of missing data for the outcome and covariates, where $\Delta_0 = 1$ implies that the outcome is observed and $\Delta_j = 1$ implies that covariate X_j is observed for $j = 1, \dots, p$. We denote the observed data by O_1, \dots, O_n , where $O_i := (\Delta_i, \Delta_{i0}Y_i, \Delta_{i1}X_{i1}, \dots, \Delta_{ip}X_{ip})$.

For each index set $s \subseteq \{1, \dots, p\}$, we consider the class of functions $\mathcal{F}_s := \{f \in \mathcal{F} : f(u) = f(v) \text{ for all } u, v \in \mathcal{X} \text{ satisfying } u_s = v_s\}$, where \mathcal{F} is a large class of functions. We also consider a scientifically meaningful predictiveness measure $V(f, P)$, where larger values of V are assumed to be better; examples of V include R^2 and classification accuracy (see, e.g., [Williamson et al., 2021](#)). For each $s \subseteq \{1, \dots, p\}$, we define the predictiveness-maximizing function $f_{0,s} \in \operatorname{argmax}_{f \in \mathcal{F}_s} V(f, P_0)$.

2.2 Ensemble-based extrinsic variable selection with complete data

We now describe our first approach to flexible feature selection, assuming that the data are fully observed; we will generalize to missing data settings in [Section 3](#). We propose to use the Super Learner ensembling procedure ([van der Laan et al., 2007](#)), a particular implementation of stacking ([Wolpert, 1992](#)) that enjoys both finite-sample and asymptotic performance guarantees ([van der Laan et al., 2007](#)). Suppose that we fit an ensemble with L candidate learners. The ensemble may include traditional learners that take as input all features, e.g., lasso, random forests, or boosted trees. The ensemble may also include screening algorithms, e.g., fit a lasso and remove features with zero coefficient, or remove any features with univariate correlation

below some prespecified rank, that are fit prior to the learners. We refer to each combination of screen and learner as a candidate learner; not all screens need necessarily be applied to all learners. As part of fitting the Super Learner, cross-validation is used to estimate a set $\{w_\ell\}_{\ell=1}^L$ of weights for each candidate learner in the final ensemble; by definition, $\sum_{\ell=1}^L w_\ell = 1$ and $w_\ell \geq 0$ for all $\ell = 1, \dots, L$. For each candidate learner, we can compute an estimate of the learner-specific, extrinsic variable importance for each feature using any method that we choose, for example, if candidate learner ℓ is the lasso with no pre-screening, variable importance for feature j , denoted by $v_{j,\ell}$, could be the absolute value of the lasso coefficient for variable j . For each learner ℓ , we then rank the extrinsic importance estimates from largest to smallest, obtaining ranks $\{r_{j,\ell}\}_{j=1}^p$, where rank 1 denotes the most important feature in learner ℓ . Finally, we select the variables with average weighted rank across learners $r_{j,L} := \sum_{\ell=1}^L w_\ell r_{j,\ell} < \kappa$, for a pre-specified threshold $\kappa \geq 1$. We summarize this procedure in Algorithm 1.

Algorithm 1 Ensemble-based extrinsic variable selection

- 1: Fit a Super Learner with L candidate learners, which results in weights $\{w_\ell\}_{\ell=1}^L$ specifying the final ensemble;
 - 2: **for** $\ell = 1, \dots, L$ **do**
 - 3: **for** $j = 1, \dots, p$ **do**
 - 4: Compute the extrinsic importance $v_{j,\ell}$;
 - 5: **end for**
 - 6: Compute the ranked importance $\{r_{j,\ell}\}_{j=1}^p$;
 - 7: **end for**
 - 8: Compute the average weighted rank across learners for each feature as $r_{j,L} := \sum_{\ell=1}^L w_\ell r_{j,\ell}$;
 - 9: Select all variables in $\{j \in \{1, \dots, p\} : r_{j,L} < \kappa\}$.
-

This ensemble-based procedure has several strengths. First, for many choices of V , e.g., R^2 , classification accuracy, and area under the receiver operating characteristic curve, the final ensemble is an estimator of $f_0 = \operatorname{argmax}_{f \in \mathcal{F}} V(f, P_0)$ (Williamson et al., 2021). Thus, extrinsic importance may provide some heuristic information about f_0 . Second, the procedure requires no meaningful additional computation time beyond fitting the ensemble. Third, the procedure should use the strengths of each individual learner, the screening algorithms, and the ensembling algorithm to the fullest advantage. Weighting the feature importance ranks accounts for the

fact that the different learners use different extrinsic importance definitions; using the ensemble weights in this average allows the ensemble to determine the priority of the features. Additionally, using aggressive screens and learners can result in a large degree of dimension reduction; this can also be accomplished by setting the tuning parameter κ to be small. Within the Super Learner, cross-validation is used to select the ensemble weights, providing robust estimation of the weighted extrinsic importance ranks. Finally, the procedure can be easily embedded within pre-existing frameworks that provide error rate control; for example, stability selection using a pre-specified threshold $\pi \in (0, 1)$. We describe such an algorithm in Algorithm 2. Stability selection has been shown to control the familywise error rate (Meinshausen and Bühlmann, 2010; Shah and Samworth, 2013).

Algorithm 2 Stability selection-based extrinsic variable selection

- 1: Generate B bootstrapped datasets $\tilde{Z}_1, \dots, \tilde{Z}_B$;
 - 2: **for** $b = 1, \dots, B$ **do**
 - 3: Using \tilde{Z}_b , generate a set of selected variables S_b using Algorithm 1;
 - 4: **end for**
 - 5: Obtain a final set of selected variables $S_B := \{j \in \{1, \dots, p\} : \frac{1}{B} \sum_{b=1}^B I(j \in S_b) > \pi\}$ for $\pi \in (0, 1)$.
-

However, the strengths of the ensemble-based extrinsic procedure must be traded off against its limitations. The main limitation of the procedure is that it relies heavily on the individual importance measures used for each candidate learner. While many of these measures are well-motivated, e.g., those for the lasso and some for random forests, they are nonetheless difficult to analyze theoretically and the importance ranks may vary if alternative measures are used. A second limitation is that even if combined with a procedure such as stability selection that provides error rate control, extrinsic procedures may not select all scientifically relevant features. These challenges motivate us to consider our second proposal for ensemble-based selection.

2.3 Intrinsic variable selection with complete data

To circumvent the need to rely on a particular algorithm-specific importance measure, we can consider intrinsic, or population-based, variable importance instead. We propose to perform intrinsic variable selection using the Shapley population variable importance measure (Williamson and Feng, 2020), which we denote by $\psi_0 := \{\psi_{0,j}\}_{j=1}^p$ and will hereafter refer to as the Shapley intrinsic importance. The Shapley intrinsic importance for feature X_j is given explicitly by

$$\psi_{0,j} := \sum_{s \in \{1, \dots, p\} \setminus \{j\}} \binom{p-1}{|s|}^{-1} \frac{1}{p} \{V(f_{0,s \cup j}, P_0) - V(f_{0,s}, P_0)\},$$

and quantifies the increase in population prediction potential, as measured by V , of including X_j in each possible subset of the remaining features $\{1, \dots, p\} \setminus \{j\}$. This definition provides a useful dichotomy: if $\psi_{0,j} > 0$, feature X_j has some utility in predicting the outcome in combination with at least one subset of the remaining features; if $\psi_{0,j} = 0$, then feature X_j does not improve population prediction potential if added to any subset of the remaining features. This key fact suggests that estimators of the Shapley intrinsic importance may be used to screen out variables with no intrinsic utility. More formally, for each $j \in \{1, \dots, p\}$, we define the null hypothesis $H_{0,j} : \psi_{0,j} = 0$. We can then define the following sets of variables:

$$S_0 \equiv S_0(P_0) := \{j \in \{1, \dots, p\} : \psi_{0,j} > 0\} \text{ and} \tag{1}$$

$$S_0^c \equiv S_0^c(P_0) := \{j \in \{1, \dots, p\} : \psi_{0,j} = 0\}. \tag{2}$$

We will refer to S_0 as the active set and S_0^c as the null set. In this context, the goal of a variable selection procedure can be recast into identifying the variables in S_0 while ignoring the variables in S_0^c ; these sets and the true Shapley intrinsic importance values are all defined relative to the underlying population P_0 .

In Williamson and Feng (2020), the authors describe the efficient influence function (see, e.g., Pfanzagl, 1982) of the true Shapley intrinsic importance and propose an estimator $\psi_{c,n} := \{\psi_{c,n,j}\}_{j=1}^p$ for each Shapley intrinsic importance that is asymptotically efficient under reg-

ularity conditions; we provide the specific conditions in the next section. Since obtaining an estimator $f_{n,s}$ of the predictiveness-maximizing function $f_{0,s}$ for each $s \subseteq \{1, \dots, p\}$ is generally computationally prohibitive, this estimation procedure is based on sampling a fraction c of all possible subsets. Under the regularity conditions provided in the next section, $n^{1/2}(\psi_{c,n} - \psi_0) \sim N_p(0, \Sigma_0)$, where $\Sigma_0 = E_0[IC_{P_0}(O)IC_{P_0}(O)^\top]$ and $IC_{P_0}(o)$ is the vector of efficient influence function values for each j . Thus, with $\sigma_{n,j}$ the j th component of the diagonal of the estimated covariance matrix based on the estimated efficient influence function, we can define test statistics $T_{n,j} := \sigma_{n,j}^{-1}(\psi_{c,n,j} - \psi_{0,j})$. The test statistics $T_n := (T_{n,1}, \dots, T_{n,p})$ follow a multivariate normal distribution under the joint null hypothesis, which we denote \mathcal{P}_0 .

Armed with these test statistics, we can define an initial set of selected variables. For a given $\alpha \in (0, 1)$ and possibly random cutoff functions $c_j(t, \mathcal{P}_0, \alpha)$, we define the sets

$$S_n(\alpha) \equiv S(T_n, \mathcal{P}_0, \alpha) := \{j \in \{1, \dots, p\} : T_{n,j} > c_j(T_n, \mathcal{P}_0, \alpha)\} \text{ and}$$

$$S_n^c(\alpha) \equiv S^c(T_n, \mathcal{P}_0, \alpha) := \{j \in \{1, \dots, p\} : j \notin S(T_n, \mathcal{P}_0, \alpha)\}.$$

Equivalently, we can define adjusted p-values (see, e.g., [Dudoit et al., 2003](#); [Dudoit and van der Laan, 2008](#))

$$\tilde{p}_{n,j} := \inf\{\alpha \in [0, 1] : T_{n,j} > c_j(T_n, \mathcal{P}_0, \alpha)\},$$

resulting in

$$S_n(\alpha) = \{j \in \{1, \dots, p\} : \tilde{p}_{n,j} \leq \alpha\}. \tag{3}$$

The procedure for determining the adjusted p-values, or equivalently the cutoffs c_j , will determine how and whether any multiple-testing control is achieved in determining $S_n(\alpha)$. Below, we will provide an example of the adjusted p-values using a Holm procedure ([Holm, 1979](#)). We define $R_n(\alpha) := |S_n(\alpha)|$ to be the number of rejected null hypotheses after this initial variable selection step.

An ideal selection procedure will result in $S_n(\alpha) \rightarrow_P S_0$ and $R_n(\alpha) \rightarrow_P |S_0|$ as $n \rightarrow \infty$ while maintaining control of the number of falsely selected variables. In other words, we want to minimize the number of type I errors $V_n(\alpha) := |S_n(\alpha) \cap S_0^c|$ while maximizing the number of selected truly important variables $|S_n(\alpha) \cap S_0|$. In the next section, we describe several procedures for augmenting the set $S_n(\alpha)$ obtained using the Shapley intrinsic importance values that provide control over commonly used error rates.

2.4 Error rate control and persistence using intrinsic selection

Before detailing our procedure and providing our main results, we introduce some additional notation. First, we define three commonly used error rates. For a given integer $k \geq 0$, the generalized family-wise error rate, of at least $k + 1$ type I errors, is defined as

$$gFWER(k) := Pr_{P_0}(V_n(\alpha) \geq k + 1) = 1 - F_{V_n(\alpha)}(k + 1), \quad (4)$$

where F_{V_n} is the cdf of V_n and $gFWER(0)$ is the family-wise error rate. The proportion of false positives among the rejected variables at level $q \in (0, 1)$ is defined as

$$PFP(q) := Pr_{P_0}(V_n(\alpha)/R_n(\alpha) > q). \quad (5)$$

Finally, we define the false discovery rate to be $FDR := E_{P_0}(V_n(\alpha)/R_n(\alpha))$.

Next, we define the collection of sets of functions $\mathcal{C}_n := \bigcup_{s \subseteq \{1, \dots, p\}: |s|=k_n} \mathcal{F}_s$ for $k_n \leq p$ and let $f_* \in \operatorname{argmax}_{f \in \mathcal{C}_n} V(f, P_0)$ denote the predictiveness-maximizing function over all function classes that make use of k_n variables. We say that a variable selection procedure S_n that selects k_n variables is persistent (see, e.g., [Greenshtein and Ritov, 2004](#); [Fan and Lv, 2010](#)) if

$$V(f_{n, S_n}, P_0) - V(f_*, P_0) \rightarrow_P 0,$$

where f_{n, S_n} is an estimator of f_{0, S_n} , the predictiveness-maximizing function that uses the variables selected by S_n . In other words, a persistent procedure ensures that the true predictiveness

of the empirical prediction function using the selected variables converges to the true predictive-ness of the best possible prediction function making use of the same number of variables. Our definition of persistence is equivalent to that of [Greenshtein and Ritov \(2004\)](#) if we consider the class of linear combinations of the predictors and take V to be R^2 .

Our results will make use of several conditions requiring additional notation. The first set of conditions is required to specify the distribution of the Shapley intrinsic importance values ([Williamson et al., 2021](#); [Williamson and Feng, 2020](#)). We define the linear space $\mathcal{R} := \{c(P_1 - P_2) : c \in \mathbb{R}, P_1, P_2 \in \mathcal{M}\}$ of finite signed measures generated by \mathcal{M} . For any $R \in \mathcal{R}$, we consider the supremum norm $\|R\|_\infty := |c| \sup_o |F_1(o) - F_2(o)|$, where F_1 and F_2 are the distribution functions corresponding to P_1 and P_2 , respectively, and we have used the representation $R = c(P_1 - P_2)$. For distribution $P_{0,\epsilon} := P_0 + \epsilon h$ with $\epsilon \in \mathbb{R}$ and $h \in \mathcal{R}$, we define $f_{0,\epsilon,s} = f_{P_{0,\epsilon},s}$ to be the oracle prediction function with respect to each subset $s \in \{1, \dots, p\}$. Let $\dot{V}(f, P_0; h)$ denote the Gâteaux derivative of $P \mapsto V(f, P)$ at P_0 in the direction $h \in \mathcal{R}$. The Gâteaux derivatives for several common choices of V are provided in [Williamson et al. \(2021\)](#). Next, we define the random function $g_{n,s} : o \mapsto \dot{V}(f_{n,s}, P_0; \delta_o - P_0) - \dot{V}(f_{0,s}, P_0; \delta_o - P_0)$, where δ_o is the degenerate distribution on $\{o\}$. For each subset $s \subseteq \{1, \dots, p\}$, we require the following conditions to hold:

- (A1) there is some $C > 0$ such that for each sequence $f_1, f_2, \dots \in \mathcal{F}_s$ with $\|f_j - f_{0,s}\|_{\mathcal{F}_s} \rightarrow 0$, there is a J such that for all $j > J$, $|V(f_j, P_0) - V(f_{0,s}, P_0)| \leq C \|f_j - f_{0,s}\|_{\mathcal{F}_s}^2$;
- (A2) there is some $\delta > 0$ such that for each sequence $\epsilon_1, \epsilon_2, \dots \in \mathbb{R}$ and $h, h_1, h_2, \dots \in \mathcal{R}$ satisfying that $\epsilon_j \rightarrow 0$ and $\|h_j - h\|_\infty \rightarrow 0$, it holds that

$$\sup_{f \in \mathcal{F}_s : \|f - f_{0,s}\|_{\mathcal{F}_s} < \delta} \left| \frac{V(f, P_0 + \epsilon_j h_j) - V(f, P_0)}{\epsilon_j} - \dot{V}(f, P_0; h_j) \right| \rightarrow 0;$$

- (A3) $\|f_{0,\epsilon,s} - f_{0,s}\|_{\mathcal{F}_s} = o(\epsilon)$ for each $h \in \mathcal{R}$;

- (A4) $f \mapsto \dot{V}(f, P_0; h)$ is continuous at $f_{0,s}$ relative to \mathcal{F}_s for each $h \in \mathcal{R}$;

- (A5) $\|f_{n,s} - f_{0,s}\|_{\mathcal{F}_s} = o_P(n^{-1/4})$;

$$(A6) \quad E_{P_0}[\int \{g_{n,s}(o)\}^2 dP_0(o)] = o_P(1);$$

(A7) for $\gamma > 0$ and sequence $\gamma_1, \gamma_2, \dots \in \mathbb{R}^+$ satisfying that $|\gamma_j - \gamma| \rightarrow 0$, $c = \gamma_n n$.

Below, we define the p-values $p_{n,j}$ from testing the null hypotheses $H_{0,j}$ for each $j \in \{1, \dots, p\}$; and the adjusted p-values $\tilde{p}_{n,j}$ arising from a multiple-testing procedure designed to provide finite-sample control of the family-wise error rate: for example, using Holm's adjusted p-values (Holm, 1979), a procedure based on the test statistics in decreasing order, or a procedure based on the p-values in increasing order (see, e.g., Dudoit et al., 2003). Based on the chosen multiple-testing control procedure, we obtain an initial set of selected variables $S_n(\alpha)$ as described in Equation (3).

To provide control over the generalized familywise error rate, proportion of false positives among the selected variables, and false discovery rate, we propose to augment the initial set $S_n(\alpha)$. For an integer $k \in \{0, \dots, p - R_n(\alpha)\}$, we define the augmentation set

$$A_n : (\alpha, k) \in (0, 1) \times \{0, \dots, p - R_n(\alpha)\} \mapsto \begin{cases} \emptyset & k = 0 \\ \{s \subseteq S_n^c(\alpha) : \tilde{p}_{n,\ell} \leq \tilde{p}_{n,(k)} \text{ for all } \ell \in s\} & k > 0, \end{cases} \quad (6)$$

where $a_{(j)}$ denotes the j th order statistic of a vector a . We also define $S_n^+(k, \alpha) = S_n(\alpha) \cup A_n(k, \alpha)$, $R_n^+(k, \alpha) = |S_n^+(k, \alpha)|$, and $V_n^+(k, \alpha) = |S_n^+(k, \alpha) \cap S_0^c|$. Finally, we define the following set of conditions:

(B1) (*finite-sample familywise error rate control*) $Pr_{P_0}(V_n(\alpha) > 0) = \alpha_n$ for all n ;

(B2) (*asymptotic familywise error rate control*) $\limsup_{n \rightarrow \infty} Pr_{P_0}(V_n(\alpha) > 0) = \alpha^* \leq \alpha$;

(B3) (*perfect asymptotic power*) $\lim_{n \rightarrow \infty} Pr_{P_0}(S_0 \subseteq S_n(\alpha)) = 1$;

(B4) (*limited number of initial rejections*) $\lim_{n \rightarrow \infty} Pr_{P_0}(S_n(\alpha) \leq p - k) = 1$.

Theorem 1. *If conditions (A1)–(A7) and (B1)–(B2) hold, then for any $k \geq 0$ and $q \in (0, 1)$, $S_n^+(k, \alpha)$ provides finite-sample control of $gFWER(k)$ and $PFP(q)$ at level α_n , that is,*

$$Pr_{P_0}(V_n^+(k, \alpha) > k) = \alpha_n, \quad Pr_{P_0}(V_n^+(k, \alpha)/R_n^+(k, \alpha) > q) = \alpha_n$$

for all n . If additionally (B3)–(B4) hold, then $S_n^+(k, \alpha)$ provides asymptotic control of these quantities, that is,

$$\limsup_{n \rightarrow \infty} Pr_{P_0}(V_n^+(k, \alpha) > k) \leq \alpha, \quad \limsup_{n \rightarrow \infty} Pr_{P_0}(V_n^+(k, \alpha)/R_n^+(k, \alpha) > q) \leq \alpha.$$

This result implies that the user can specify a tolerable threshold for the tail probability of a number of false discoveries, which can result in increased power over the potentially strict initial procedure $S_n(\alpha)$ while still providing error control. This holds in finite samples and asymptotically, so long as the initial procedure $S_n(\alpha)$ has high asymptotic power. Additionally, a simple extension of this result provides control of the false discovery rate (see, e.g., [Dudoit and van der Laan, 2008](#)).

Conditions (A1)–(A7) are necessary to characterize the distribution of the Shapley intrinsic importance estimator. The deterministic conditions (A1)–(A4) hold for many common choices of the predictiveness function V , including R^2 , classification accuracy, and the area under the receiver operating characteristic curve. The stochastic conditions (A5)–(A7) depend on the number of sampled subsets and the chosen estimator of the oracle prediction functions. These conditions are satisfied for many common estimators, and have been shown to hold approximately in numerical experiments with estimators that are not guaranteed to satisfy the conditions.

Conditions (B1)–(B4) describe the initial variable selection procedure $S_n(\alpha)$. While a number of procedures satisfy these conditions under (A1)–(A7), we consider here a Holm-based procedure for simplicity. Based on the p-values $\{p_{n,j}\}_{j=1}^p$ from the individual, unadjusted null

hypothesis tests, we can construct Holm-adjusted p-values

$$\tilde{p}_{n,(j)} := \max_{\ell \in \{1, \dots, j\}} \{\min\{p_{n,(\ell)}(p - \ell + 1), 1\}\}. \quad (7)$$

For $\alpha \in (0, 1)$, we set $S_n(\alpha) = \{j \in \{1, \dots, p\} : \tilde{p}_{n,j} < \alpha\}$, which guarantees control of the familywise error rate. Next, to control the generalized familywise error rate, select $k \in \{0, \dots, p - R_n(\alpha)\}$; to control the proportion of false positives among the selected variables, select $q \in (0, 1)$ and set $k = \max\{j \in \{0, \dots, p - R_n(\alpha)\} : j\{j + R_n(\alpha)\}^{-1} \leq q\}$. Define $A_n(k, \alpha)$ as in Equation (6), and augment the initial set to obtain $S_n^+(k, \alpha)$. Other procedures may satisfy (B1)–(B4) and could result in increased power (see, e.g., [Dudoit and van der Laan, 2008](#)). The general procedure based on any familywise error rate-controlling initial selection step is summarized in Algorithm 3.

Algorithm 3 Intrinsic variable selection with error rate control

- 1: For a given $\alpha \in (0, 1)$ and Shapley intrinsic importance estimators $\psi_{c,n,j}$ with corresponding standard error estimators $\sigma_{n,j}$, compute unadjusted p-values $p_{n,j}$ for each hypothesis test $H_{0,j}$;
 - 2: Compute adjusted p-values $\tilde{p}_{n,j}$ according to the desired familywise error rate-controlling procedure, e.g., Holm adjusted p-values as in Equation (7);
 - 3: Set $S_n(\alpha) = \{j \in \{1, \dots, p\} : \tilde{p}_{n,j} < \alpha\}$ as in Equation (3);
 - 4: For a given $k \in \{0, \dots, p - R_n(\alpha)\}$, obtain $A_n(k, \alpha)$ as in Equation (6);
 - 5: Set $S_n^+(k, \alpha) = S_n(\alpha) \cup A_n(k, \alpha)$.
-

Suppose that we use Algorithm 3 to perform variable selection, resulting in a set $S_n^+(k, \alpha)$.

The following lemma states that this procedure is persistent.

Lemma 1. *If conditions (A1), (A2), (A5) and (A6) hold for all $s \subseteq \{1, \dots, p\}$ and conditions (A7) and (B3) hold, then the procedure described in Algorithm 3 is persistent, that is,*

$$V(f_{n,S_n^+(k,\alpha)}, P_0) - V(f_*, P_0) \rightarrow_P 0.$$

This result implies that $S_n^+(k, \alpha)$ returns a collection of features that has predictiveness converging to the best possible predictiveness among all procedures that select $R_n^+(k, \alpha)$ variables.

3 Extrinsic and intrinsic selection with multiple imputation

In all algorithms studied so far, we focused on complete data. As noted above, in many cases, including our analysis in Section 5, data on covariates, the outcome, or some subset of these are missing. In these cases, a strategy for properly handling these missing data is necessary to perform variable selection and establish control of error rates. If an inverse probability weighting procedure is deemed appropriate, then the intrinsic selection procedure defined in Algorithm 3 can be updated with the inverse probability weights both in estimation and inference (van der Vaart, 2000; Williamson et al., 2021). However, as we mentioned above, in many cases with non-monotone patterns of missing data, correct estimation of the weights is difficult. Additionally, inverse probability weighting can be inefficient in cases with non-monotone missingness.

Multiple imputation is an appealing approach both due to the availability of easy-to-use software (e.g., `mice`; van Buuren and Groothuis-Oudshoorn, 2010) and the ability to flexibly model both monotone and non-monotone missing data patterns. We adopt a multiple imputation approach in this article due to this potential for flexibility. Each of our proposed algorithms can easily be used within a multiple imputation framework. Once a variable selection algorithm is determined, two additional procedures must be specified. The first is the imputation model: this must be appropriately flexible to avoid the risk of misspecification. Once the imputation model is determined, M imputed datasets $\tilde{Z}_1, \dots, \tilde{Z}_M$ are created. On each of these datasets, we use the chosen variable selection algorithm to obtain a set $S_{m,n}$ of selected variables, this may include an appropriate augmentation procedure to control the desired error rate using intrinsic selection. At this stage, the M selected sets must be harmonized; this is the second procedure that must be specified to embed one of our proposed algorithms within multiple imputation.

There are two common approaches to this harmonization step. The approach of Long and Johnson (2015) uses a single imputation within an outer layer of bootstrapping, and a stability-selection-type criterion for selecting final variables. While this approach has been shown to have good finite-sample characteristics, it can be computationally expensive, since there may be many

more bootstrap datasets than imputed datasets. An alternative is to select any variables that appear in at least πM selected variable sets, where $\pi \in [0, 1]$ is a threshold parameter (Heymans et al., 2007; Wood et al., 2008; Lachenbruch, 2011). Our proposed variable selection algorithm with multiple imputation is summarized in Algorithm 4; while we have chosen here not to embed the procedure within a bootstrap, it would be straightforward to extend Algorithm 4 to this case. This bootstrap-with-multiple-imputation algorithm can be seen as a natural generalization of the approach of Long and Johnson (2015) using our proposed extrinsic or intrinsic selection procedures.

Algorithm 4 Flexible variable selection with multiple imputation

- 1: Choose a variable selection procedure (e.g., Algorithm 1, 2, or 3);
 - 2: Using the chosen multiple imputation algorithm, obtain M imputed datasets $\tilde{Z}_1, \dots, \tilde{Z}_M$;
 - 3: **for** $m \in \{1, \dots, M\}$ **do**
 - 4: Using \tilde{Z}_m , obtain a selected set $S_{m,n}$ based on the procedure chosen in Step 1;
 - 5: **end for**
 - 6: Obtain a final set of selected variables $S_{M,n} := \{j \in \{1, \dots, p\} : M^{-1} \sum_{m=1}^M I(j \in S_{m,n}) > \pi\}$.
-

While the procedure described in Algorithm 4 holds for each of the three flexible selection algorithms we proposed in Sections 2.2 and 2.3, its generality must be traded off with the difficulty in providing formal error control. In particular, the results of Section 2.4 may fail to hold in settings with missing data, rendering the procedure of Algorithm 3 incorrect. In particular, the standard error based on the complete-data efficient influence function does not appropriately incorporate the additional variability due to the imputation step. However, as we shall see, if the imputation model is flexible enough to contain the true missing data mechanism, we can largely ignore this variance contribution.

Before stating a formal result, we first introduce a regularity condition. For intrinsic selection, we can use Rubin’s rules (Rubin, 1987) to combine estimates from a multiple imputation procedure. Suppose that for each of the M imputed datasets, we have computed Shapley intrinsic importance estimator $\psi_{m,c,n}$ of ψ_0 and its corresponding variance estimator $\sigma_{m,n}^2$. Define $\psi_{M,c,n} := M^{-1} \sum_{m=1}^M \psi_{m,c,n}$, $\sigma_{M,n}^2 := M^{-1} \sum_{m=1}^M \sigma_{m,n}^2$, and $\tau_{M,n}^2 := (M - 1)^{-1} \sum_{m=1}^M (\psi_{m,c,n} -$

$\psi_{M,c,n})^2$. Below, all expectations are with respect to the full data Z .

(A8) (*consistency of imputations*)

$$(A8a) \lim_{M \rightarrow \infty} E(\psi_{M,c,n} \mid Z) = \psi_{c,n};$$

$$(A8b) \lim_{M \rightarrow \infty} E(\sigma_{M,n}^2 \mid Z) = \sigma_n^2;$$

$$(A8c) \lim_{M \rightarrow \infty} E(\tau_{M,n}^2 \mid Z) = \lim_{M \rightarrow \infty} \text{var}(\psi_{M,c,n} \mid Z).$$

These conditions are commonly referred to as the essential conditions for proper multiple imputation (see, e.g., [Rubin, 1996](#)), and in turn provide conditions for the approximate asymptotic normality of appropriately centered and scaled version of $\psi_{M,c,n}$.

Lemma 2. *Provided that conditions (A1)–(A8) hold, then $n^{1/2}(\psi_{M,c,n} - \psi_0)$ is approximately asymptotically normally distributed with consistent variance estimator $\sigma_{M,n}^2 + (M+1)M^{-1}\tau_{M,n}^2$.*

This result indicates that, under a regularity condition, it is possible to use the estimators $\psi_{M,c,n}$ and appropriate variance estimators to compute adjusted p-values for use within Algorithm 3. The resulting procedure provides error rate control as described in Theorem 1. In finite samples, however, the approach detailed in Algorithm 4 also has favorable performance, as we describe below.

4 Numerical experiments

4.1 Experimental setup

We provide several experiments that are designed to describe the operating characteristics of our proposed extrinsic and intrinsic importance-based variable selection procedures, and compare these procedures with other well-established algorithms. In all cases, our simulated dataset consisted of independent replicates of (X, Y) , where $X = (X_1, \dots, X_p)$ and Y followed a Bernoulli distribution with success probability $\Phi\{\beta_{00} + f(\beta_0, x)\}$ conditional on $X = x$, where Φ denotes the cumulative distribution function of the standard normal distribution. Under this specification, Y followed a probit model.

In Scenario 1, we vary $p \in \{30, 500\}$, set $f(\beta_0, x) = x\beta_0$, and specify $\beta_{00} = 0.5$ and $\beta_0 = (-1, 1, -0.5, 0.5, 1/3, -1/3, \mathbf{0}_{p-6})^\top$, where $\mathbf{0}_k$ denotes a zero-vector of dimension k . We consider $X \sim MVN(0, I_p)$, where I_p is the $p \times p$ identity matrix. In this scenario, procedures that are based on a generalized linear model are correctly specified.

In Scenario 2, we consider a nonlinear outcome regression model, set $p = 6$, and add correlation between the variables. We center and scale each variable by its population mean and standard deviation using a function c_j ; then

$$\begin{aligned}
f(\beta_0, x) &= 2[\beta_{0,1}f_1\{c_1(x_1)\} + \beta_{0,2}f_2\{c_2(x_2), c_3(x_3)\} + \beta_{0,3}f_3\{c_3(x_3)\} \\
&\quad + \beta_{0,4}f_4\{c_4(x_4)\} + \beta_{0,5}f_2\{c_5(x_5), c_1(x_1)\} + \beta_{0,6}f_5\{c_6(x_6)\}], \quad (8) \\
f_1(x) &= \sin\left(\frac{\pi}{4}x\right), f_2(x, y) = xy, f_3(x) = \tanh(x), \\
f_4(x) &= \cos\left(\frac{\pi}{4}x\right), f_5(x) = -\tanh(x),
\end{aligned}$$

where \tanh denotes the hyperbolic tangent. In this scenario, $\beta_{00} = 0.5$, $\beta_0 = (0, 1, 0, 0, 0, 1)^\top$, and $X \sim MVN(0, \Sigma)$, where $\Sigma_{i,j} = \rho_1^{|i-j|}$ for i, j not in the active set, and $\Sigma_{i,j} = I_p + \rho_2(J_p - I_p)$ for i, j in the active set, where J_p is a $p \times p$ matrix of ones. We set $\rho_1 = 0.3$ and $\rho_2 = 0.95$. In this scenario, procedures that are based on a generalized linear model are misspecified.

We generate observed data by first generating complete (X, Y) and then generating missing data using amputation ([van Buuren and Groothuis-Oudshoorn, 2010](#)) as implemented in the `mice` package in R. The outcome and certain features always have complete data, i.e., $\delta_j = 1$ for $j \in \{0, 1, 3, 5\}$. The missing data are missing at random and have the following possible specifications for the noise features and important features. When $p = 500$, 40 noise features can be missing; when $p = 30$, 3 noise features can be missing; and the remaining noise features are fully observed. The truly important features (X_2, X_4, X_6) have a monotone pattern of missingness, where observing X_2 implies that both X_4 and X_6 are observed. In all scenarios, we consider fully observed data, a maximum of 20% missing data within each column, and a maximum of 40% missing data within each column.

For each sample size $n \in \{200, 500, 1500, 3000\}$, we generated 1000 replicates from each

combination of data-generating mechanism, number of features, and proportion of missing data. We additionally generated an independent test dataset following the same distribution but with no missing data and with sample size 10,000. Prior to fitting any procedure, we used multiple imputation with a single round and predictive mean matching, implemented in `mice`, to impute any missing feature information. We used $M = 1$ in these simulations to allow for a more feasible computation time; in most applications, we advocate for larger M . Thus, in all cases in this section, we are evaluating Algorithm 4 with $M = 1$ and $\pi = 0$. To provide a performance benchmark, in each case we fit a Super Learner with no variable selection, implemented in the `SuperLearner` package (Polley et al., 2019). The candidate algorithms for the Super Learner were the lasso using cross-validation-based tuning; and boosted trees and random forests with default tuning parameters. The specific algorithms and their tuning parameters are discussed more fully in the Supplementary Material. We used five-fold cross-validation to select the ensemble that minimized the cross-validated negative log likelihood loss function.

We considered three base estimation procedures for performing variable selection: lasso; Super Learner with our proposed extrinsic selection, specified in Algorithm 1; and intrinsic selection, specified in Algorithm 3, with generalized familywise error rate, proportion of false positives among the selected variables, and false discovery rate control. In the latter case, we used a simple Super Learner library consisting of boosted trees with pre-screening based on univariate correlation to estimate intrinsic importance. In this case, since $M = 1$, the intrinsic importance-based procedures are equivalent to the approach based on Rubin’s rules. Finally, we used both the Super Learner and the lasso as part of a stability selection algorithm, implemented in the `stabs` package (Hofner and Hothorn, 2017); and we used the lasso with knockoffs, implemented in the `knockoff` package (Patterson and Sesia, 2020). The values of the tuning parameters used in each procedure for error rate control are provided in the Supplementary Material.

After performing variable selection, we estimated the prediction performance of the selected variables by fitting a regression of the outcome on these variables. We used a probit regression in the case of variables selected by the lasso-based methods and used the Super Learner in all other

cases. We then computed the test-set area under the receiver operating characteristic curve based on the independent sample. We additionally computed the sensitivity and specificity of the selected set of variables. Finally, we evaluated the average test-set area under the receiver operating characteristic curve based of the selected variables and the average sensitivity and specificity of each procedure over the 1000 samples.

4.2 Primary empirical results

In Figure 1, we display the results of the experiment conducted under Scenario 1; the features are multivariate normal and the outcome-feature relationship follows a linear model. We only show results for no missing data and 40% missing data; the results for 20% missing data are similar and are presented in the Supplementary Material. In this scenario, the lasso-based estimators are correctly specified. We observe that for both feature-space dimensions $p \in \{30, 500\}$, all estimators have increasing test-set area under the receiver operating characteristic curve regardless of the proportion of missing data. However, test-set area under the receiver operating characteristic curve decreases with the proportion of missing data, especially at smaller sample sizes; we suspect that this could be mitigated by using a larger number of imputations. In this experiment, lasso with knockoffs and the benchmark Super Learner tend to have the largest test-set area under the receiver operating characteristic curve, followed by the extrinsic ensemble selector with stability selection described in Algorithm 2. The proportion of false positives and false discovery rate-controlling intrinsic selection procedures tend to have lower area under the receiver operating characteristic curve, particularly at smaller sample sizes, reflecting the fact that these procedures provide stricter control of specificity at the cost of sensitivity. In Figure 1, we observe that empirical sensitivity increases towards one for all algorithms regardless of the feature-space dimension. Worryingly, the specificity of the base lasso decreases with n in both moderate and high dimensions. In the $p = 500$ case, while the lasso again has decreasing specificity, stability selection appears to mitigate this behavior.

In Figure 2, we display the results of the experiment conducted under Scenario 2; the fea-

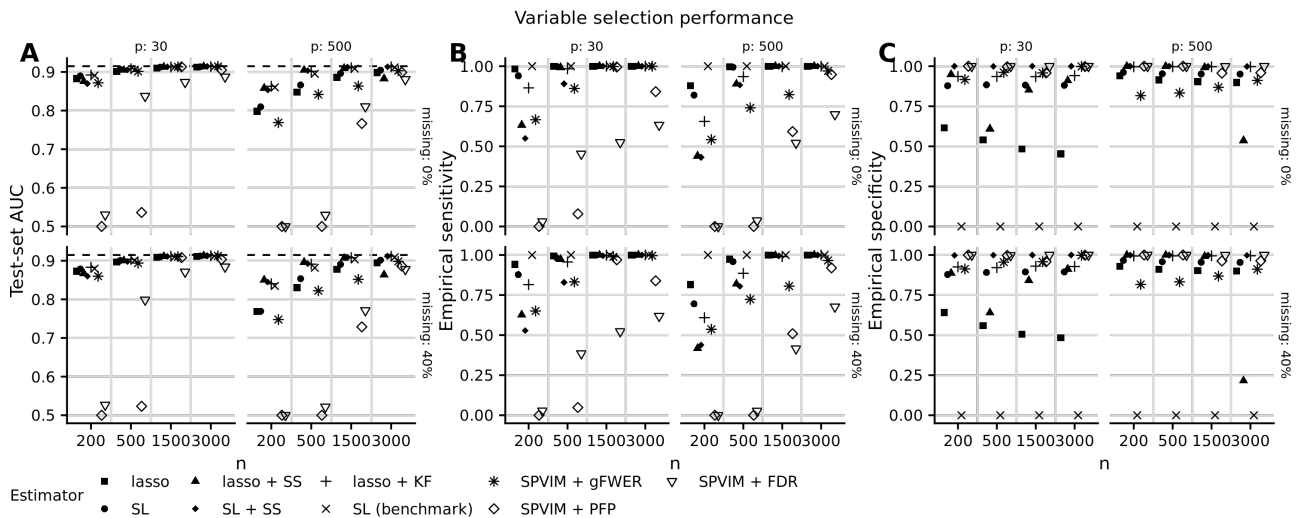


Figure 1: Test-set area under the receiver operating characteristic curve (AUC) (panel A) and empirical variable selection sensitivity (panel B) and specificity (panel C) vs n for each estimator and missing data proportion, in Scenario 1 (a linear model for the outcome and multivariate normal features). The dotted line in panel A shows the true (optimal) test-set AUC. The methods compared are: lasso; lasso + SS, lasso with stability selection; lasso + KF, lasso with knockoffs; SL (benchmark), the Super Learner with no variable selection; SL, extrinsic variable selection; SL + SS, extrinsic variable selection with stability selection; SPVIM + gFWER, intrinsic selection to control the generalized familywise error rate; SPVIM + PFP, intrinsic selection to control the proportion of false positives among the rejected variables; and SPVIM + FDR, intrinsic selection to control the false discovery rate.

tures are correlated multivariate normal and the outcome-feature relationship is nonlinear. We observe test-set area under the receiver operating characteristic curve near the optimal value for the extrinsic and intrinsic selection procedures, while test-set area under the receiver operating characteristic curve is much lower for the lasso-based procedures. We again observe lower test-set area under the receiver operating characteristic curve for the proportion of false positives and false discovery rate-controlling intrinsic procedures, particularly in smaller samples; this is due to these procedures having lower sensitivity, shown in panel B of Figure 2, suggesting that the error control is too tight in this case. We observe poor empirical sensitivity for all lasso-based estimators in this scenario, while we observe high sensitivity for the extrinsic and generalized familywise error rate-controlling intrinsic procedures. Empirical specificity also tends to be high for this intrinsic procedure; among lasso-based estimators, lasso with knockoffs has the highest empirical specificity, which tends to be lower than specificity for the generalized familywise error rate-controlling intrinsic procedure.

This simulation study suggests that the extrinsic and intrinsic variable selection procedures proposed here have good practical performance, as suggested by theory. As is the case with other procedures, we observed a tradeoff between sensitivity and specificity for our proposed procedures. Our findings suggest that in cases where variable selection is not a goal, using a flexible algorithm with all features tends to result in test-set area under the receiver operating characteristic curve close to the optimal value. In the Scenario 2, where procedures based on a generalized linear model were misspecified, we observed poor variable selection and prediction performance when using lasso-based estimators, whereas our proposed methods protected against this model misspecification.

4.3 Additional empirical results

In the Supplementary Material, we present the 20% missing data case for Scenarios 1 and 2, observing similar results to those presented in Figures 1 and 2. We also consider six additional scenarios scrutinizing the effect of intermediate departures from the linear outcome regression

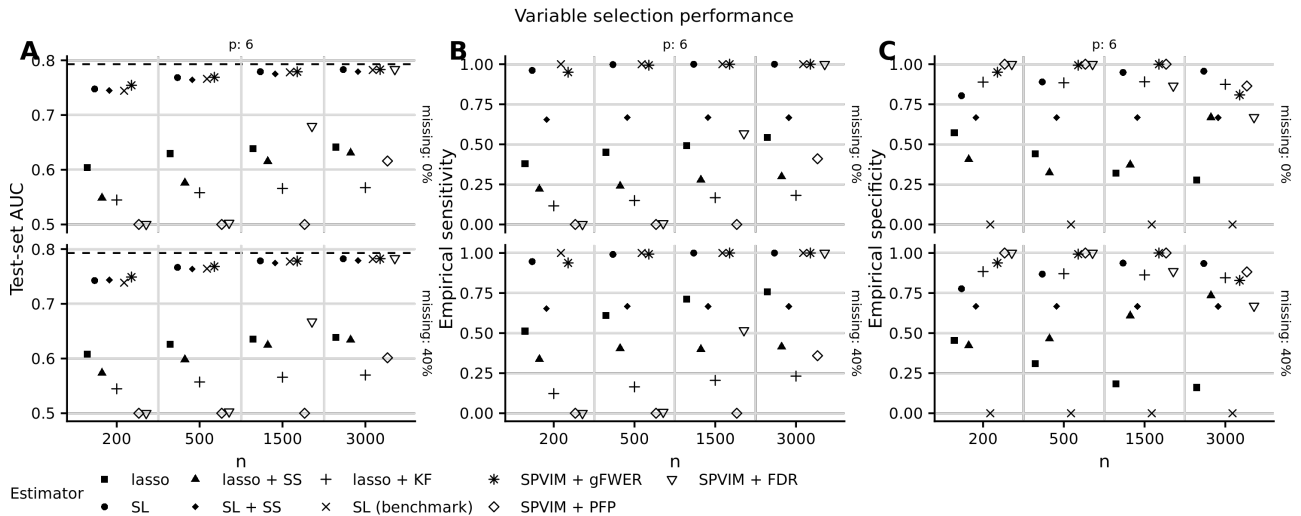


Figure 2: Test-set area under the receiver operating characteristic curve (AUC) (panel A) and empirical variable selection sensitivity (panel B) and specificity (panel C) vs n for each estimator, in Scenario 2 (a nonlinear model for the outcome and correlated multivariate normal features). The dotted line in panel A shows the true (optimal) test-set AUC. The methods compared are: lasso; lasso + SS, lasso with stability selection; lasso + KF, lasso with knockoffs; SL (benchmark), the Super Learner with no variable selection; SL, extrinsic variable selection; SL + SS, extrinsic variable selection with stability selection; SPVIM + gFWER, intrinsic selection to control the generalized familywise error rate; SPVIM + PFP, intrinsic selection to control the proportion of false positives among the rejected variables; and SPVIM + FDR, intrinsic selection to control the false discovery rate.

and independent normal feature distribution. We found that a nonnormal feature distribution had a minimal effect on both variable selection and prediction performance. In contrast, a non-linear outcome regression resulted in decreased test-set prediction performance and decreased probability of selecting some important variables. In a setting with equally, but weakly, important variables and a linear outcome regression model, we observed that adding correlation resulted in poorer performance of lasso-based estimators, whereas our proposed methods continued to perform well. We observed similar performance to Scenario 2 in an identical case except for with uncorrelated features. We also further investigated our proposed extrinsic selection algorithm by incorporating knockoffs and variable screens. We found that the Super Learner did not perform well with the knockoff statistic that we evaluated. We also found that caution must be exercised if variable screens are used in the Super Learner. In some cases, e.g., a strong nonlinear association between the outcome and covariates, the Super Learner can be heavily influenced by the variable screens, resulting in poor selection and estimation performance. The appropriate screens to use within a Super Learner are likely to depend on context. Our results suggest that if variable selection is a scientific goal, a well-calibrated selection procedure should be combined with an algorithm for the final outcome regression that is flexible enough to avoid misspecification.

5 Developing a biomarker panel for pancreatic cancer early detection

Pancreatic ductal adenocarcinoma is the fourth-leading cause of cancer death in the United States, with an estimated five-year survival rate of 8%. Since pancreatic ductal adenocarcinoma typically results from a multi-step process, there is increasing focus on early detection of intraductal precursor lesions, with the goal of identifying pancreatic cancer at an early stage, when treatment should be most effective. Mucinous cysts are one potential precursor lesion to pancreatic ductal adenocarcinoma and might be identified using routine imaging. However,

imaging can be prohibitively expensive, and the ability of current radiographic tests to differentiate between benign and pre-malignant cystic neoplasms is limited (Brugge et al., 2004). This has spurred development of fluid biomarkers that can be assayed using pancreatic cyst fluid, which is routinely collected during clinical care.

The analysis cohort we consider consists of specimens from 321 participants with confirmed surgical pathology diagnosis from the Pancreatic Cyst Biomarker Validation Study sponsored by the Early Detection & Research Network (Liu et al., 2020), which is a collaborative effort evaluating multiple cystic fluid biomarkers measured by biomarker labs in several research institutes across the United States. Measurements are also available for the standard carcinoembryonic antigen biomarker for mucinous cysts (Meng et al., 2017). There are 21 candidate biomarkers, consisting of both continuous scores and binary calls; some of the binary calls correspond to an available continuous score, while others do not. The biomarkers are described further in the Supplementary Material.

A main objective of the Pancreatic Cyst Biomarker Validation Study is to develop biomarkers or biomarker panels that can be used to separate pancreatic cysts with differential malignant potentials. A major complication in achieving this study objective is the limited cystic fluid volume available from each study participant. Measuring all proposed biomarkers would require 1.1 ml cystic fluid per individual, but only 0.35 to 1.1 ml is available from each participant. The study statistical team thus designed a scheme to randomly assign available specimens to each validation site such that biomarkers in each research lab were only measured in a subset of the total study participants. This results in a highly non-monotone pattern of missingness in the biomarker data. Here the missing at random assumption holds since the probability of measuring a biomarker from an individual depends on that individual’s specimen volume based on the specimen allocation scheme. Our primary goal in this analysis is to develop biomarker panels to separate mucinous cysts from non-mucinous cysts, where a mucinous cyst is thought to have some malignant potential. In the Supplementary Material, we present an analysis focused on separating cysts with high malignant potential from cysts with low or no malignant potential.

Our procedure for obtaining a final set of selected biomarkers, which we refer to as a panel, and assessing the panel’s prediction performance involves several steps. We use the same variable selection and prediction procedures that we evaluated in the previous section: lasso, including with knockoffs and stability selection, for variable selection, with final predictions made using logistic regression; Super Learner with no selection, extrinsic selection, and extrinsic selection with stability selection; and intrinsic selection designed to control the generalized familywise error rate, proportion of false positives, and false discovery rate, both with and without using Rubin’s rules via Lemma 2. Final predictions for the extrinsic and intrinsic procedures are made using the Super Learner. We assessed the prediction performance of each procedure through repeating an imputation-within-cross-validation procedure 100 times. We used multiple imputation with $M = 10$ in all cases, and used an outer layer of five-fold cross-validation to assess prediction performance. We obtained a final set of biomarkers selected by each procedure using the full dataset, selecting variables that were selected in 7 or more of 10 imputed datasets. More details on the approaches to estimating prediction performance and obtaining the final panel are provided in the Supplementary Material.

We present the results of our analysis in Figure 3. We see that with the exception of the proportion of false positives- and false discovery rate-controlling intrinsic selection procedures, all procedures have high predictiveness, as measured by cross-validated area under the receiver operating characteristic curve. The top-performing algorithms are the Super Learner with no variable selection and the generalized familywise error rate-controlling intrinsic selection procedure, with average estimated cross-validated area under the receiver operating characteristic curve of 0.958 and 0.959, respectively, with 95% confidence intervals of [0.91, 1] and [0.911, 1], respectively. Similar performance between these two procedures suggests that we do not lose much information by performing variable selection in this case. Additionally, similar performance between the intrinsic selection procedures with and without using Rubin’s rules suggests that the approach of Algorithm 4 is well-calibrated in this setting. Performance is slightly worse for the lasso-based estimators, with an average estimated cross-validated area under the receiver operating characteristic curve of 0.949 [0.891, 1] for the lasso with knockoffs. On av-

erage, the proportion of false positives- and false discovery rate-controlling intrinsic selection procedures did not select any variables, suggesting that the tuning parameters we selected were too conservative. In the Supplementary Material, we display the final set of biomarkers selected by each procedure. Encouragingly, the biomarkers selected by both intrinsic selection procedures are identical. No biomarkers are selected across all seven procedures. However, several biomarkers are selected by five or more procedures: continuous scores for methylated DNA levels, amphiregulin overexpression, fluorescent protease activity, and expression of the protein MUC3AC; and binary variables based on amphiregulin and the combination of amphiregulin and glucose.

6 Discussion

We have proposed several variable selection procedures that are robust to model misspecification and are valid in settings with missing data. These extrinsic and intrinsic selection procedures provide an alternative to existing, model-based approaches to variable selection that may be invalid under model misspecification. We proved that our intrinsic selection procedure is persistent, in other words, the predictiveness of the selected set converges to the predictiveness of the best possible set of the same size as the selected set; and that control of the generalized family-wise error rate, proportion of false positives, or false discovery rate can be achieved through the use of a tuning parameter. In cases with missing data, we identified conditions under which Rubin’s rules can be used with this procedure to achieve control over these same error rates while formally incorporating the imputation variance into the variable selection procedure. We also proposed an extrinsic variable selection procedure based on ensembling, and found that this procedure can be embedded within stability selection. In the extrinsic case, the results from multiply-imputed datasets are combined by selecting those variables that appear in a user-defined proportion of the individual-imputation selected sets. We found in simulated examples that all of our proposals had high sensitivity and specificity, and that the prediction performance of a prediction algorithm built using the selected variables converged to the pre-

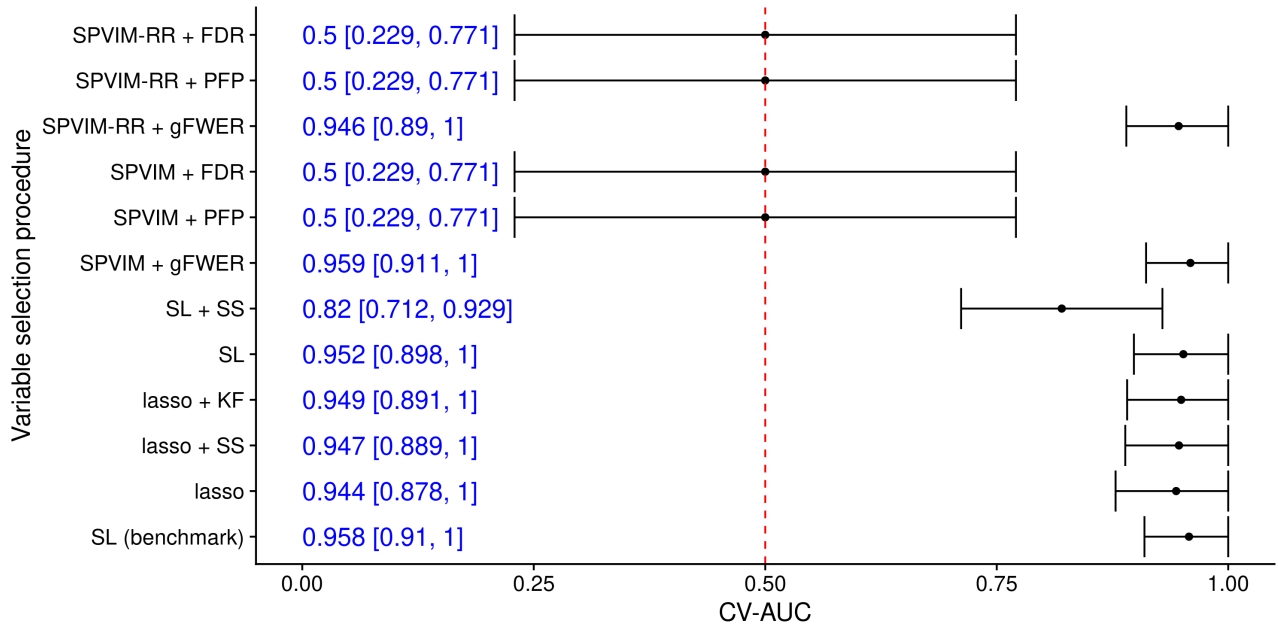


Figure 3: Cross-validated area under the receiver operating characteristic curve (CV-AUC) for predicting whether a cyst is mucinous averaged over 100 replicates of the imputation-within-cross-validated procedure for each variable selection algorithm. Prediction performance for lasso-based methods is based on logistic regression on the selected variables, while performance for Super Learner-based methods is based on a Super Learner. Error bars denote 95% confidence intervals based on the average variance over the 100 replications. The methods compared are: lasso; lasso + SS, lasso with stability selection; lasso + KF, lasso with knockoffs; SL (benchmark), the Super Learner with no variable selection; SL, extrinsic variable selection; SL + SS, extrinsic variable selection with stability selection; SPVIM + gFWER, intrinsic selection to control the generalized familywise error rate; SPVIM + PFP, intrinsic selection to control the proportion of false positives among the rejected variables; SPVIM + FDR, intrinsic selection to control the false discovery rate; SPVIM-RR + gFWER, intrinsic selection with Rubin’s rules to control the generalized familywise error rate; SPVIM-RR + PFP, intrinsic selection with Rubin’s rules to control the proportion of false positives among the rejected variables; and SPVIM-RR + FDR, intrinsic selection with Rubin’s rules to control the false discovery rate. The first eight methods use Algorithm 4 to combine sets of variables across imputed datasets, while the final four methods use Rubin’s rules.

diction performance of the best possible prediction algorithm. Importantly, in settings where a simple linear model is correctly specified, our proposed approaches have similar operating characteristics to three commonly-used procedures: the lasso, lasso with stability selection, and lasso with knockoffs. In settings with a nonlinear outcome regression model, weakly important features, and correlated features, we observed that our proposals maintained high sensitivity and specificity, while the performance of the lasso-based procedures suffered; this degraded performance was suggested by theory (see, e.g., [Leng et al., 2006](#)). In settings with a larger number of features, some of which were strongly important, lasso-based procedures had higher overall performance. This performance was robust to nonnormal features, but was not robust to a misspecified outcome regression model, particularly in selecting the more weakly important features.

In settings with missing data, many variable selection procedures require post-hoc harmonization of many selected sets resulting from multiply imputed datasets. A benefit of our proposed intrinsic selection procedure is that Rubin’s rules can be used to obtain a single set of point and variance estimates, thereby resulting in a single set of selected variables that explicitly account for the across-imputation variance. In cases where the imputation mechanism is misspecified and incongenial with the analytic approach, it may be necessary to update the variance estimator ([Robins and Wang, 2000](#)); however, the form of this estimator is complex. A procedure that explicitly accounts for across-imputation variance in our proposed extrinsic selection procedures, and in other procedures that currently require post-hoc harmonization with multiply imputed data, is also of interest. These ideas are being pursued in ongoing research.

Software and supplementary materials

The proposed methods are implemented in the R package `flevr`, freely available on [GitHub](#). Supplementary Materials, including all technical proofs and code to reproduce all numerical experiments and data analyses, are available on GitHub at https://github.com/bdwilliamson/ensembleselect_supplementary.

Acknowledgements

This work was supported by the National Institutes of Health (NIH) grants R37AI054165, R01GM106177, U24CA086368 and S10OD028685. The opinions expressed in this article are those of the authors and do not necessarily represent the official views of the NIH.

References

- Bach, F. (2008). Bolasso: model consistent lasso estimation through the bootstrap. In *Proceedings of the 25th International Conference on Machine Learning*, pp. 33–40.
- Bang, H. and J. Robins (2005). Doubly robust estimation in missing data and causal inference models. *Biometrics* 61(4), 962–973.
- Barber, R. and E. Candès (2015). Controlling the false discovery rate via knockoffs. *Annals of Statistics* 43(5), 2055–2085.
- Barber, R. F., E. J. Candès, and R. J. Samworth (2020). Robust inference with knockoffs. *arXiv preprint arXiv:1801.03896*.
- Barron, A. (1989). Statistical properties of artificial neural networks. In *Proceedings of the 28th IEEE Conference on Decision and Control*, pp. 280–285. IEEE.
- Breiman, L. (2001). Random forests. *Machine Learning* 45(1), 5–32.
- Brugge, W., K. Lewandrowski, E. Lee-Lewandrowski, B. Centeno, T. Szydlo, S. Regan, C. del Castillo, A. Warshaw, and The Investigators of the CPC Study (2004). Diagnosis of pancreatic cystic neoplasms: a report of the cooperative pancreatic cyst study. *Gastroenterology* 126(5), 1330–1336.
- Candès, E., Y. Fan, L. Janson, and J. Lv (2018). Panning for gold: Model-X knockoffs for high-dimensional controlled variable selection. *Journal of the Royal Statistical Society: Series B (Statistical Methodology)* 80, 551–577.
- Cao, Z., K. Maupin, B. Curnutte, B. Fallon, C. Feasley, E. Brouhard, R. Kwon, C. West, J. Cunningham, R. Brand, P. Castelli, S. Crippa, Z. Feng, P. Allen, D. Simeone, and B. Haab (2013). Specific

- glycoforms of MUC5AC and endorepellin accurately distinguish mucinous from nonmucinous pancreatic cysts. *Molecular & Cellular Proteomics* 12(10), 2724–2734.
- Chen, T., T. He, M. Benesty, V. Khotilovich, Y. Tang, H. Cho, K. Chen, R. Mitchell, I. Cano, T. Zhou, M. Li, J. Xie, M. Lin, Y. Geng, and Y. Li (2019). *xgboost: Extreme Gradient Boosting*. R package version 0.82.1.
- Das, K., H. Xiao, X. Geng, C. Fernandez-del Castillo, V. Morales-Oyarvide, E. Daglilar, D. Forcione, B. Bounds, W. Brugge, M. Pitman, M. Mino-Kenudson, and K. Das (2014). mAb Das-1 is specific for high-risk and malignant intraductal papillary mucinous neoplasm (IPMN). *Gut* 63(10), 1626–1634.
- Dudoit, S., J. Shaffer, and J. Boldrick (2003). Multiple hypothesis testing in microarray experiments. *Statistical Science* 18(1), 71–103.
- Dudoit, S. and M. van der Laan (2008). *Multiple testing procedures with applications to genomics*. Springer Science & Business Media.
- Fan, J. and R. Li (2001). Variable selection via nonconcave penalized likelihood and its oracle properties. *Journal of the American Statistical Association* 96(456), 1348–1360.
- Fan, J. and J. Lv (2010). A selective overview of variable selection in high dimensional feature space. *Statistica Sinica* 20(1), 101.
- Friedman, J. (2001). Greedy function approximation: a gradient boosting machine. *Annals of Statistics* 29(5), 1189–1232.
- Friedman, J., T. Hastie, and R. Tibshirani (2010). Regularization paths for generalized linear models via coordinate descent. *Journal of Statistical Software* 33(1), 1–22.
- Garcia, R., J. Ibrahim, and H. Zhu (2010). Variable selection for regression models with missing data. *Statistica Sinica* 20(1), 149.
- Greenshtein, E. and Y. Ritov (2004). Persistence in high-dimensional linear predictor selection and the virtue of overparametrization. *Bernoulli* 10(6), 971–988.

- Guan, D., W. Yuan, Y. Lee, K. Najeebullah, and M. Rasel (2014). A review of ensemble learning based feature selection. *IETE Technical Review* 31(3), 190–198.
- Hata, T., M. Dal Molin, S. Hong, K. Tamura, M. Suenaga, J. Yu, H. Sedogawa, M. Weiss, C. Wolfgang, A. Lennon, R. Hruban, and M. Goggins (2017). Predicting the grade of dysplasia of pancreatic cystic neoplasms using cyst fluid DNA methylation markers. *Clinical Cancer Research* 23(14), 3935–3944.
- Hata, T., M. Dal Molin, M. Suenaga, J. Yu, M. Pittman, M. Weiss, M. Canto, C. Wolfgang, A. Lennon, R. Hruban, and M. Goggins (2016). Cyst fluid telomerase activity predicts the histologic grade of cystic neoplasms of the pancreas. *Clinical Cancer Research* 22(20), 5141–5151.
- Heymans, M., S. Van Buuren, D. Knol, W. Van Mechelen, and H. De Vet (2007). Variable selection under multiple imputation using the bootstrap in a prognostic study. *BMC Medical Research Methodology* 7(1), 1–10.
- Hofner, B., L. Boccutto, and M. Göker (2015). Controlling false discoveries in high-dimensional situations: boosting with stability selection. *BMC Bioinformatics* 16(1), 1–17.
- Hofner, B. and T. Hothorn (2017). *stabs: Stability Selection with Error Control*. R package version 0.6-3.
- Holm, S. (1979). A simple sequentially rejective multiple test procedure. *Scandinavian Journal of Statistics*, 65–70.
- Ivry, S., J. Sharib, D. Dominguez, N. Roy, S. Hatcher, M. Yip-Schneider, C. Schmidt, R. Brand, W. Park, M. Hebrok, G. Kim, A. O’Donoghue, K. Kirkwood, and C. Craik (2017). Global protease activity profiling provides differential diagnosis of pancreatic cysts. *Clinical Cancer Research* 23(16), 4865–4874.
- Johnson, B., D. Lin, and D. Zeng (2008). Penalized estimating functions and variable selection in semiparametric regression models. *Journal of the American Statistical Association* 103(482), 672–680.
- Karatzoglou, A., A. Smola, K. Hornik, and A. Zeileis (2004). kernlab – an S4 package for kernel methods in R. *Journal of Statistical Software* 11(9), 1–20.

- Lachenbruch, P. (2011). Variable selection when missing values are present: a case study. *Statistical Methods in Medical Research* 20(4), 429–444.
- Leng, C., Y. Lin, and G. Wahba (2006). A note on the lasso and related procedures in model selection. *Statistica Sinica* 16, 1273–1284.
- Little, R. and M. Schluchter (1985). Maximum likelihood estimation for mixed continuous and categorical data with missing values. *Biometrika* 72(3), 497–512.
- Liu, L., Y. Qiu, L. Natarajan, and K. Messer (2019). Imputation and post-selection inference in models with missing data: An application to colorectal cancer surveillance guidelines. *Annals of Applied Statistics* 13(3), 1370–1396.
- Liu, Y., S. Kaur, Y. Huang, J. Fahrman, J. Rinaudo, S. Hanash, S. Batra, A. Singhi, R. Brand, A. Maitra, and B. Haab (2020). Biomarkers and strategy to detect preinvasive and early pancreatic cancer: State of the field and the impact of the EDRN. *Cancer Epidemiology, Biomarkers & Prevention* 29(12), 2513–2523.
- Long, Q. and B. Johnson (2015). Variable selection in the presence of missing data: resampling and imputation. *Biostatistics* 16(3), 596–610.
- Majumder, S., W. Taylor, T. Yab, C. Berger, B. Dukek, X. Cao, P. Foote, C. Wu, D. Mahoney, H. Aslanian, C. Fernandez-Del Castillo, L. Doyle, J. Farrell, W. Fisher, L. Lee, Y. Lee, W. Park, C. Rodrigues, B. Rothberg, R. Salem, D. Simeone, S. Urs, G. Van Buren, T. Smyrk, H. Allawi, G. Lidgard, M. Raimondo, S. Chari, M. Kendrick, J. Kisiel, M. Topazian, and D. Ahlquist (2019). Novel methylated DNA markers discriminate advanced neoplasia in pancreatic cysts: marker discovery, tissue validation, and cyst fluid testing. *The American journal of Gastroenterology* 114(9), 1539.
- Meinshausen, N. and P. Bühlmann (2010). Stability selection. *Journal of the Royal Statistical Society: Series B (Statistical Methodology)* 72(4), 417–473.
- Meng, Q., S. Shi, C. Liang, D. Liang, W. Xu, S. Ji, B. Zhang, Q. Ni, J. Xu, and X. Yu (2017). Diagnostic and prognostic value of carcinoembryonic antigen in pancreatic cancer: A systematic review and meta-analysis. *OncoTargets and therapy* 10, 4591.

- Murdoch, W., C. Singh, K. Kumbier, R. Abbasi-Asl, and B. Yu (2019). Interpretable machine learning: definitions, methods, and applications. *arXiv:1901.04592*.
- Neidich, S. D., Y. Fong, S. S. Li, D. E. Geraghty, B. D. Williamson, W. C. Young, D. Goodman, K. E. Seaton, X. Shen, S. Sawant, et al. (2019). Antibody Fc effector functions and IgG3 associate with decreased HIV-1 risk. *The Journal of Clinical Investigation* 129(11), 4838–4849.
- Patterson, E. and M. Sesia (2020). *knockoff: The Knockoff Filter for Controlled Variable Selection*. R package version 0.3.3.
- Pes, B. (2020). Ensemble feature selection for high-dimensional data: a stability analysis across multiple domains. *Neural Computing and Applications* 32, 5951–5973.
- Pfanzagl, J. (1982). *Contributions to a general asymptotic statistical theory*. Springer.
- Polley, E., E. LeDell, C. Kennedy, and M. van der Laan (2019). *SuperLearner: Super Learner Prediction*. R package version 2.0-26.
- Raghunathan, T., J. Lepkowski, J. Van Hoewyk, and P. Solenberger (2001). A multivariate technique for multiply imputing missing values using a sequence of regression models. *Survey Methodology* 27(1), 85–96.
- Robins, J. and N. Wang (2000). Inference for imputation estimators. *Biometrika* 87(1), 113–124.
- Rubin, D. (1987). *Multiple Imputation for Nonresponse in Surveys*. John Wiley & Sons.
- Rubin, D. (1996). Multiple imputation after 18+ years. *Journal of the American Statistical Association* 91(434), 473–489.
- Saeys, Y., T. Abeel, and Y. Van de Peer (2008). Robust feature selection using ensemble feature selection techniques. In *Joint European Conference on Machine Learning and Knowledge Discovery in Databases*, pp. 313–325.
- Shah, R. and R. Samworth (2013). Variable selection with error control: another look at stability selection. *Journal of the Royal Statistical Society: Series B (Statistical Methodology)* 75(1), 55–80.

- Shin, S., Y. Liu, S. Cole, and J. Fine (2020). Ensemble estimation and variable selection with semi-parametric regression models. *Biometrika* 107(2), 433–448.
- Singhi, A., K. McGrath, R. Brand, A. Khalid, H. Zeh, J. Chennat, K. Fasanella, G. Papachristou, A. Slivka, D. Bartlett, A. Dasyam, M. Hogg, K. Lee, J. Marsh, S. Monaco, N. Ohori, J. Pingpank, A. Tsung, A. Zureikat, A. Wald, and M. Nikiforova (2018). Preoperative next-generation sequencing of pancreatic cyst fluid is highly accurate in cyst classification and detection of advanced neoplasia. *Gut* 67(12), 2131–2141.
- Sun, B. and E. Tchetgen Tchetgen (2018). On inverse probability weighting for nonmonotone missing at random data. *Journal of the American Statistical Association* 113(521), 369–379.
- Tibshirani, R. (1996). Regression shrinkage and selection via the lasso. *Journal of the Royal Statistical Society: Series B (Statistical Methodology)*, 267–288.
- Tsiatis, A. (2007). *Semiparametric theory and missing data*. Springer Science & Business Media.
- Tun, M., R. Pai, S. Kwok, A. Dong, A. Gupta, B. Visser, J. Norton, G. Poultsides, S. Banerjee, J. Van Dam, A. Chen, S. Friedland, B. Scott, R. Verma, A. Lowe, and W. Park (2012). Diagnostic accuracy of cyst fluid amphiregulin in pancreatic cysts. *BMC Gastroenterology* 12(1), 1–6.
- van Buuren, S. (2007). Multiple imputation of discrete and continuous data by fully conditional specification. *Statistical Methods in Medical Research* 16(3), 219–242.
- van Buuren, S. and K. Groothuis-Oudshoorn (2010). mice: multivariate imputation by chained equations in R. *Journal of Statistical Software*, 1–68.
- van der Laan, M., E. Polley, and A. Hubbard (2007). Super learner. *Statistical Applications in Genetics and Molecular Biology* 6(1), Online Article 25.
- van der Vaart, A. (2000). *Asymptotic Statistics*, Volume 3. Cambridge University Press.
- Williamson, B. and J. Feng (2020). Efficient nonparametric statistical inference on population feature importance using Shapley values. In *Proceedings of the 37th International Conference on Machine Learning*, Volume 119 of *Proceedings of Machine Learning Research*, pp. 10282–10291.

- Williamson, B., P. Gilbert, N. Simon, and M. Carone (2021). A general framework for inference on algorithm-agnostic variable importance. *Journal of the American Statistical Association (Theory & Methods)*.
- Wolpert, D. (1992). Stacked generalization. *Neural Networks* 5(2), 241–259.
- Wood, A., I. White, and P. Royston (2008). How should variable selection be performed with multiply imputed data? *Statistics in Medicine* 27(17), 3227–3246.
- Wright, M. N. and A. Ziegler (2017). ranger: A fast implementation of random forests for high dimensional data in C++ and R. *Journal of Statistical Software* 77(1), 1–17.
- Xin, L. and M. Zhu (2012). Stochastic stepwise ensembles for variable selection. *Journal of Computational and Graphical Statistics* 21(2), 275–294.
- Zhao, Y. and Q. Long (2017). Variable selection in the presence of missing data: Imputation-based methods. *Wiley Interdisciplinary Reviews: Computational Statistics* 9(5), e1402.
- Zikos, T., K. Pham, R. Bowen, A. Chen, S. Banerjee, S. Friedland, M. Dua, J. Norton, G. Poultsides, B. Visser, and W. Park (2015). Cyst fluid glucose is rapidly feasible and accurate in diagnosing mucinous pancreatic cysts. *American Journal of Gastroenterology* 110(6), 909–914.

SUPPLEMENTARY MATERIAL

7 Proofs of theorems

7.1 Proof of Theorem 1

Before proving the theorem, we first state and prove a lemma that will be useful.

Lemma S3. *For any $\alpha \in (0, 1)$, $k \in \{0, \dots, p - R_n(\alpha)\}$ and $q \in (0, 1)$, if conditions (A1)–(A6) hold for each $s \subseteq \{1, \dots, p\}$ and (A7) holds, then the procedure $S_n(\alpha)$ satisfies the following: (a) when based on Holm-adjusted p -values, $FWER \leq \alpha$ both in finite samples and asymptotically; and (b) when based on a step-down $\max T$ or $\min P$ procedure, $FWER \leq \alpha$ asymptotically.*

Proof. Under the collection of conditions (A1)–(A7), $\sqrt{n}(\psi_{c,n} - \psi_0) \rightarrow_d Z \sim N(0, \Sigma_0)$ by Theorem 1 in [Williamson and Feng \(2020\)](#), where $\Sigma_0 = E_0\{\phi_0(O)\phi_0(O)^\top\}$ and ϕ_0 is the vector of efficient influence function values provided in [Williamson and Feng \(2020\)](#) for each j . Therefore, the centered and scaled test statistics T_n follow a multivariate Gaussian distribution.

Thus, by Proposition 3.8 in [Dudoit and van der Laan \(2008\)](#), when $S_n(\alpha)$ is based on Holm-adjusted p -values the procedure has finite-sample and asymptotic control of the FWER. When $S_n(\alpha)$ is based on a step-down $\max T$ or $\min P$ procedure, the procedure has asymptotic control of the FWER as a result of Theorems 5.2 and 5.7 in [Dudoit and van der Laan \(2008\)](#), respectively. \square

Under conditions (A1)–(A7) and (B1)–(B2), an application of Lemma S3 and Theorem 6.3 in [Dudoit and van der Laan \(2008\)](#) to the procedure $S_n^+(k, \alpha)$ yields that

$$Pr_{P_0}(V_n^+(k, \alpha) > k) = \alpha_n \text{ and } Pr_{P_0}(V_n^+(k, \alpha)/R_n^+(k, \alpha) > q) = \alpha_n \text{ for all } n,$$

i.e., the $gFWER(k)$ and $PFP(q)$ are controlled in finite samples at level α_n .

If additionally conditions (B3)–(B4) hold, then an application of Lemma S3 and Theorem

6.5 in [Dudoit and van der Laan \(2008\)](#) to the procedure $S_n^+(k, \alpha)$ yields that

$$\limsup_{n \rightarrow \infty} Pr_{P_0}(V_n^+(k, \alpha) > k) \leq \alpha \text{ and } \limsup_{n \rightarrow \infty} Pr_{P_0}(V_n^+(k, \alpha)/R_n^+(k, \alpha) > q) \leq \alpha,$$

i.e., the gFWER(k) and PFP(q) are controlled asymptotically at level α .

Finally, under the above conditions, an application of Lemma [S3](#) and Theorem 6.6 in [Dudoit and van der Laan \(2008\)](#) to the procedure $S_n^+(k, \alpha)$ yields that the FDR is controlled asymptotically.

7.2 Proof of Lemma [1](#)

Without loss of generality, suppose that we use Holm-adjusted p-values to construct the initial set of selected variables and that the augmented set is chosen so as to control the gFWER(k). For a fixed sample size n and constant k_n , this results in selected set $S_n := S_n^+(k_n, \alpha)$, where $|S_n| = k_n$. The claim of persistence is equivalent to showing that

$$V(f_{n, S_n}, P_0) - V(f_*, P_0) \rightarrow_P 0.$$

We can decompose the left-hand side of the above expression into two terms:

$$V(f_{n, S_n}, P_0) - V(f_*, P_0) = \{V(f_{n, S_n}, P_0) - V(f_{0, S_n}, P_0)\} - \{V(f_{0, S_n}, P_0) - V(f_*, P_0)\}. \quad (\text{S9})$$

The first term in [\(S9\)](#) is the contribution to the limiting behavior of $V(f_{n, S_n}, P_0) - V(f_*, P_0)$ from estimating f_0 for a fixed S_n ; by condition [\(A1\)](#),

$$|V(f_{n, S_n}, P_0) - V(f_{0, S_n}, P_0)| \leq C \|f_{n, S_n} - f_{0, S_n}\|_{\mathcal{F}_{S_n}}^2 \rightarrow_P 0.$$

The second term in [\(S9\)](#) is the contribution to the limiting behavior of $V(f_{n, S_n}, P_0) - V(f_*, P_0)$ from selecting S_n compared to the population-optimal set. To study this term, recall that for a fixed p , we have under conditions [\(A1\)](#), [\(A2\)](#), [\(A5\)](#), [\(A6\)](#), and [\(A7\)](#) that $\psi_{c, n, j} \rightarrow_P \psi_{0, j}$

for each $j \in \{1, \dots, p\}$. Thus, for each $j \in S_0$, the p-value $p_{n,j}$ associated with testing the null hypothesis $H_{0,j} : \psi_{0,j} = 0$ converges to 0. This implies that as $n \rightarrow \infty$, $S_n(\alpha) \rightarrow_P S_0$. Moreover, by condition (B3), $S_0 \subseteq S_n^+(k_n, \alpha)$ as $n \rightarrow \infty$. By definition, $\psi_{0,j} > 0$ if and only if $V(f_{0,s \cup \{j\}}, P_0) - V(f_{0,s}, P_0) > 0$ for some $s \subseteq \{1, \dots, p\}$. This implies that for $j \in S_0^c$, $V(f_{0,s \cup \{j\}}, P_0) - V(f_{0,s}, P_0) = 0$ for all $s \subseteq \{1, \dots, p\}$. In particular, for $j \in S_0^c$,

$$V(f_{0,S_0 \cup \{j\}}, P_0) - V(f_{0,S_0}, P_0) = 0.$$

This implies that $S_n^+(k_n, \alpha) \rightarrow_P S_0$, which further implies that $\{V(f_{0,S_n}, P_0) - V(f_*, P_0)\} \rightarrow_P 0$, proving the claim with

$$V(f_{n,S_n}, P_0) - V(f_*, P_0) = o_P(n^{-1/2}).$$

7.3 Proof of Lemma 2

The result follows under conditions (A1)–(A8) and an application of results in Chapter 4 of [Rubin \(1987\)](#). Using this result, we can write that

$$\sqrt{n}(\psi_{M,c,n} - \psi_0) \rightarrow_d W \sim N(0, \sigma^2),$$

where a consistent estimator of σ^2 is given by $\sigma_{M,n}^2 + \frac{m+1}{m}\tau_{M,n}^2$. This variance estimator, in turn, can be used in the p-value computations of [Algorithm 3](#); this will provide error control under the conditions of [Theorem 1](#).

8 Additional numerical experiments

8.1 Replicating all numerical experiments

All numerical experiments presented here and in the main manuscript can be replicated using code available on GitHub.

| Scenario | Outcome regression | Feature distribution | Importance | p |
|----------|--------------------|-----------------------|------------|-----------|
| 1 | Linear | Independent normal | Mix | {30, 500} |
| 2 | Nonlinear | Correlated normal | Weak | 6 |
| 3 | Linear | Independent nonnormal | Mix | {30, 500} |
| 4 | Nonlinear | Independent normal | Mix | {30, 500} |
| 5 | Nonlinear | Independent nonnormal | Mix | {30, 500} |
| 6 | Linear | Independent normal | Weak | 6 |
| 7 | Linear | Correlated normal | Weak | 6 |
| 8 | Nonlinear | Independent normal | Weak | 6 |

Table S1: Summary of the eight data-generating scenarios considered in the numerical experiments.

In all cases, our simulated dataset consisted of independent replicates of (X, Y) , where $X = (X_1, \dots, X_p)$ and Y followed a Bernoulli distribution with success probability $\Phi\{\beta_{00} + f(\beta_0, x)\}$ conditional on $X = x$, where Φ denotes the cumulative distribution function of the standard normal distribution. Under this specification, Y followed a probit model. A summary of the eight scenarios is provided in Table S1.

In Scenarios 3–5, we investigate the effect of departures from a multivariate normal feature distribution and a linear outcome regression model under a similar setup to Scenario 1. We set $\beta_{00} = 0.5$ and $\beta_0 = (-1, 1, -0.5, 0.5, 1/3, -1/3, \mathbf{0}_{p-6})^\top$, where $\mathbf{0}_k$ denotes a zero-vector of dimension k . We vary $p \in \{30, 500\}$. In Scenario 3, we set $f(\beta_0, x) = x\beta_0$, but in contrast to Scenario 1, X follows a nonnormal feature distribution specified by

$$\begin{aligned}
X_1 &\sim N(0.5, 1); \quad X_2 \sim \text{Binomial}(0.5); \quad X_3 \sim \text{Weibull}(1.75, 1.9); \quad X_4 \sim \text{Lognormal}(0.5, 0.5); \\
X_5 &\sim \text{Binomial}(0.5); \quad X_6 \sim N(0.25, 1); \quad (X_7, \dots, X_p) \sim \text{MVN}(0, I_{p-6}).
\end{aligned}
\tag{S10}$$

In Scenarios 4 and 5, the outcome regression follows the same nonlinear specification as in

Scenario 2. Specifically, using a centering and scaling function c_j for each variable,

$$\begin{aligned}
f(\beta_0, x) &= 2[\beta_{0,1}f_1\{c_1(x_1)\} + \beta_{0,2}f_2\{c_2(x_2), c_3(x_3)\} + \beta_{0,3}f_3\{c_3(x_3)\} \\
&\quad + \beta_{0,4}f_4\{c_4(x_4)\} + \beta_{0,5}f_2\{c_5(x_5), c_1(x_1)\} + \beta_{0,6}f_5\{c_6(x_6)\}], \quad (\text{S11}) \\
f_1(x) &= \sin\left(\frac{\pi}{4}x\right), f_2(x, y) = xy, f_3(x) = \tanh(x), \\
f_4(x) &= \cos\left(\frac{\pi}{4}x\right), f_5(x) = -\tanh(x),
\end{aligned}$$

where \tanh denotes the hyperbolic tangent. In Scenario 4, $X \sim MVN(0, I_p)$, while in Scenario 5, X follows the distribution specified in Equation (S10). In these scenarios, only the first six features truly influence the outcome; some of the features are strongly important, while others are more weakly important.

In the final scenarios, we investigate the effect of correlated features and departures from a linear outcome regression model in a setting where the features are equally, and weakly, important; these settings are similar to Scenario 2. In these cases, we set $p = 6$, $\beta_{00} = 0.5$, $\beta_0 = (0, 1, 0, 0, 0, 1)^\top$, and $X \sim MVN(0, \Sigma)$, where $\Sigma_{i,j} = \rho_1^{|i-j|}$ for i, j not in the active set, and $\Sigma_{i,j} = I_p + \rho_2(J_p - I_p)$ for i, j in the active set, where J_p is a $p \times p$ matrix of ones. In Scenarios 6 and 7 we set $f(\beta_0, x) = x\beta_0$, while in Scenario 8 f is specified as in Equation (S11). In Scenarios 6 and 8 we set $\rho_1 = \rho_2 = 0$, while in Scenario 7 we set $\rho_1 = 0.3$ and $\rho_2 = 0.95$.

8.2 Tuning parameters for variable selection

The tuning parameters that specify each variable selection procedure are as follows. For the extrinsic selection algorithm, we set $\kappa \in \{4, 10, 36\}$ for $p \in \{6, 30, 500\}$, respectively. For the intrinsic selection algorithm, we determined k and q for error control using a target specificity at $n = 3000$ of 75% for $p = 6$, 85% for $p = 30$, and 95% for $p = 500$. For target specificity denoted by s_p and $s_0 = \sum_{j=1}^p I(\beta_{0j} > 0)$, we set $k = \lceil (1 - s_p)(p - s_0) \rceil$, where $\lceil \cdot \rceil$ denotes the ceiling; and set $q = k\{p^{-1}(p - s_0)(n/200)^{1/2} + k\}^{-1}$. The exact values of k (for $gFWER(k)$ control) and q (for $PFP(q)$ control) are provided in Table S2. For stability selection (both using the

| n | p | SS_q | Target specificity | k | q |
|------|-----|--------|--------------------|-----|-------|
| 200 | 30 | 23 | 0.762 | 6 | 0.882 |
| 500 | 30 | 23 | 0.774 | 6 | 0.826 |
| 1500 | 30 | 23 | 0.809 | 5 | 0.695 |
| 3000 | 30 | 23 | 0.854 | 4 | 0.564 |
| 200 | 500 | 91 | 0.812 | 94 | 0.990 |
| 500 | 500 | 91 | 0.824 | 88 | 0.983 |
| 1500 | 500 | 91 | 0.861 | 69 | 0.962 |
| 3000 | 500 | 91 | 0.904 | 48 | 0.926 |

Table S2: Values of: the number of variables selected in each bootstrap run of stability selection (SS_q), target specificity for $gFWER(k)$ and $PFP(q)$ control, and k and q used for $gFWER$ and PFP control, respectively, in the numerical experiments.

lasso and extrinsic selection), we specified stability selection threshold equal to 0.9 and target per-comparison type I error rate of 0.04. For the lasso with knockoffs, we set target FDR equal to 0.2. The methods compared are: lasso; lasso + SS, lasso with stability selection; lasso + KF, lasso with knockoffs; SL (benchmark), the Super Learner with no variable selection; SL, extrinsic variable selection; SL + SS, extrinsic variable selection with stability selection; SPVIM + gFWER, intrinsic selection to control the generalized familywise error rate; SPVIM + PFP, intrinsic selection to control the proportion of false positives among the rejected variables; and SPVIM + FDR, intrinsic selection to control the false discovery rate.

8.3 Super Learner specification

The specific candidate learners and their corresponding tuning parameters for our Super Learner library are provided in Tables S3 (Scenarios 1, 3–5) and S4 (Scenarios 2, 6–8). For the internal library in our intrinsic selection procedure in Scenarios 1 and 3–5, we first pre-screened variables based on their univariate rank correlation with the outcome, and then fit boosted trees with maximum depth equal to three and shrinkage equal to 0.1. In Scenarios 2 and 6–8, we again first pre-screened variables based on their univariate rank correlation with the outcome, and then fit a logistic regression or boosted trees with maximum depth equal to four, shrinkage equal to 0.1, and number of rounds equal to 100. Recall that within the intrinsic selection procedure, we estimate the optimal prediction function for each subset s of the p features. The univariate rank

| Candidate Learner | R Implementation | Tuning Parameter and possible values | Tuning parameter description |
|-------------------------|---|--|---|
| Random forests | <code>ranger</code> (Wright and Ziegler, 2017) | <code>mtry</code> $\in \{1/2, 1, 2\}\sqrt{p}$ [†] | Number of variables to possibly split at in each node |
| Gradient boosted trees | <code>xgboost</code> (Chen et al., 2019) | <code>max.depth</code> $\in \{1, 3\}$ | Maximum tree depth |
| Support vector machines | <code>ksvm</code> (Karatzoglou et al., 2004) | | |
| Lasso | <code>glmnet</code> (Friedman et al., 2010) | λ chosen via 10-fold CV | ℓ_1 regularization parameter |

Table S3: Candidate learners in the Super Learner ensemble for Scenarios 1 and 3–5 along with their R implementation, tuning parameter values, and description of the tuning parameters. All tuning parameters besides those listed here are set to their default values. In particular, the random forests are grown with 500 trees, a minimum node size of 5 for continuous outcomes and 1 for binary outcomes, and a subsampling fraction of 1; the boosted trees are grown with a maximum of 1000 trees, shrinkage rate of 0.1, and a minimum of 10 observations per node; and the SVMs are fit with radial basis kernel, cost of constraints violation equal to 1, upper bound on training error (`nu`) equal to 0.2, `epsilon` equal to 0.1, and three-fold cross-validation with a sigmoid for calculating class probabilities.

[†]: p denotes the total number of predictors.

correlation screen operated as follows: if $|s| \leq 2$, we did no screening; if $2 < |s| < 100$, we picked the top two variables ranked by univariate correlation with the outcome; and if $|s| \geq 100$, we picked the top ten variables ranked by univariate correlation with the outcome. This screening substantially reduced the computation time for the intrinsic selection procedure, and reflects the type of aggressive screen that is used in some cases (Neidich et al., 2019).

8.4 Additional results from Scenarios 1 and 2

In the main manuscript, we presented results with no missing data and with a maximum of 40% missing data in some variables in Scenarios 1 and 2. In Figure S1 we present results in an intermediate setting with a maximum of 20% missing data in some variables. The results tend to be worse than the results with no missing data, but better than the results with maximum 40% missing data.

In Figures S2–S4, we display the empirical selection probability for each active-set variable

| Candidate Learner | R Implementation | Tuning Parameter and possible values | Tuning parameter description |
|-------------------------|----------------------|--|-----------------------------------|
| Random forests | <code>ranger</code> | <code>min.node.size</code> \in $\{1, 20, 50, 100, 250, 500\}$ | Minimum node size |
| Gradient boosted trees | <code>xgboost</code> | <code>shrinkage</code> \in $\{1 \times 10^{-2}, 1 \times 10^{-1}\}$ <code>ntrees</code> \in $\{100, 1000\}$ | Shrinkage Number of trees |
| Support vector machines | <code>ksvm</code> | | |
| Lasso | <code>glmnet</code> | λ chosen via 10-fold CV | ℓ_1 regularization parameter |

Table S4: Candidate learners in the Super Learner ensemble for Scenarios 2 and 6–8 along with their R implementation, tuning parameter values, and description of the tuning parameters. All tuning parameters besides those listed here are set to their default values. In particular, the random forests are grown with 500 trees and a subsampling fraction of 1; the boosted trees are grown with a minimum of 10 observations per node; and the SVMs are fit with radial basis kernel, cost of constraints violation equal to 1, upper bound on training error (`nu`) equal to 0.2, `epsilon` equal to 0.1, and three-fold cross-validation with a sigmoid for calculating class probabilities.

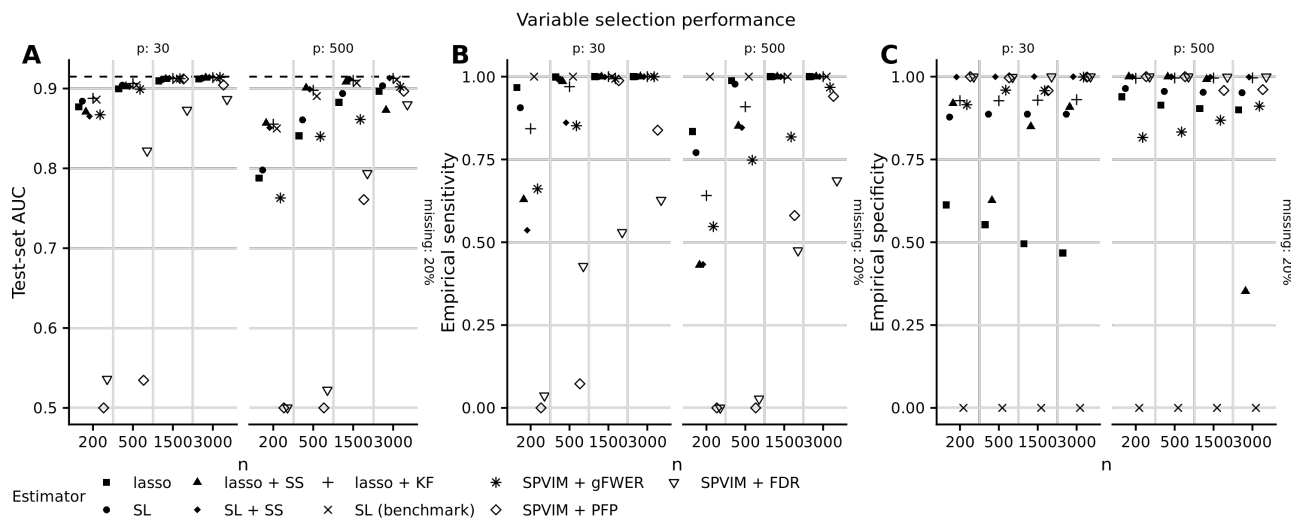


Figure S1: Test-set AUC (panel A) and empirical variable selection sensitivity (panel B) and specificity (panel C) vs n for each estimator and missing data proportion equal to 0.2, in Scenario 1 (a linear model for the outcome and multivariate normal features). The dotted line in panel A shows the true (optimal) test-set AUC.

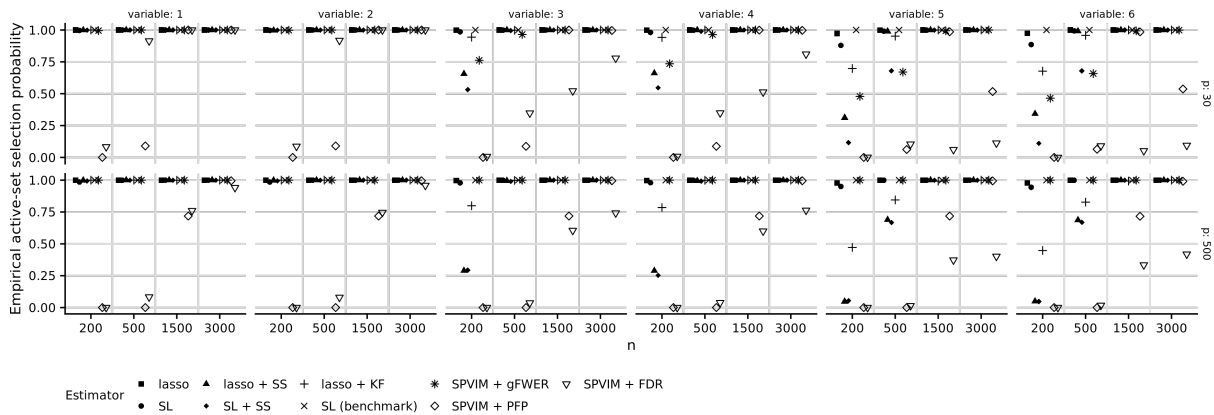


Figure S2: Empirical selection probability for each active-set variable vs n for each estimator and dimension with missing data proportion equal to 0, in Scenario 1 (a linear model for the outcome and multivariate normal features).

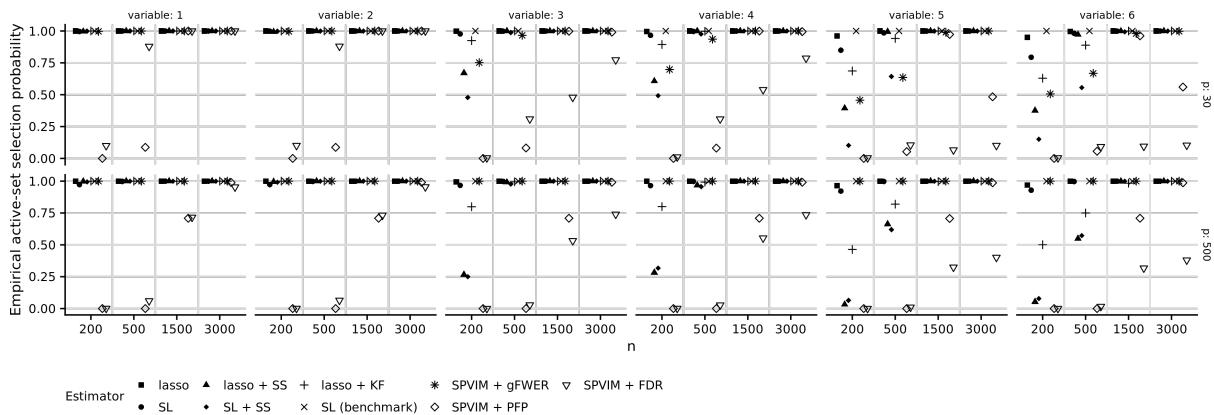


Figure S3: Empirical selection probability for each active-set variable vs n for each estimator and dimension with missing data proportion equal to 0.2, in Scenario 1 (a linear model for the outcome and multivariate normal features).

under each selection algorithm in Scenario 1. All active-set variables are selected with high probability in large samples by the lasso-based procedures, SL and SL + SS, and SPVIM + gFWER. In small samples, lasso + KF and lasso + SS sometimes fail to select variables 3–6; these variables are selected with low probability by SPVIM + PFP and SPVIM + FDR at all sample sizes considered here. This reflects the low true importance of these variables combined with tuning parameters that provide strict PFP and FDR control. As the proportion of missing data increases, the selection probabilities tend to decrease slightly.

In Figures S5–S7, we display the empirical selection probability for each active-set variable under each selection algorithm in Scenario 2. In this scenario, as expected, the selection prob-

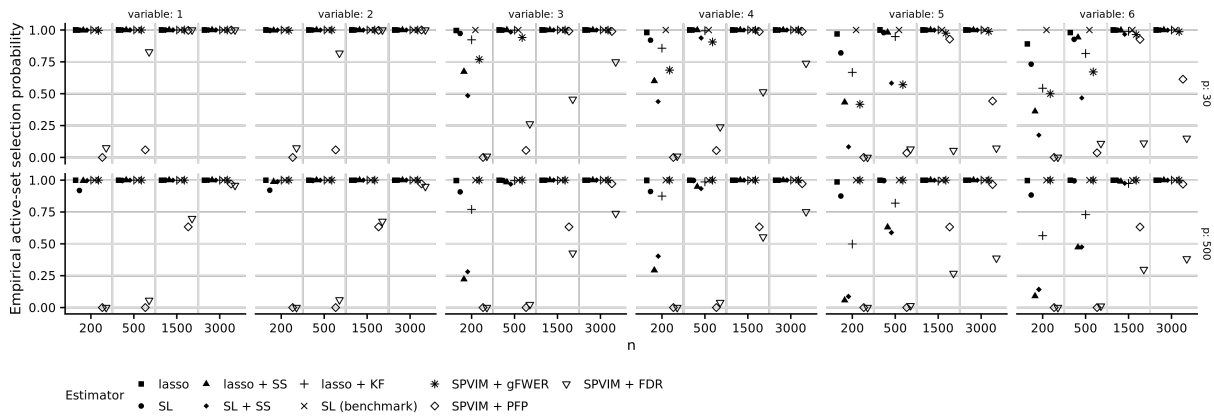


Figure S4: Empirical selection probability for each active-set variable vs n for each estimator and dimension with missing data proportion equal to 0.4, in Scenario 1 (a linear model for the outcome and multivariate normal features).

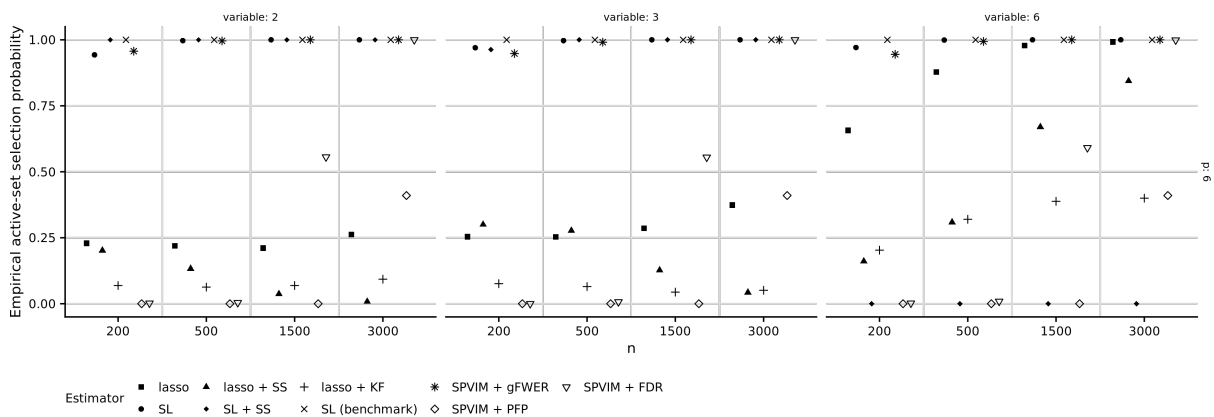


Figure S5: Empirical selection probability for each active-set variable vs n for each estimator, in Scenario 2 (a nonlinear model for the outcome and correlated multivariate normal features).

ability is low for all lasso-based procedures and high for SL, SL + SS, and SPVIM + gFWER (as reflected in the empirical sensitivity presented in the main manuscript). Variables 2 and 3, which are highly correlated and include an interaction term not modelled by the lasso, have the lowest selection probability for lasso-based procedures, as expected. Here, we observe increasing selection probability for the lasso-based estimators as the proportion of missing data increases, particularly for variables 2 and 3. This may be due to the fact that when data are missing for variable 2, the imputation procedure ignores that variables 2 and 3 are correlated, which may reduce the observed correlation.

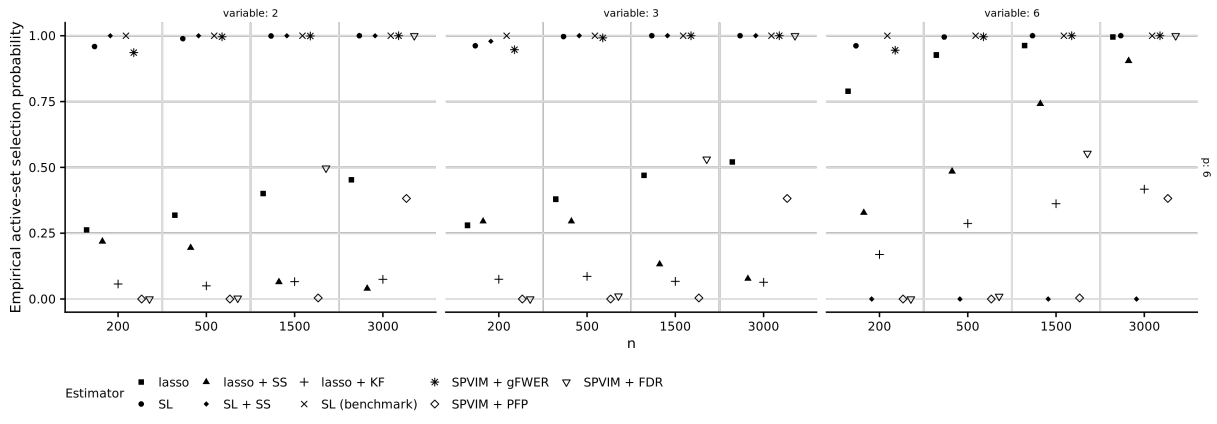


Figure S6: Empirical selection probability for each active-set variable vs n for each estimator, in Scenario 2 (a nonlinear model for the outcome and correlated multivariate normal features).

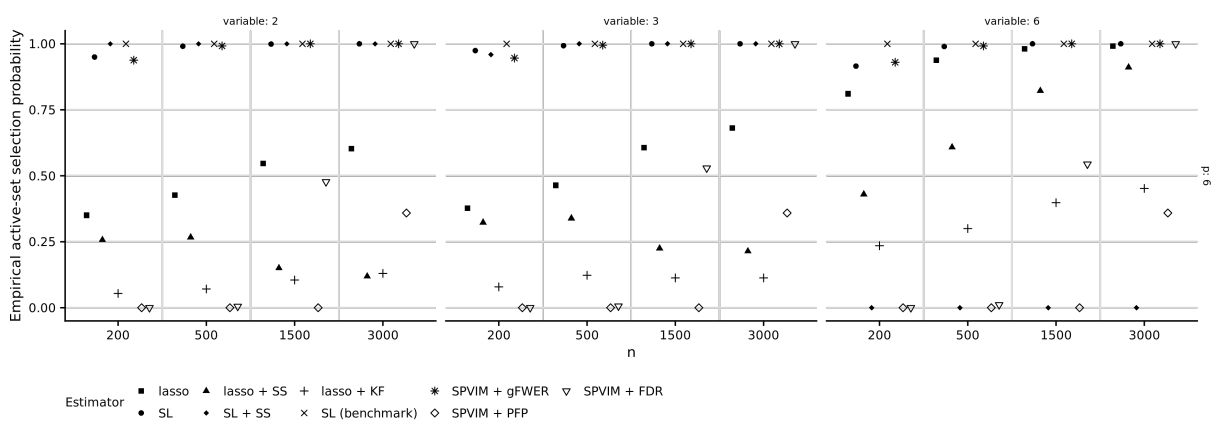


Figure S7: Empirical selection probability for each active-set variable vs n for each estimator, in Scenario 2 (a nonlinear model for the outcome and correlated multivariate normal features).

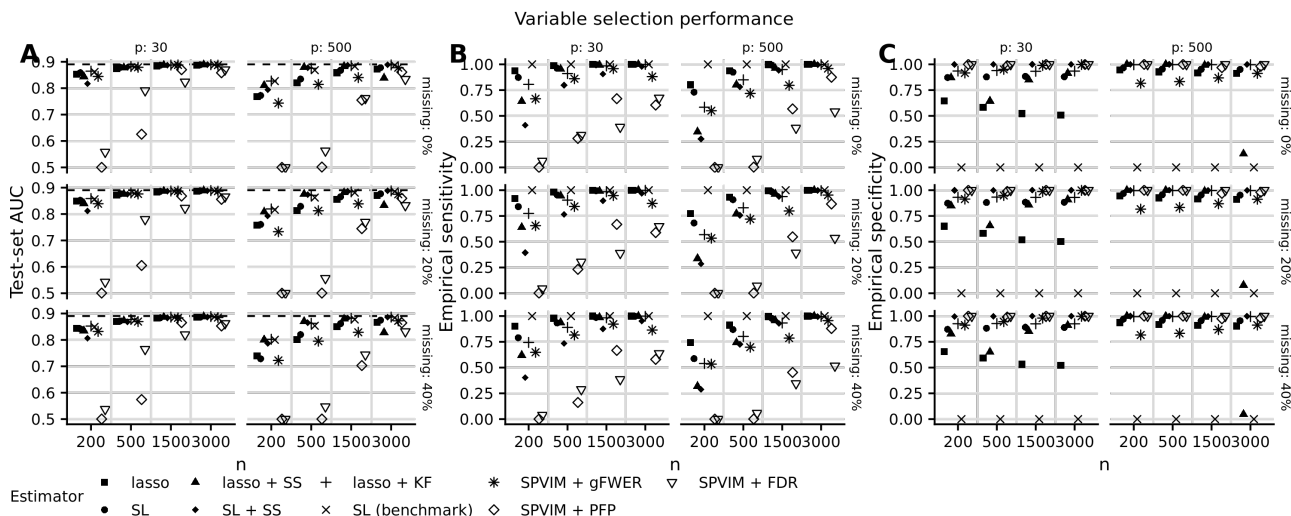


Figure S8: Test-set AUC (panel A) and empirical variable selection sensitivity (panel B) and specificity (panel C) vs n for each estimator and missing data proportion, in Scenario 3 (a linear model for the outcome and nonnormal features). The dotted line in panel A shows the true (optimal) test-set AUC.

8.5 Results from Scenarios 3–8

In Scenario 3, we generate features from a nonnormal joint distribution and the outcome is a linear combination of these features. We display the results of this experiment in Figure S8. We observe similar performance in this scenario to the performance we observed in Scenario 1: test-set AUC increases towards the optimal value with increasing sample size for all estimators; empirical sensitivity and specificity tend to both increase, with the exception of the base lasso and lasso with stability selection (particularly in low dimensions).

In Scenario 4, we generate features from a multivariate normal distribution and the outcome is a nonlinear combination of these features. We display the results of this experiment in Figure S9. We observe that test-set AUC tends to increase quickly towards the optimal AUC with increasing sample size for all Super Learner-based estimators, but increases more slowly for lasso-based estimators; empirical sensitivity and specificity tend to both increase, with the exception of the base lasso and lasso with stability selection (particularly in low dimensions).

In Figure S10, we display the results of the experiment conducted under Scenario 5, in which the features are nonnormal and the outcome-feature relationship is nonlinear. In this case, the lasso-based methods are misspecified. In panel A, we observe that all variants of the

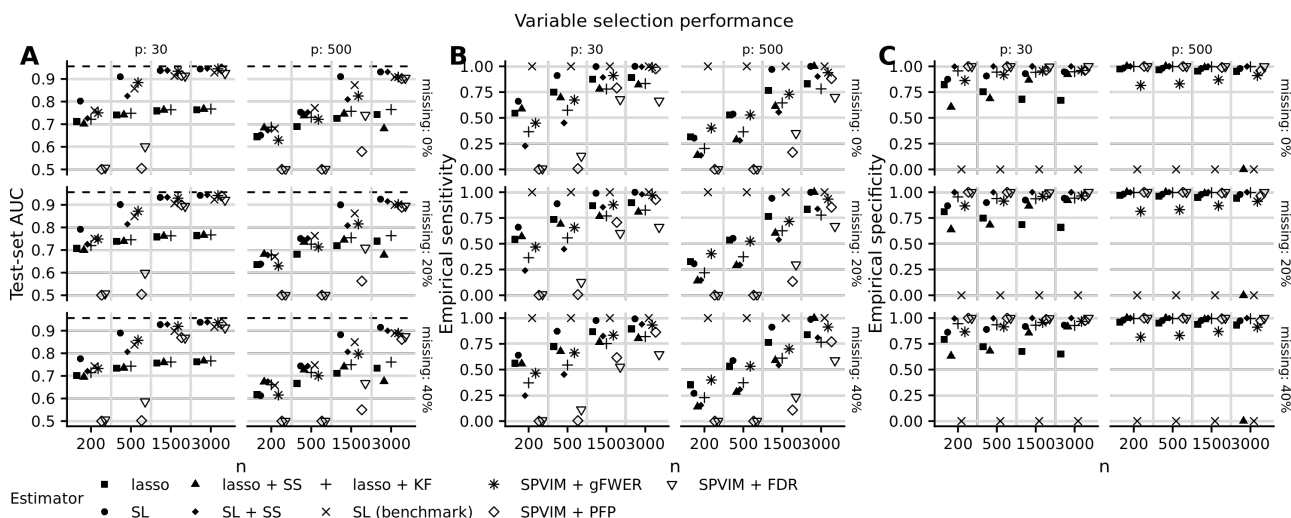


Figure S9: Test-set AUC (panel A) and empirical variable selection sensitivity (panel B) and specificity (panel C) vs n for each estimator and missing data proportion, in Scenario 4 (a nonlinear model for the outcome and normal features). The dotted line in panel A shows the true (optimal) test-set AUC.

lasso have test-set AUC increasing slowly with n , while all other procedures have test-set AUC approaching the optimal value more quickly. In panels B and C, we see that sensitivity tends to be lower than in Scenario 1 for all procedures, though still increasing towards one; and that specificity trends are similar to those in Scenario 1.

In Scenarios 6–8, the features are more weakly important. We present the results of the experiments under these scenarios in Figures S11–S13. In Scenario 7, we observe reduced variable selection performance for the lasso-based procedures compared to Scenario 6. In Scenario 8, we observe similar trends to Scenario 2, though performance for the lasso-based methods tends to be better than the performance we observed in Scenario 2, reflecting that this scenario does not involve correlation among the features. These experiments suggest that correlation makes variable selection more difficult, particularly in combination with a misspecified outcome regression model.

In Figures S14–S31, we display the empirical selection probability for each active-set variable under each selection algorithm in Scenarios 6–8. We observe similar performance in Scenario 3 as in Scenario 1. In Scenarios 3 and 4, we observe that most procedures select variables 1, 2, 3, 5, and 6 with high probability as sample size increases. However, lasso-based procedures

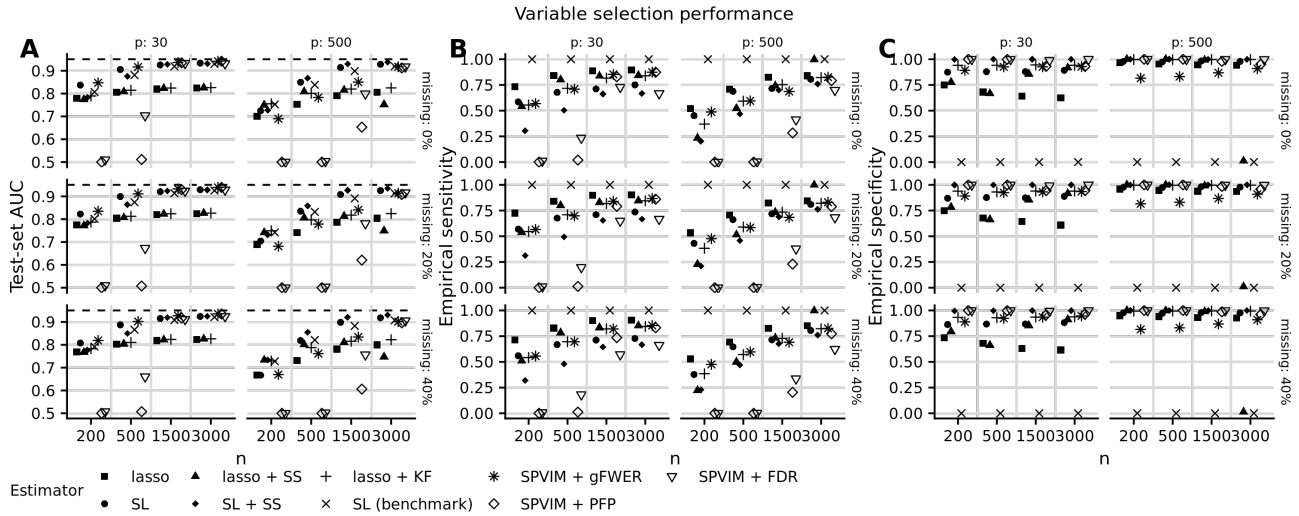


Figure S10: Test-set AUC (panel A) and empirical variable selection sensitivity (panel B) and specificity (panel C) vs n for each estimator and missing data proportion, in Scenario 5 (a nonlinear model for the outcome and nonnormal features). The dotted line in panel A shows the true (optimal) test-set AUC.

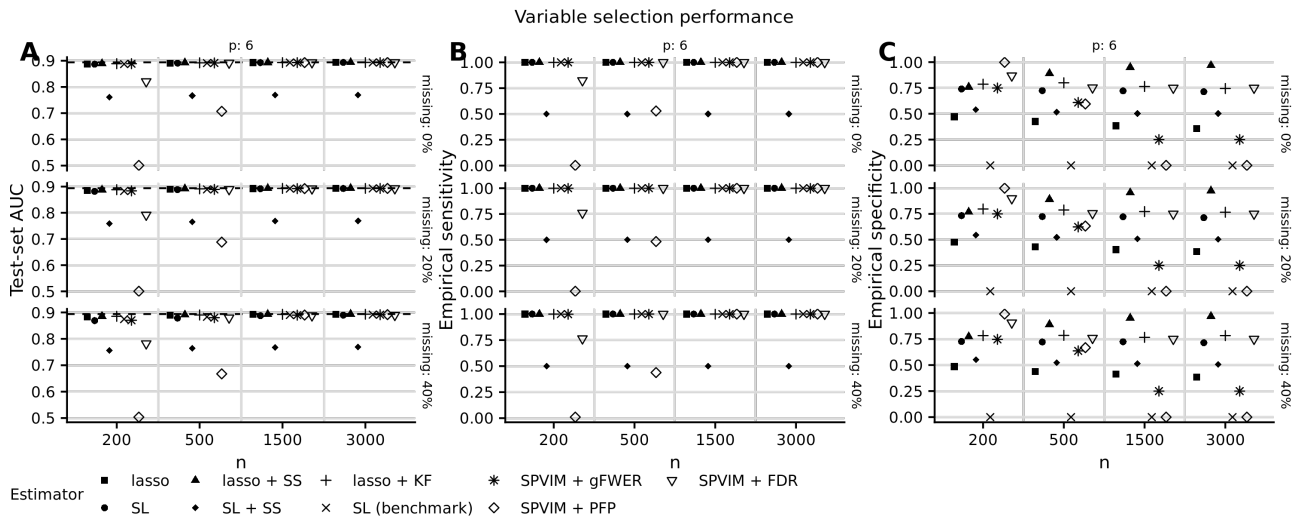


Figure S11: Test-set AUC (panel A) and empirical variable selection sensitivity (panel B) and specificity (panel C) vs n for each estimator and missing data proportion, in Scenario 6 (a weak linear model for the outcome and normal features). The dotted line in panel A shows the true (optimal) test-set AUC.

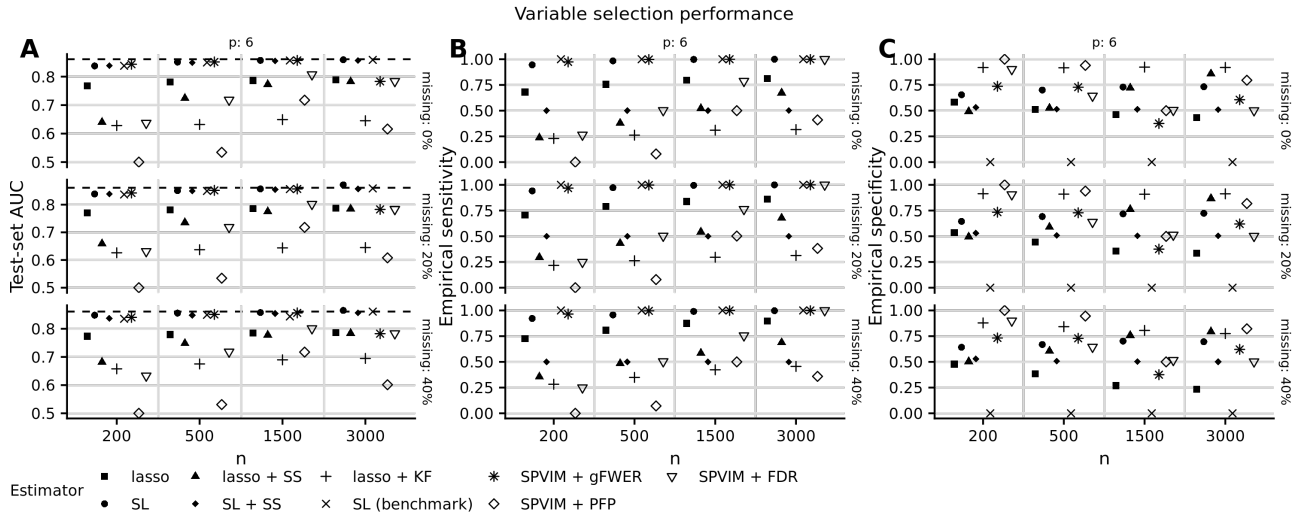


Figure S12: Test-set AUC (panel A) and empirical variable selection sensitivity (panel B) and specificity (panel C) vs n for each estimator and missing data proportion, in Scenario 7 (a weak nonlinear model for the outcome and correlated normal features). The dotted line in panel A shows the true (optimal) test-set AUC.

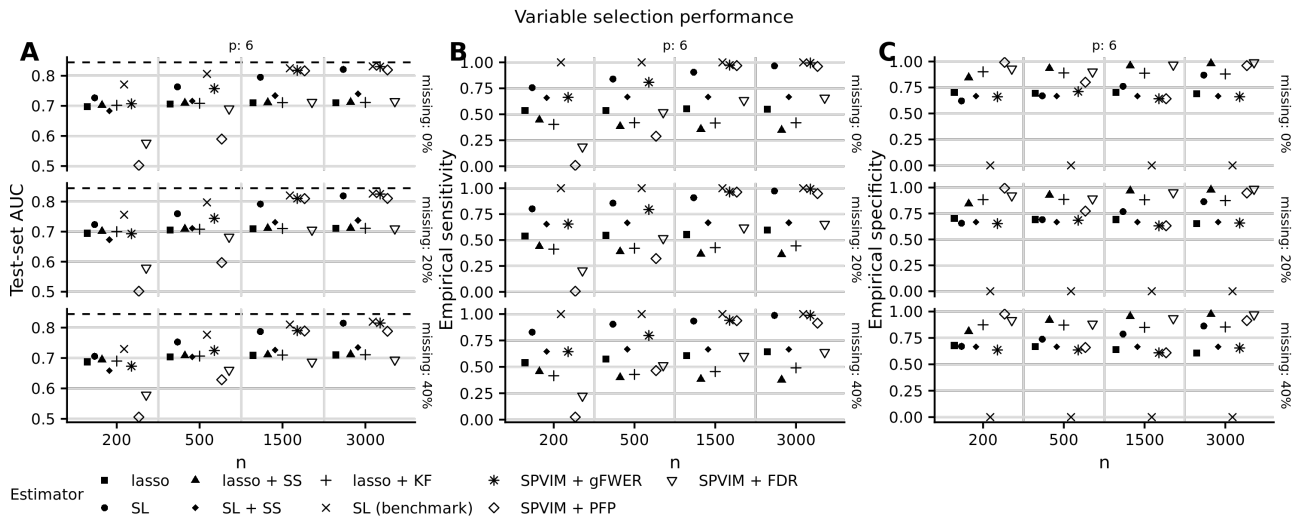


Figure S13: Test-set AUC (panel A) and empirical variable selection sensitivity (panel B) and specificity (panel C) vs n for each estimator and missing data proportion, in Scenario 8 (a weak nonlinear model for the outcome and normal features). The dotted line in panel A shows the true (optimal) test-set AUC.

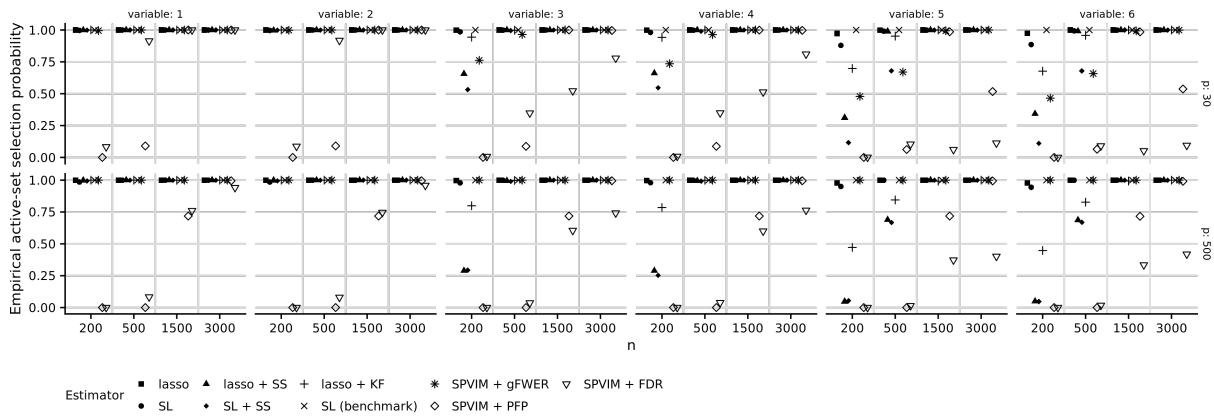


Figure S14: Empirical selection probability for each active-set variable vs n for each estimator and dimension with missing data proportion equal to 0, in Scenario 3 (a linear model for the outcome and nonnormal features).

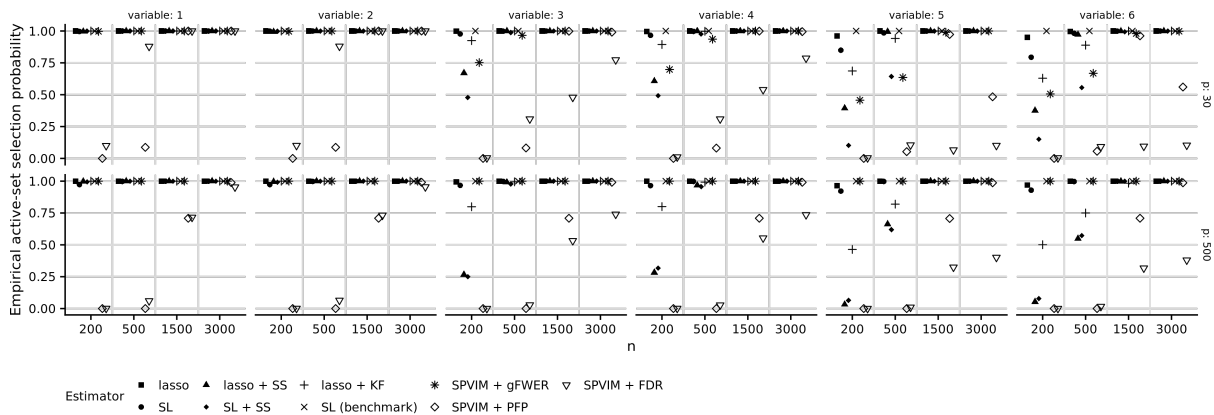


Figure S15: Empirical selection probability for each active-set variable vs n for each estimator and dimension with missing data proportion equal to 0.2, in Scenario 3 (a linear model for the outcome and nonnormal features).

select variable 4 with lower probability than our proposed extrinsic and intrinsic selection procedures. Variable 4 is moderately important (its coefficient is 1, compared to a maximum coefficient of 2), but the function relating this variable to the outcome is highly nonlinear over its support. In Scenario 6, we observe similar patterns to Scenario 5: variables 2 and 3 tend to be selected infrequently by the lasso-based procedures, but with high frequency by the extrinsic and intrinsic selection procedures; and as the missing data proportion increases, the selection proportion for variables 2 and 3 increases somewhat for the lasso-based methods.

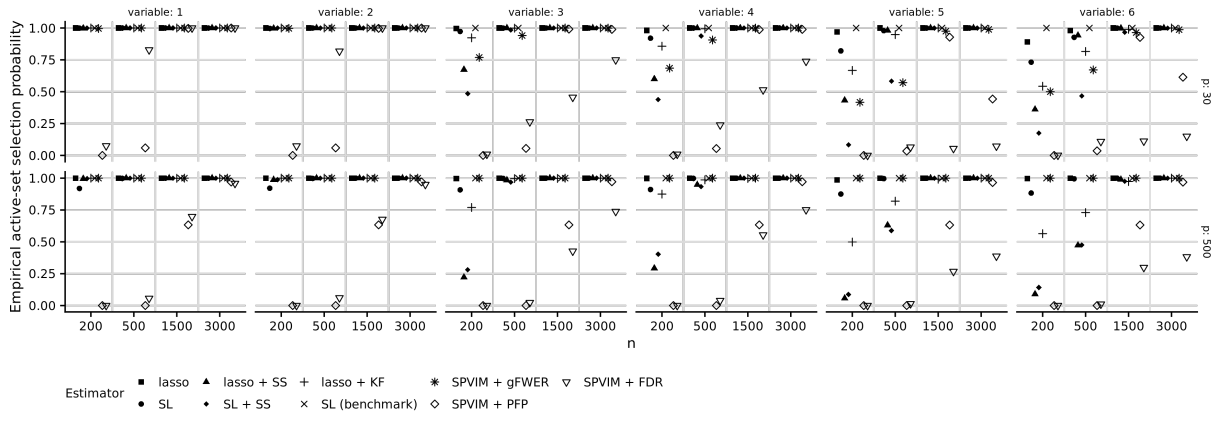


Figure S16: Empirical selection probability for each active-set variable vs n for each estimator and dimension with missing data proportion equal to 0.4, in Scenario 3 (a linear model for the outcome and nonnormal features).

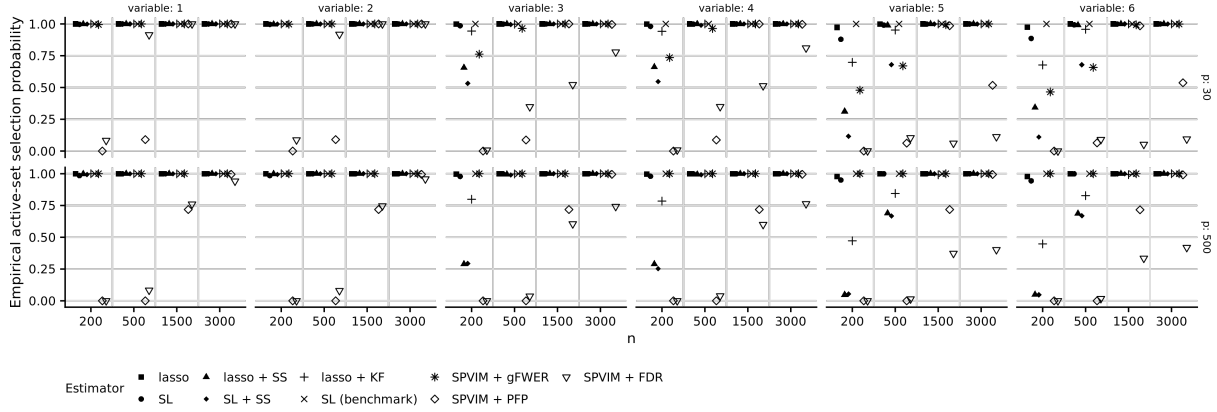


Figure S17: Empirical selection probability for each active-set variable vs n for each estimator and dimension with missing data proportion equal to 0, in Scenario 4 (a nonlinear model for the outcome and multivariate normal features).

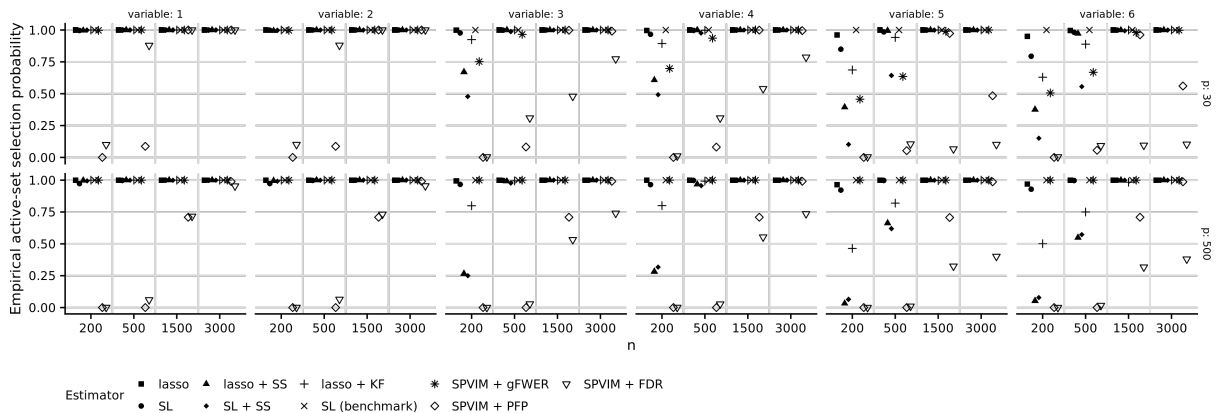


Figure S18: Empirical selection probability for each active-set variable vs n for each estimator and dimension with missing data proportion equal to 0.2, in Scenario 4 (a nonlinear model for the outcome and multivariate normal features).

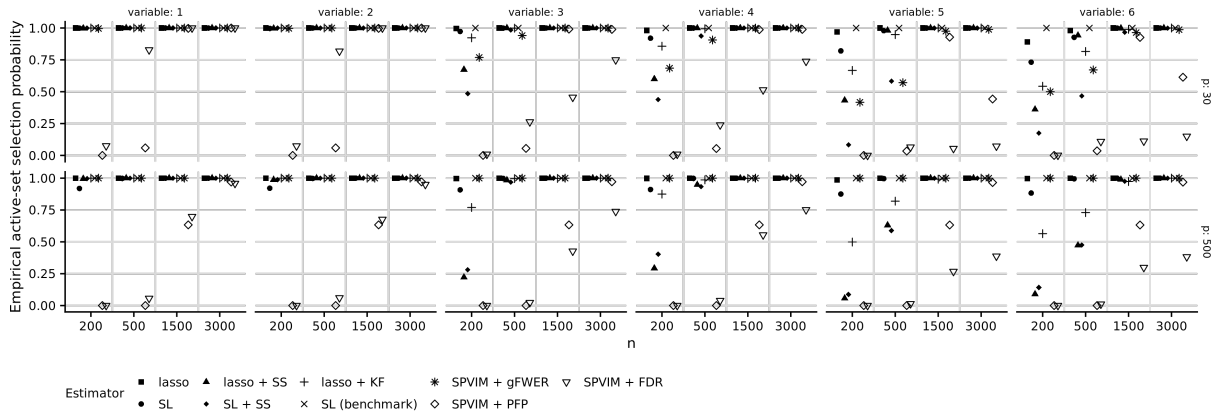


Figure S19: Empirical selection probability for each active-set variable vs n for each estimator and dimension with missing data proportion equal to 0.4, in Scenario 4 (a nonlinear model for the outcome and multivariate normal features).

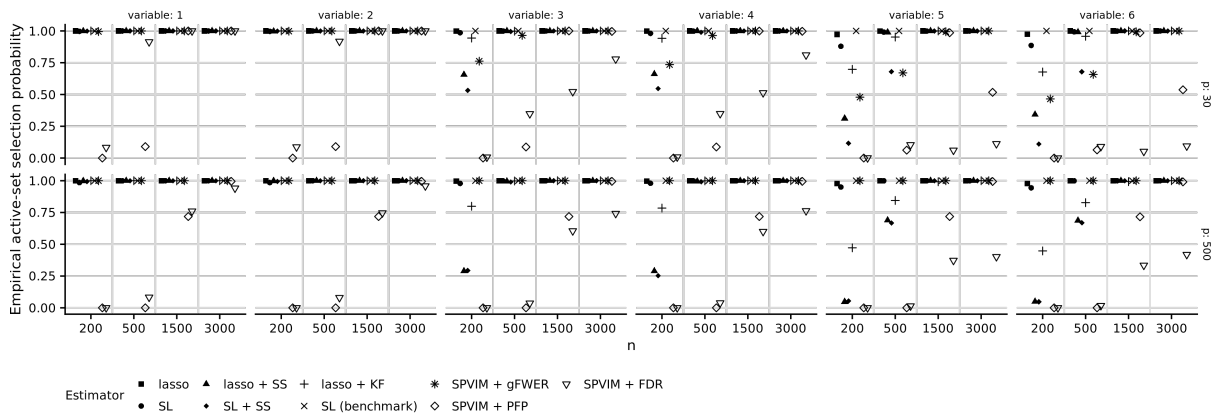


Figure S20: Empirical selection probability for each active-set variable vs n for each estimator and dimension with missing data proportion equal to 0, in Scenario 5 (a nonlinear model for the outcome and nonnormal features).

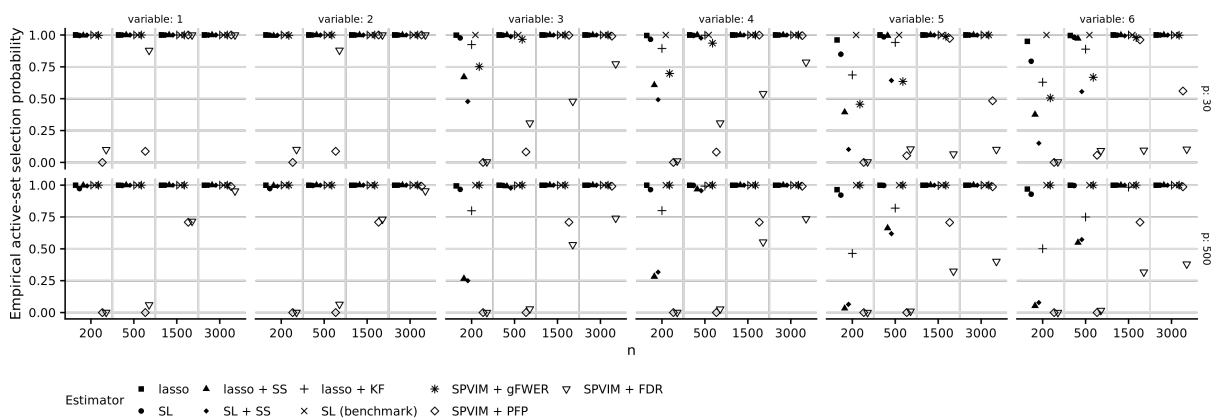


Figure S21: Empirical selection probability for each active-set variable vs n for each estimator and dimension with missing data proportion equal to 0.2, in Scenario 5 (a nonlinear model for the outcome and nonnormal features).

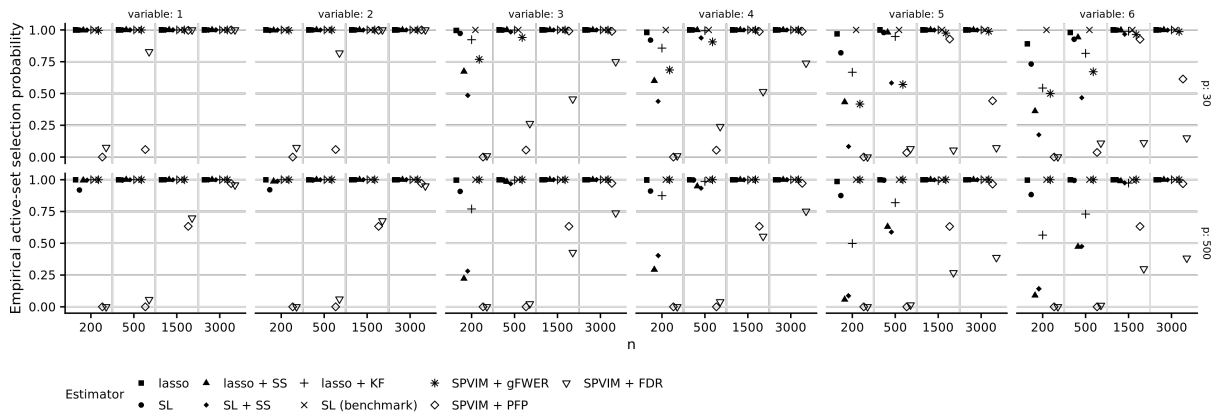


Figure S22: Empirical selection probability for each active-set variable vs n for each estimator and dimension with missing data proportion equal to 0.4, in Scenario 5 (a nonlinear model for the outcome and nonnormal features).

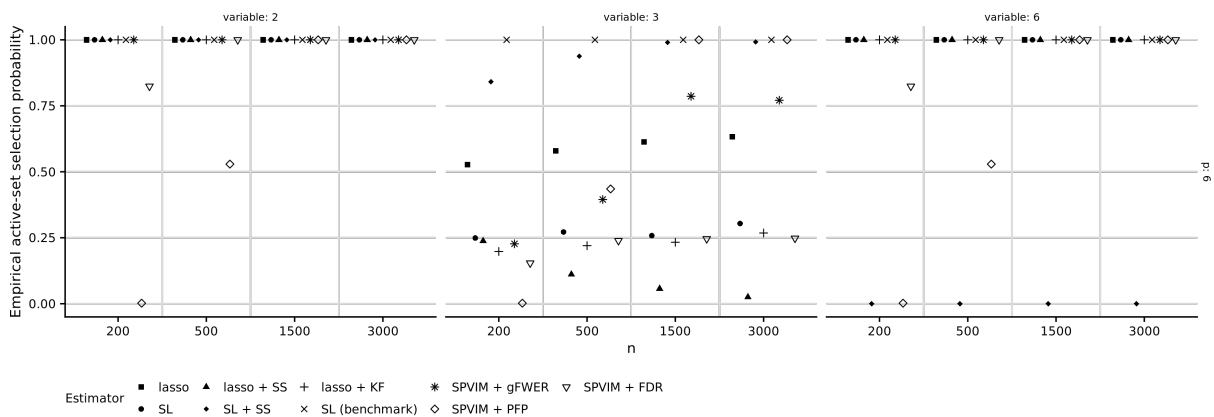


Figure S23: Empirical selection probability for each active-set variable vs n for each estimator, in Scenario 6 (a weak linear model for the outcome and normal features).

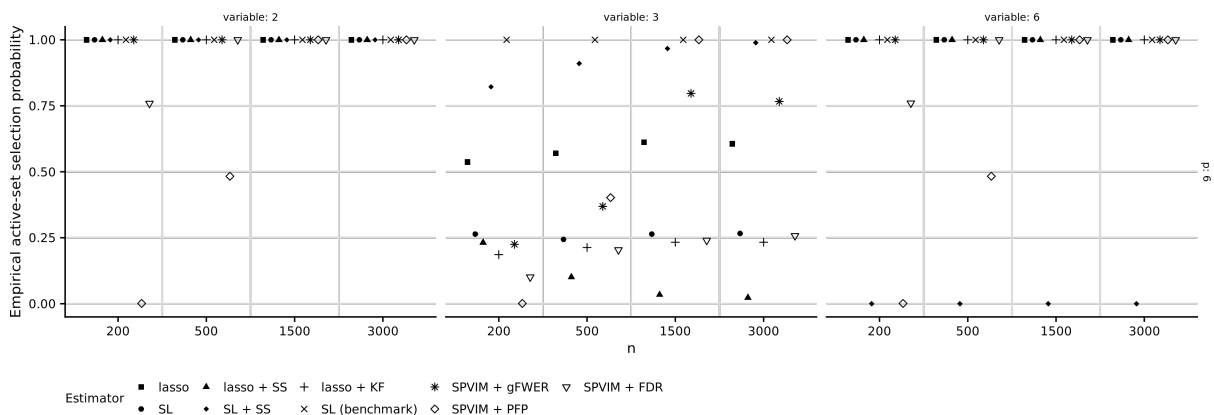


Figure S24: Empirical selection probability for each active-set variable vs n for each estimator, in Scenario 6 (a weak linear model for the outcome and normal features).

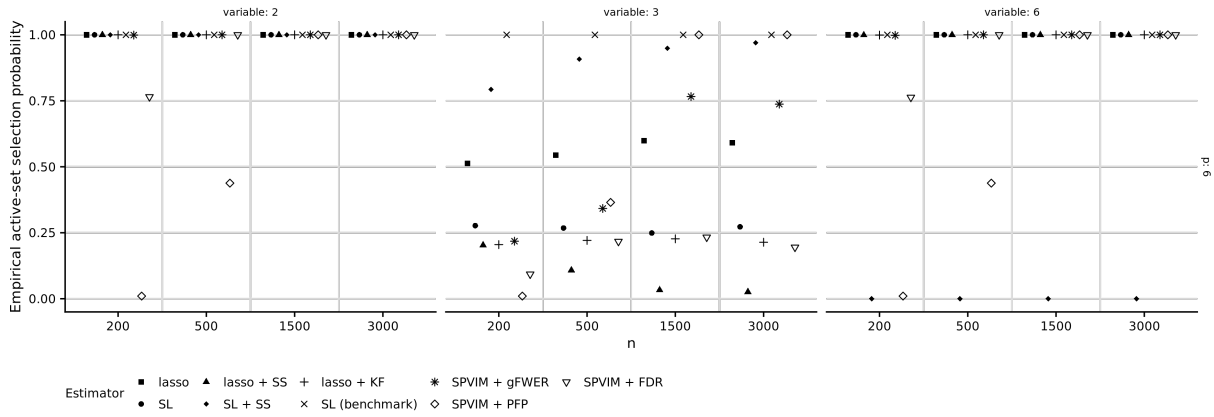


Figure S25: Empirical selection probability for each active-set variable vs n for each estimator, in Scenario 6 (a weak linear model for the outcome and normal features).

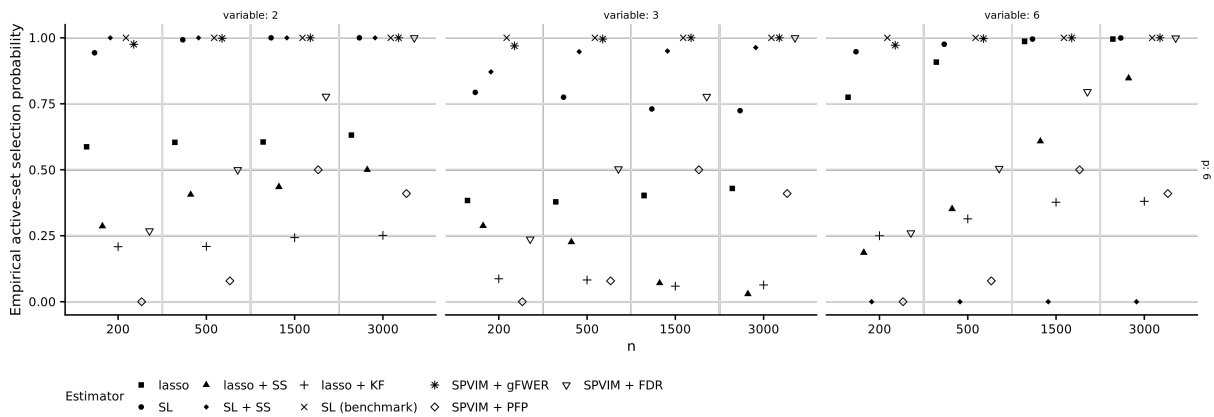


Figure S26: Empirical selection probability for each active-set variable vs n for each estimator, in Scenario 7 (a weak linear model for the outcome and correlated normal features).

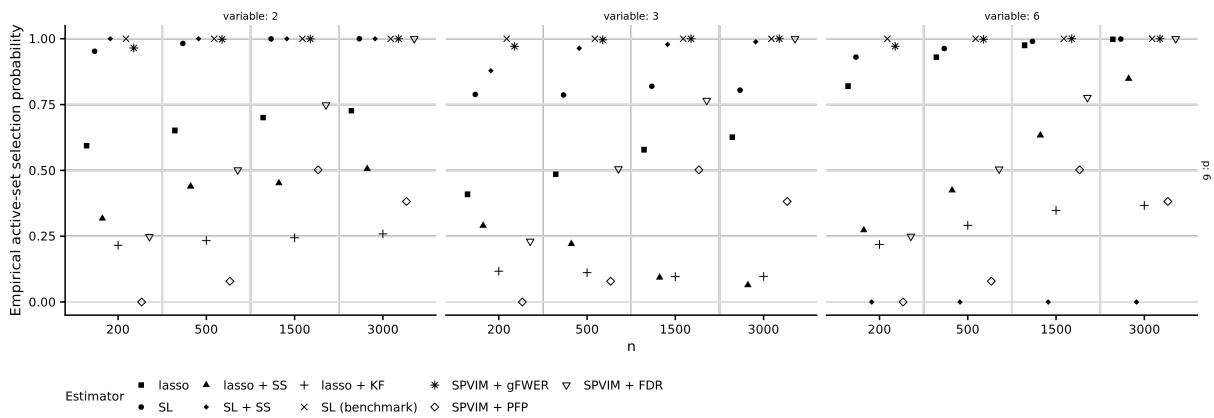


Figure S27: Empirical selection probability for each active-set variable vs n for each estimator, in Scenario 7 (a weak linear model for the outcome and correlated normal features).

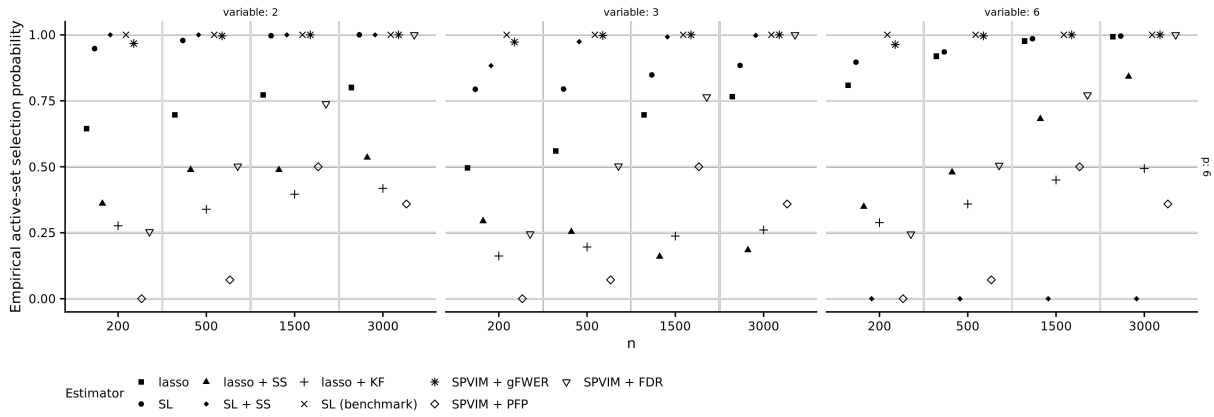


Figure S28: Empirical selection probability for each active-set variable vs n for each estimator, in Scenario 7 (a weak linear model for the outcome and correlated normal features).

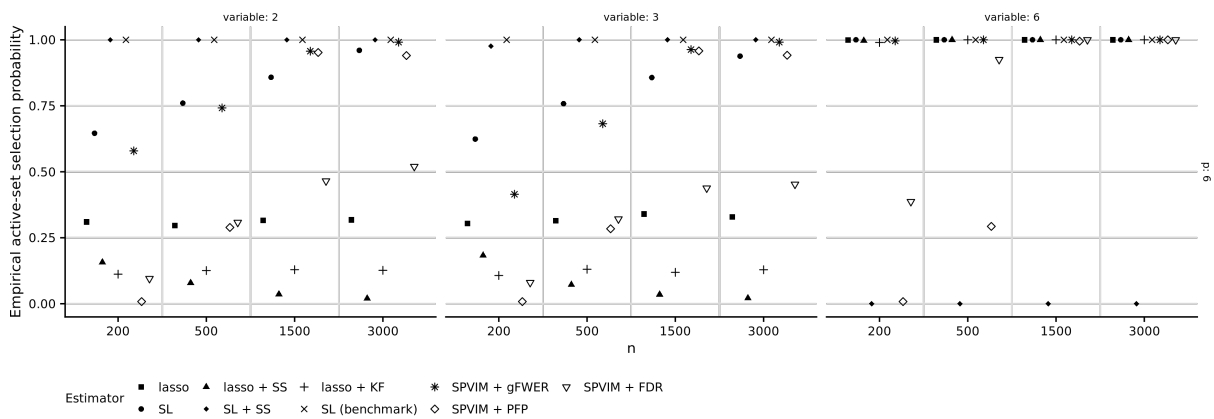


Figure S29: Empirical selection probability for each active-set variable vs n for each estimator, in Scenario 8 (a weak nonlinear model for the outcome and normal features).

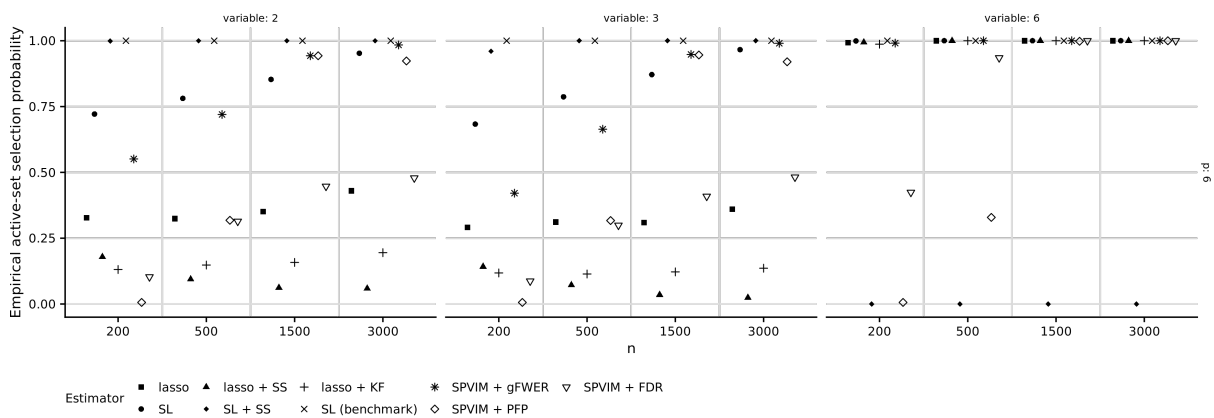


Figure S30: Empirical selection probability for each active-set variable vs n for each estimator, in Scenario 8 (a weak nonlinear model for the outcome and normal features).

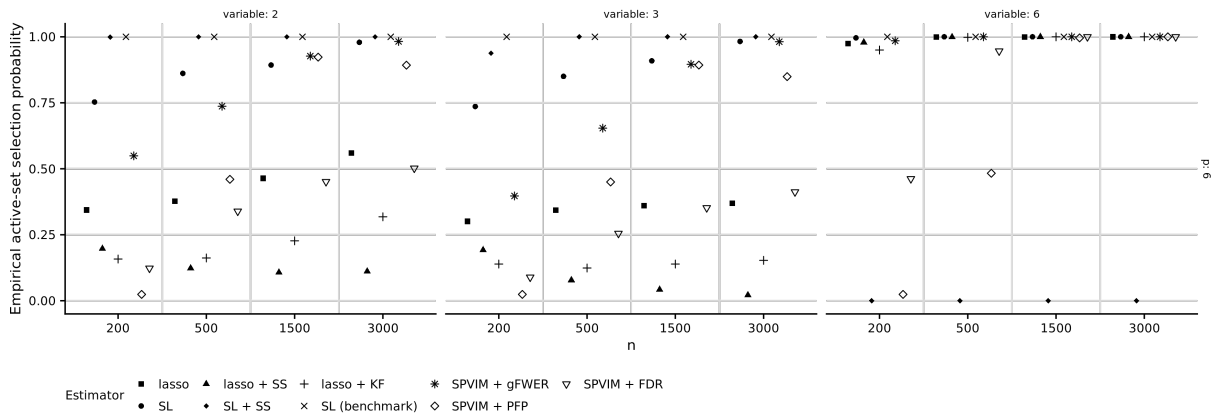


Figure S31: Empirical selection probability for each active-set variable vs n for each estimator, in Scenario 8 (a weak nonlinear model for the outcome and normal features).

8.6 Summary of results from Scenarios 1–8

Taken together, these results suggest that (a) as the missing data proportion increases, performance tends to degrade; (b) the outcome distribution (linear vs nonlinear) appears to have a larger effect on test-set AUC than the covariate distribution (normal vs nonnormal); (c) weakly important variables are less likely to be selected by lasso-based procedures than strongly important variables; and (d) correlation causes further degradation in performance for lasso-based methods. Variable selection performance (sensitivity and specificity) is similar asymptotically across Scenarios 1 and 3–5. This last finding is surprising, since the variable selection performance of the lasso is not guaranteed in misspecified settings. However, as we saw in Scenarios 2, 7, and 8, in adversarial cases the lasso-based estimators can have poor variable selection performance, as suggested by theory. Additionally, in the plots describing empirical selection probability for lasso-based estimators, we saw that while lasso-based procedures may have good overall selection performance, some important variables may still be missed, even in the non-adversarial settings.

8.7 Further investigating selection performance

In the extrinsic selection procedure (Algorithm 1), we need to specify a tuning parameter κ that determines the maximum number of variables that can be selected. In the main manuscript,

| Selection algorithm | Tuning parameter | Description | Possible values |
|--------------------------------|------------------|--------------------------------------|---|
| Extrinsic selection | κ | Rank threshold | $\{1, \dots, 25\}$ ($p = 30$) $\{5, 30, \dots, 400\}$ ($p = 500$) |
| Stability selection | π | Threshold for stability | $\{0.7, 0.71, \dots, 1\}$ |
| Intrinsic selection (gFWER) | k | Allowed number of type I errors | $\{1, \dots, 25\}$ ($p = 30$) $\{10, 20, \dots, 250\}$ ($p = 500$) |
| Intrinsic selection (PFP) | q | Desired false-positive proportion | $\{0.2, 0.25, \dots, 1\}$ |

Table S5: Selection algorithm, tuning parameter, description, and values used for computing receiver operating characteristic (ROC) curves. The total number of variables is denoted by p .

we set $\kappa = 10$ in the moderate-dimensional case ($p = 30$) and $\kappa = 36$ in the higher-dimensional case ($p = 500$). These tuning parameters were chosen in an effort to harmonize the analysis with the stability selection-based procedure: with a threshold of 0.85 and a target per-family error rate of 5, the maximum number of variables selected by stability selection can be shown to be $q = \sqrt{5(p/2)}$ (Hofner et al., 2015), which in this case yields:

$$q \approx \begin{cases} 9 & p = 30 \\ 35 & p = 500. \end{cases}$$

Since κ directly determines the maximum number of variables selected by the extrinsic selection procedure, we can vary κ in each of Scenarios 1–4 to obtain different values for sensitivity and specificity. Similarly, for the stability selection-based estimators, we can vary the cutoff threshold π ; and for intrinsic selection, we can vary the gFWER and PFP controlling parameters k and q , respectively. We computed sensitivity and specificity based on the values of κ , π , k , and q provided in Table S5. Based on these values for sensitivity and specificity, we can plot a receiver operating characteristic (ROC) curve for each setting and selection procedure.

We display the ROC curves for Scenarios 1–4 in Figures S32–S35. In all scenarios and in both dimensions, we see that as the sample size increases, the sensitivity and specificity of all procedures increases, though this effect is most pronounced in the moderate-dimensional case. Additionally, we see that the larger missing data proportion results in reduced sensitivity and specificity in smaller samples, though this difference tends to decrease with increasing sample

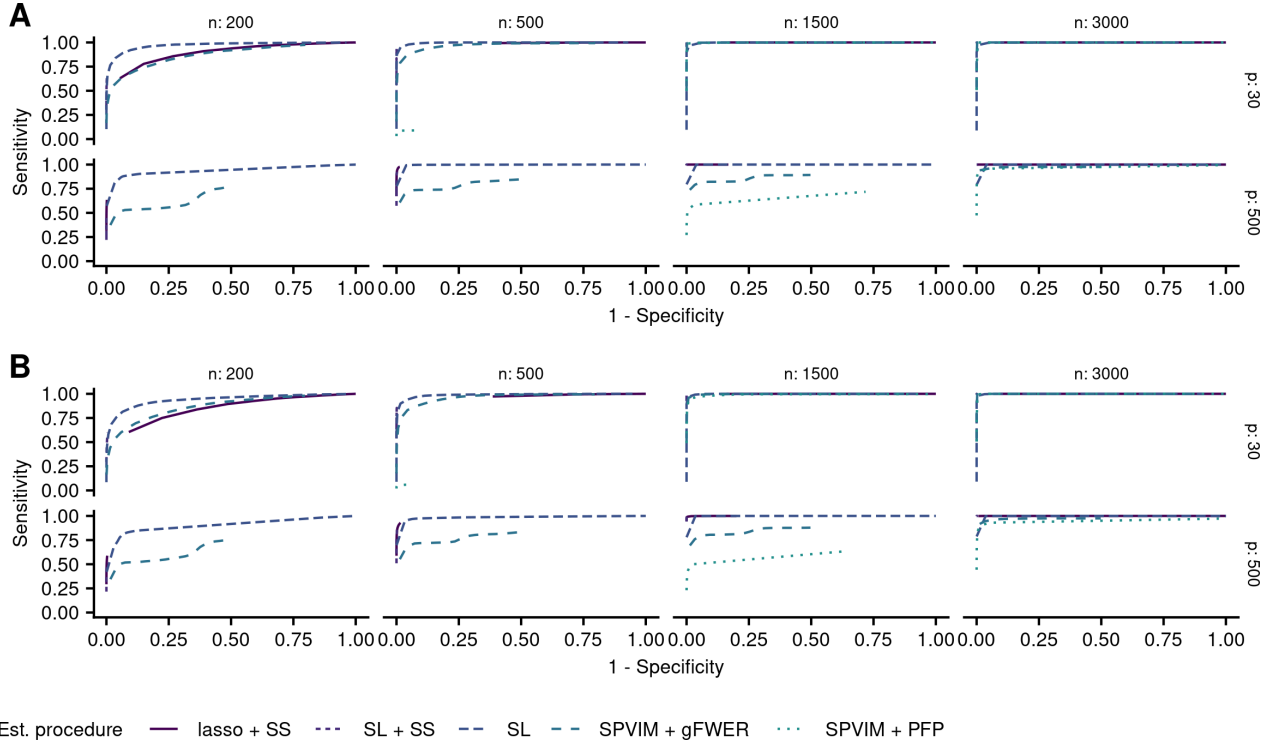


Figure S32: Receiver operating characteristic curves for procedures with externally-specified tuning parameters in Scenario 1 (linear conditional distribution, multivariate normal features). Panel A: no missing data; panel B: maximum of 40% missing data in some variables.

size. Comparing across scenarios, we see the largest sensitivity and specificity in Scenarios 1 and 2, with both sensitivity and specificity reduced in Scenarios 3 and 4. Overall, the sensitivity and specificity of the lasso with stability selection and the PFP-controlling intrinsic selection procedure tend to be lowest. Finally, we use these ROC curves to determine the sensitivity for a fixed target specificity of approximately 85% – due to the discrete grid of values considered, the estimated specificity may not equal exactly 85%. The maximum achievable sensitivity for each algorithm and this specificity, along with the tuning parameter value for which this sensitivity is achieved, are given in Tables S6–S9 for the case where $n = 200$ and there is no missing data.

8.8 Further investigating extrinsic variable selection

We further investigated the performance of the extrinsic ensemble selector in two ways. We first compared the rank threshold-based selector (used in the main manuscript) to a weighted

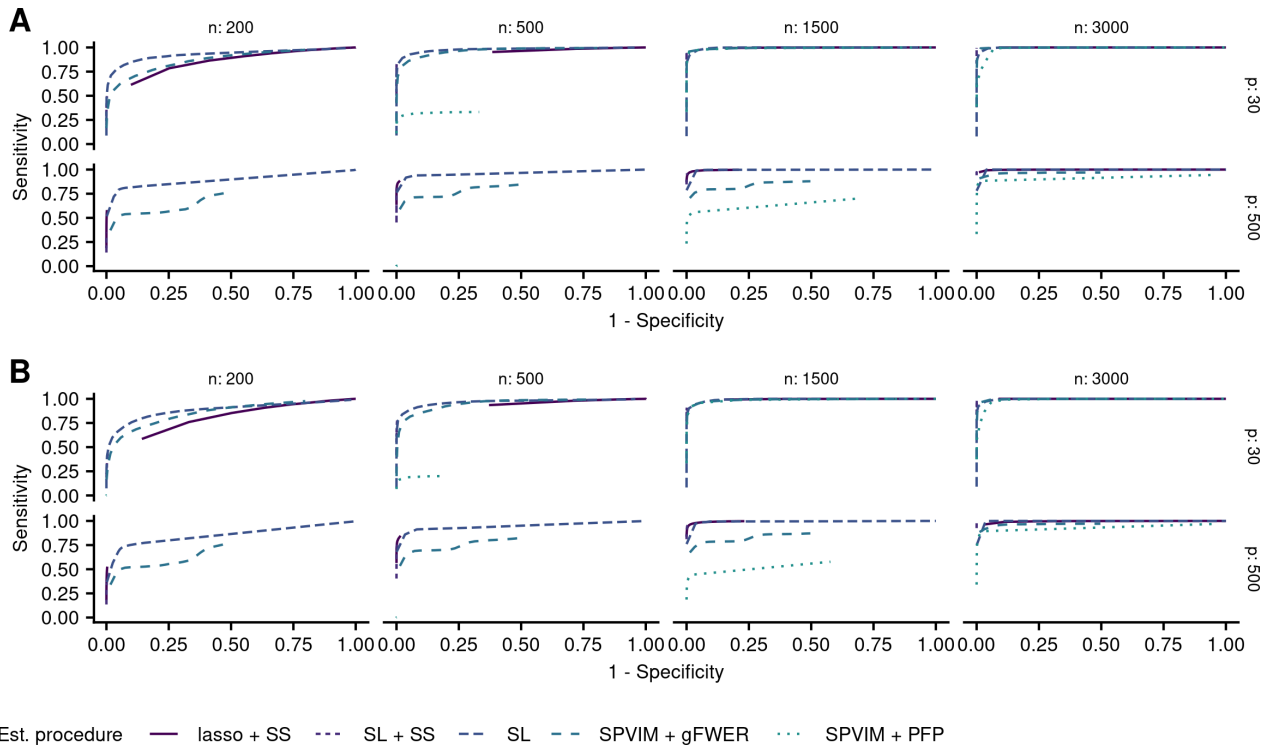


Figure S33: Receiver operating characteristic curves for procedures with externally-specified tuning parameters in Scenario 3 (linear conditional distribution, nonnormal features). Panel A: no missing data; panel B: maximum of 40% missing data in some variables.

Table S6: Mean sensitivity for mean specificity closest to 0.85 at $n = 200$ with no missing data, for each p and estimator in setting A.

| Estimator | Extra layer | p | Tuning parameter value | Mean sensitivity | Mean specificity |
|-----------|-------------|-----|------------------------|------------------|------------------|
| SL | none | 30 | 10.00 | 0.943 | 0.867 |
| SL | SS | 30 | 0.70 | 0.630 | 0.998 |
| lasso | SS | 30 | 0.99 | 0.778 | 0.850 |
| SPVIM | gFWER | 30 | 8.00 | 0.740 | 0.852 |
| SL | none | 500 | 255.00 | 0.903 | 0.867 |
| lasso | SS | 500 | 0.70 | 0.635 | 0.998 |
| SL | SS | 500 | 0.70 | 0.499 | 1.000 |
| SPVIM | gFWER | 500 | 80.00 | 0.539 | 0.845 |

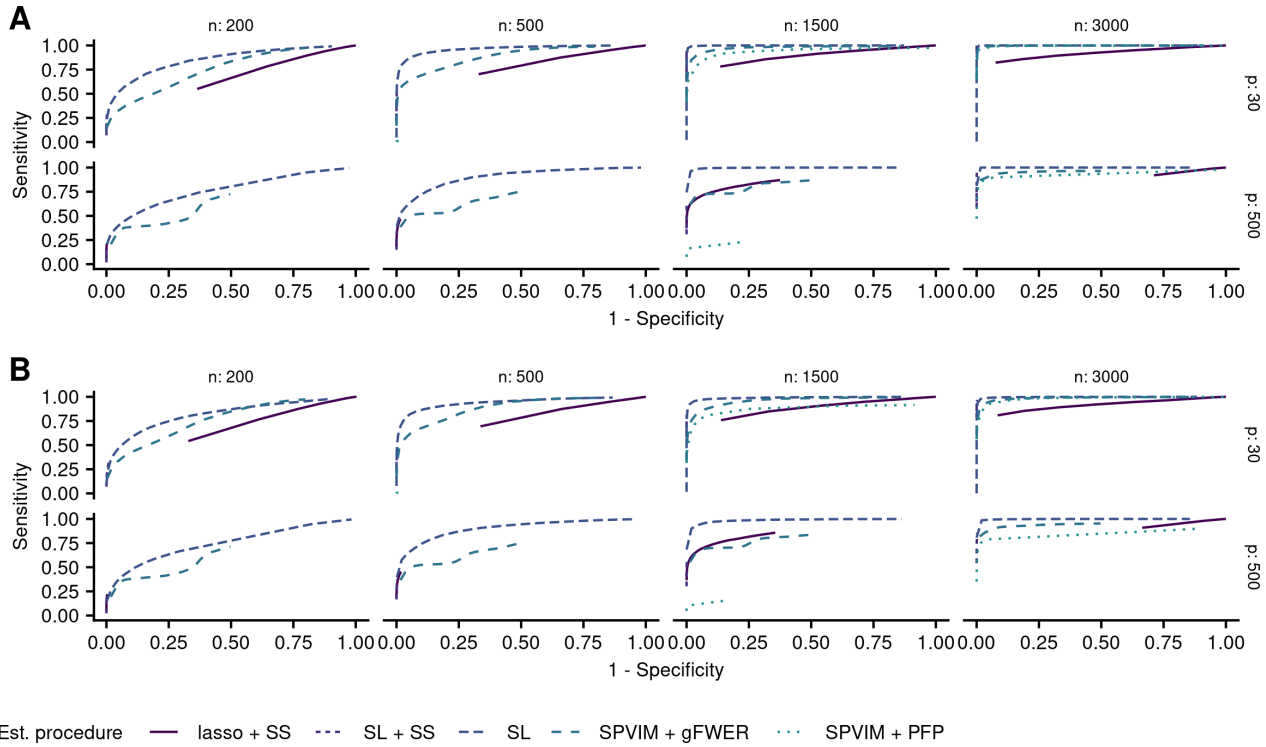


Figure S34: Receiver operating characteristic curves for procedures with externally-specified tuning parameters in Scenario 3 (nonlinear conditional distribution, multivariate normal features). Panel A: no missing data; panel B: maximum of 40% missing data in some variables.

Table S7: Mean sensitivity for mean specificity closest to 0.85 at $n = 200$ with no missing data, for each p and estimator in setting B.

| Estimator | Extra layer | p | Tuning parameter value | Mean sensitivity | Mean specificity |
|-----------|-------------|-----|------------------------|------------------|------------------|
| SL | none | 30 | 10.0 | 0.874 | 0.862 |
| SL | SS | 30 | 0.7 | 0.496 | 0.998 |
| lasso | SS | 30 | 1.0 | 0.613 | 0.902 |
| SPVIM | gFWER | 30 | 8.0 | 0.735 | 0.850 |
| SL | none | 500 | 255.0 | 0.829 | 0.852 |
| lasso | SS | 500 | 0.7 | 0.581 | 0.998 |
| SL | SS | 500 | 0.7 | 0.348 | 1.000 |
| SPVIM | gFWER | 500 | 80.0 | 0.547 | 0.845 |

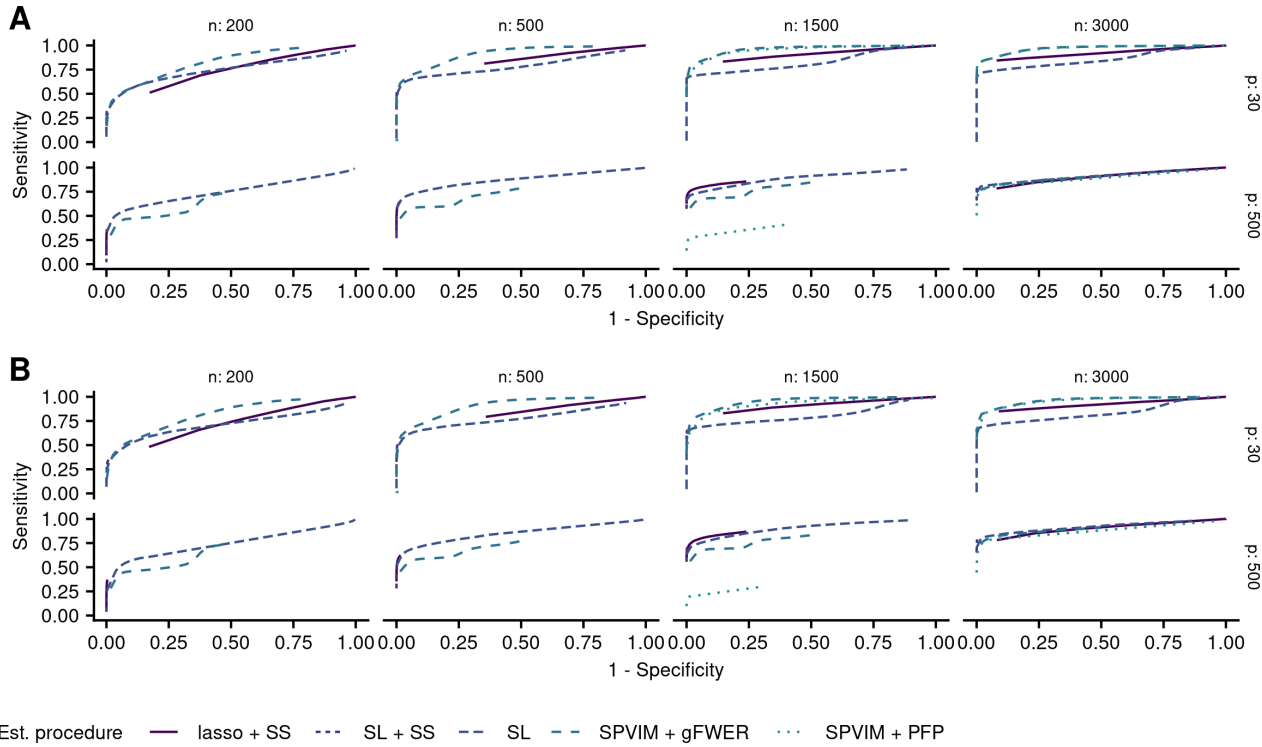


Figure S35: Receiver operating characteristic curves for procedures with externally-specified tuning parameters in Scenario 4 (nonlinear conditional distribution, nonnormal features). Panel A: no missing data; panel B: maximum of 40% missing data in some variables.

Table S8: Mean sensitivity for mean specificity closest to 0.85 at $n = 200$ with no missing data, for each p and estimator in setting C.

| Estimator | Extra layer | p | Tuning parameter value | Mean sensitivity | Mean specificity |
|-----------|-------------|-----|------------------------|------------------|------------------|
| SL | none | 30 | 11.0 | 0.708 | 0.840 |
| SL | SS | 30 | 0.7 | 0.292 | 0.997 |
| lasso | SS | 30 | 1.0 | 0.550 | 0.636 |
| SPVIM | gFWER | 30 | 6.0 | 0.449 | 0.862 |
| SL | none | 500 | 205.0 | 0.571 | 0.841 |
| lasso | SS | 500 | 0.7 | 0.215 | 0.998 |
| SL | SS | 500 | 0.7 | 0.169 | 1.000 |
| SPVIM | gFWER | 500 | 80.0 | 0.397 | 0.843 |

Table S9: Mean sensitivity for mean specificity closest to 0.85 at $n = 200$ with no missing data, for each p and estimator in setting D.

| Estimator | Extra layer | p | Tuning parameter value | Mean sensitivity | Mean specificity |
|-----------|-------------|-----|------------------------|------------------|------------------|
| SL | none | 30 | 11.0 | 0.612 | 0.839 |
| SL | SS | 30 | 0.7 | 0.338 | 0.997 |
| lasso | SS | 30 | 1.0 | 0.511 | 0.826 |
| SPVIM | gFWER | 30 | 7.0 | 0.599 | 0.858 |
| SL | none | 500 | 230.0 | 0.600 | 0.858 |
| lasso | SS | 500 | 0.7 | 0.362 | 0.998 |
| SL | SS | 500 | 0.7 | 0.248 | 1.000 |
| SPVIM | gFWER | 500 | 80.0 | 0.483 | 0.844 |

screened rank-based selector; we will refer to these as the rank-based and screen-based selectors, respectively. In the latter Super Learner algorithm, variable screens are fit prior to any candidate algorithm in the library – one example of such a screen is to fit a lasso and only advance features with nonzero coefficient. Then, the ranks for each feature were weighted by the proportion of variable screens that selected the feature. We also compared using knockoffs with both the rank- and screen-based selectors, with knockoff statistic equal to $(|-r_K| - |\tilde{r}_K|)$, where $r_K := (r_{1,K}, \dots, r_{p,K})$ is the vector of average weighted original feature ranks from the ensemble, \tilde{r}_K is defined similarly but for the knockoff features, and $-r_j$ denotes the reverse rank (i.e., large reverse ranks imply important features). A large difference between the ranks of the original and knockoff feature implies a large knockoff statistic using this formulation; heuristically, small knockoff statistics imply that the feature is not important. This knockoff statistic should satisfy both the exchangeability and flip-sign properties necessary for a valid knockoff statistic (Barber and Candès, 2015; Candès et al., 2018).

We considered eight estimators: the Super Learner (SL) with no variable selection and no screens; SL with screens and no variable selection [denoted by SL (screen)]; the ensemble selector (denoted by SL + rank); the weighted screened selector (SL + screened rank); and each selector with knockoffs (+ KF) and stability selection (+ SS). To evaluate these estimators, we generated 100 features $X \sim N_{100}(0, \Sigma)$, where $\Sigma = I$ (the identity matrix). The conditional

distribution of the outcome given covariates was

$$Y \mid X = x \sim \text{Bernoulli}[\text{expit}\{f(x)\}].$$

The function f was specified as $f(x) = \begin{bmatrix} 1 & x \end{bmatrix} \beta$ (generalized linear model) or

$$f(x) = \beta_0 + \sum_{j=1}^6 \beta_j f_j(x_j)$$

$$f_1(x) = x^2; f_2(x) = I(x > 0); f_3(x) = x^3$$

$$f_4(x) = I(x < 0); f_5(x) = |x|; f_6(x) = x^2/2 + x^3/3.$$

In both cases, $\beta = (\beta_0, \beta_1)$; $\beta_0 = 2.5$; and $\beta_1 = (-3, -1, 1, -1.5, -0.5, 0.5, \mathbf{0}_{\mathbf{p}-6})$ (strong association) or $\beta_1 = (-1, -0.5, 0.5, -0.25, -0.25, 0.25, \mathbf{0}_{\mathbf{p}-6})$ (weak association). We refer to these distinct data-generating mechanisms as settings SA (strong linear association), SB (strong nonlinear conditional distribution), and SC (weak linear association). For each data-generating mechanism, we generated 1,000 random datasets with $p = 100$ features and $n \in \{200, 350, 500, 1000, \dots, 4000\}$. We then fit the estimator specified above, using the same library of candidate learners as in the main manuscript. The following variable screens were used in the screened Super Learner: (a) a lasso screen, where features were selected if their point estimate in a lasso regression with tuning parameter chosen by cross-validation was greater than zero; and (b) a univariate correlation screen, where features were selected if their marginal correlation with the outcome was ranked in the top 25. We chose threshold $\kappa = 25$ for extrinsic selection; SS threshold of 0.7 and target per-family error rate of 4; and used knockoff target false discovery rate of 0.75. We assessed performance in the same manner as in the main manuscript, and include Monte-Carlo error bars in each figure below.

We display the results of this experiment in Figures [S36–S41](#). First, we focus on scaled MSE for estimating the test-set AUC (Figures [S36](#), [S38](#), and [S40](#)). Interestingly, even in the case of a strong linear association (setting SA), scaled MSE for the Super Learner with screens

and either KF or SS increases with sample size. Additionally, the Super Learner with KF has increasing MSE. This behavior is more pronounced in the case of a strong nonlinear association (setting SB); in this case, the only estimators with controlled MSE are the benchmark Super Learner (without screens), the ensemble selector without screens, and the ensemble selector with SS and no screens. In this setting, the benchmark Super Learner with screens also has increasing MSE. In the case of a weak linear association (setting SC), again the procedures using KF have increasing MSE, as does the Super Learner with screens and SS.

Focusing on sensitivity and specificity (Figures S37, S39, and S41), we see that the benchmark Super Learner (with and without screens) has perfect sensitivity and zero specificity across all simulations, as expected. For the procedures that performed variable selection, the minimum specificity was $(1 - \frac{25}{100-6}) \times 100\% \approx 73\%$ (if no truly important variables were selected); if all truly important variables and 25 total variables were selected, the specificity should converge to approximately 80%. In a given simulation, the number of selected variables may be less than κ . In setting SA, we see that the procedures with the largest scaled MSE – SL + screened rank + SS and both procedures with KF – also have the lowest sensitivity. We also see that sensitivity and specificity for the best-performing selection algorithms converges to approximately 100% and 80%, respectively, indicating that these algorithms are selecting the truly important variables and several unimportant variables. In setting SB, sensitivity converges to 100% most quickly for the ensemble selector without screens; adding stability selection to this procedure results in higher specificity at the expense of a slower increase in sensitivity. The sensitivity of procedures with screens is much lower, peaking at less than 75%. In setting SC, specificity tends to be higher than in setting SA, while sensitivity tends to be lower.

Based on these results, where screens appear to result in decreased Super Learner selection performance – and poor benchmark Super Learner performance in the case of a nonlinear association – we recommend that caution be exercised when considering using screens in our proposed extrinsic selection procedure. Additionally, our results suggest that the knockoff statistic for SL that we used here may not be valid, and that further work should be done to understand the performance of SL with knockoffs for variable selection.

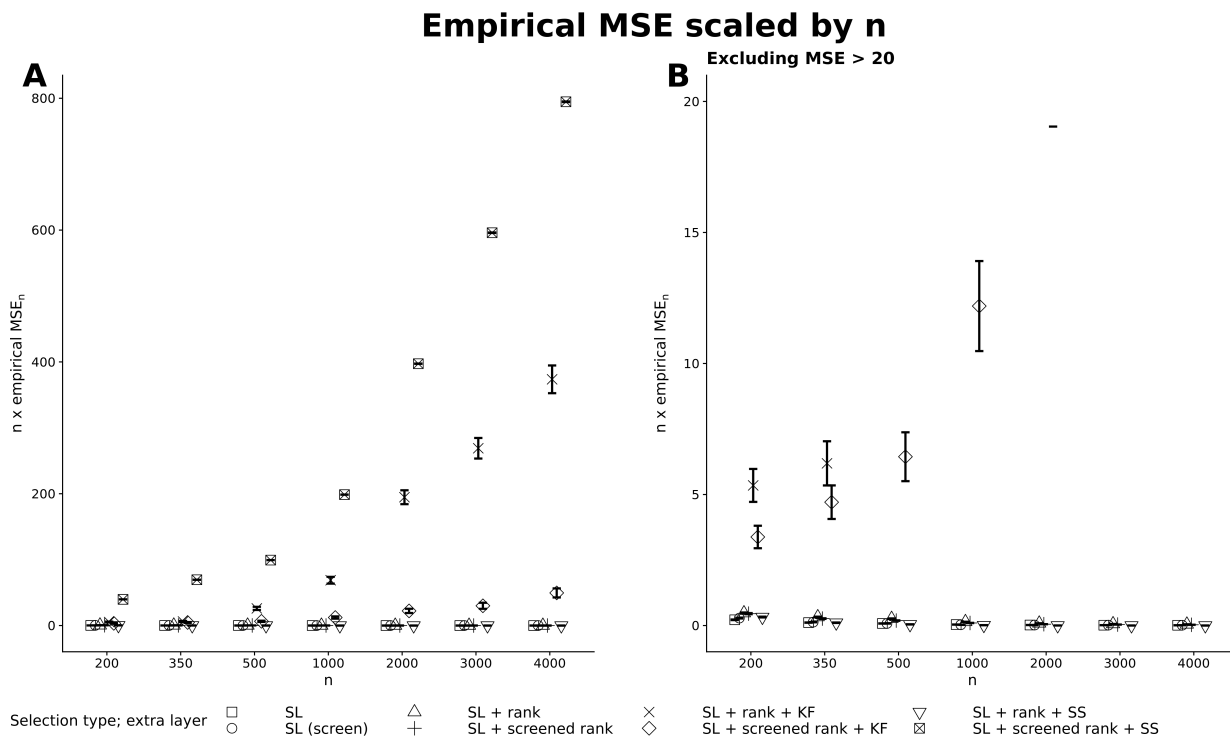


Figure S36: Empirical mean squared error for estimating the test-set AUC scaled by n vs n for each estimator, in setting SA (a strong linear association). The right-hand panel zooms in on MSE < 20. Monte-Carlo error is displayed in vertical bars.

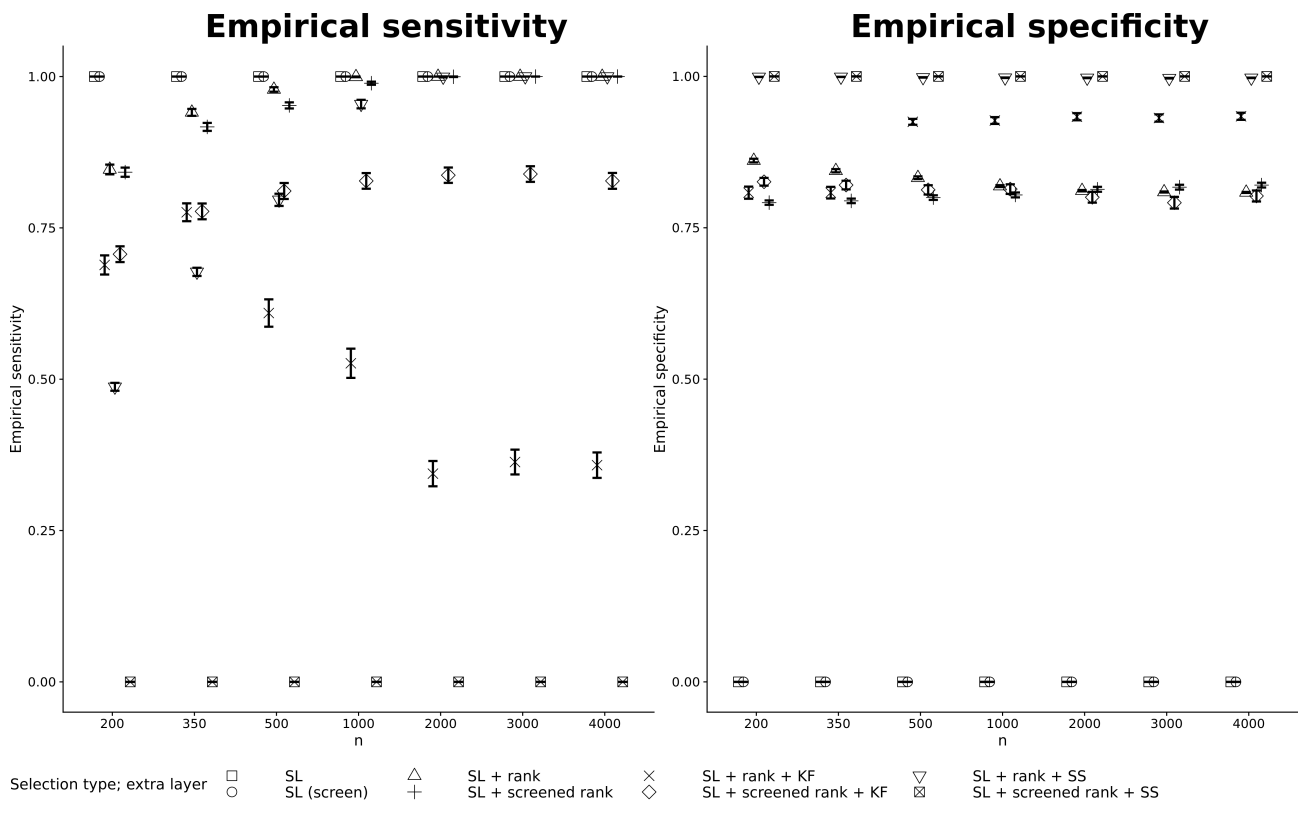


Figure S37: Empirical variable selection sensitivity (left-hand column) and specificity (right-hand column) vs n for each estimator, in setting SA (a strong linear association). Monte-Carlo error is displayed in vertical bars.

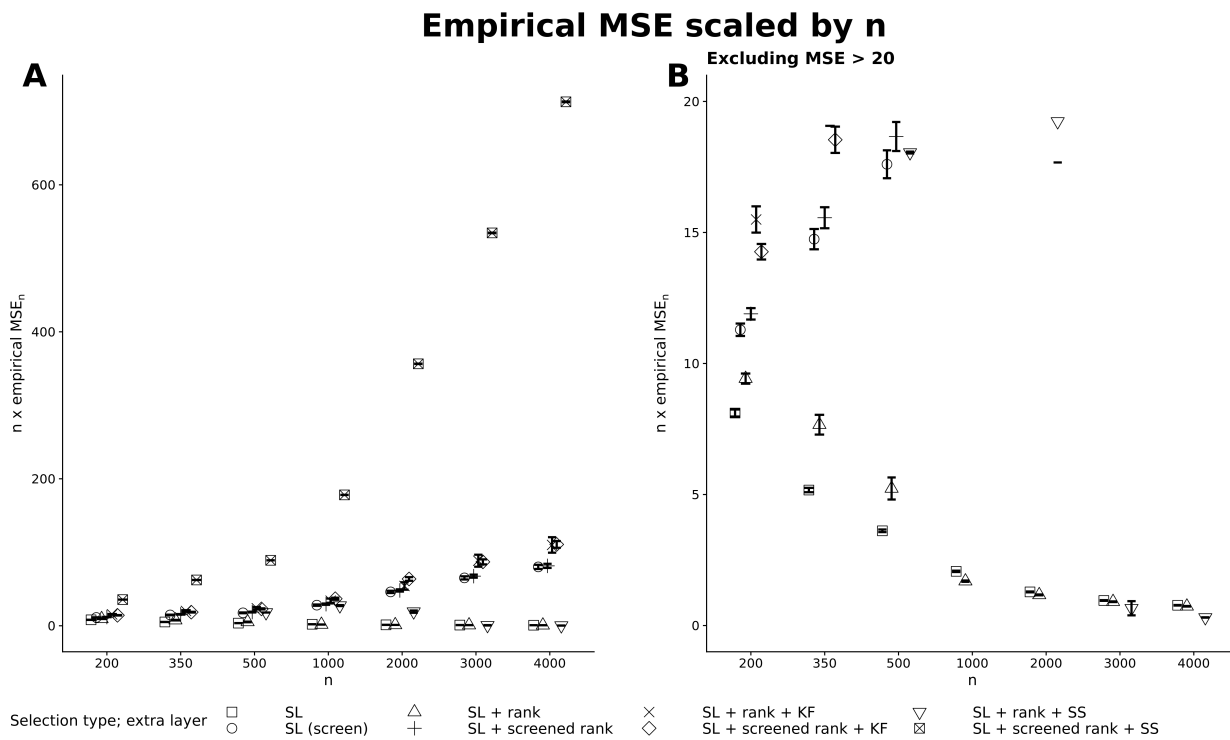


Figure S38: Empirical mean squared error for estimating the test-set AUC scaled by n vs n for each estimator, in setting SB (a strong nonlinear association). The right-hand panel zooms in on $\text{MSE} < 20$. Monte-Carlo error is displayed in vertical bars.

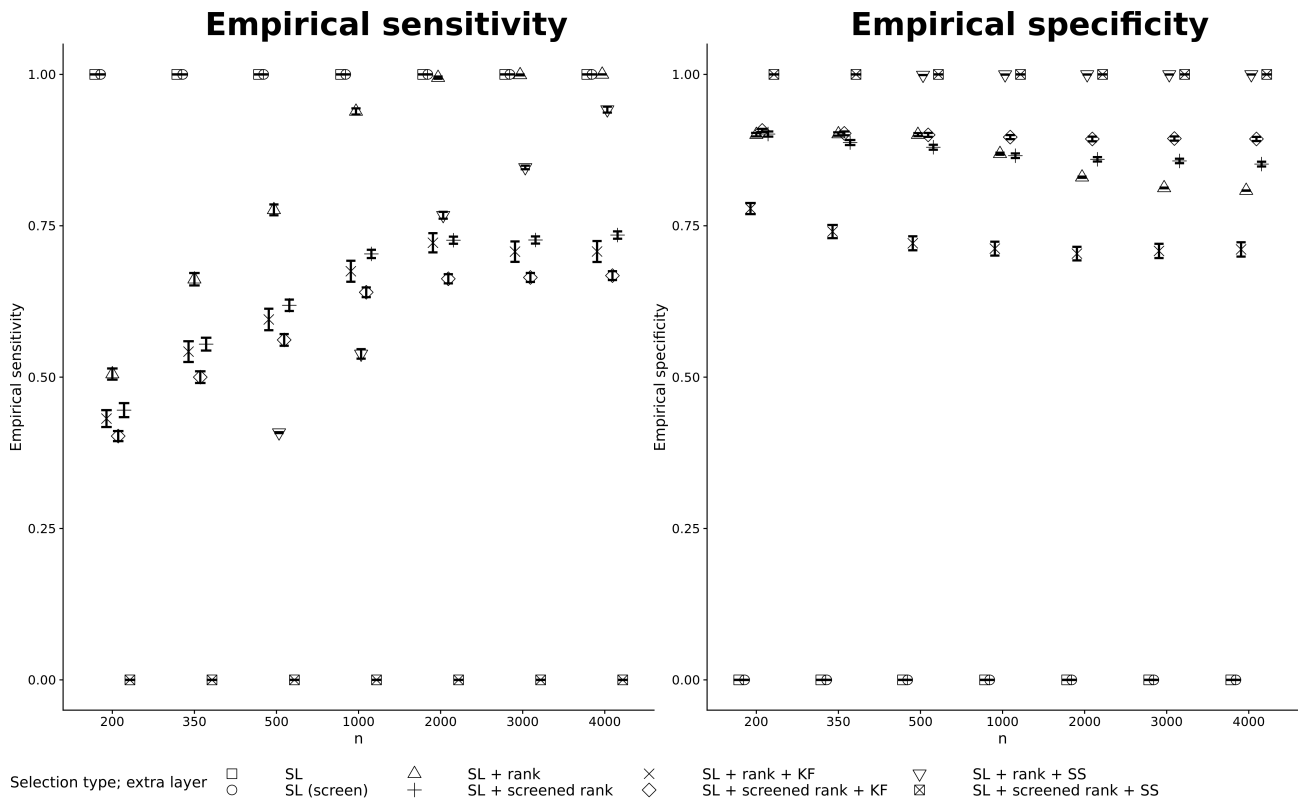


Figure S39: Empirical variable selection sensitivity (left-hand column) and specificity (right-hand column) vs n for each estimator, in setting SB (a strong nonlinear association). Monte-Carlo error is displayed in vertical bars.

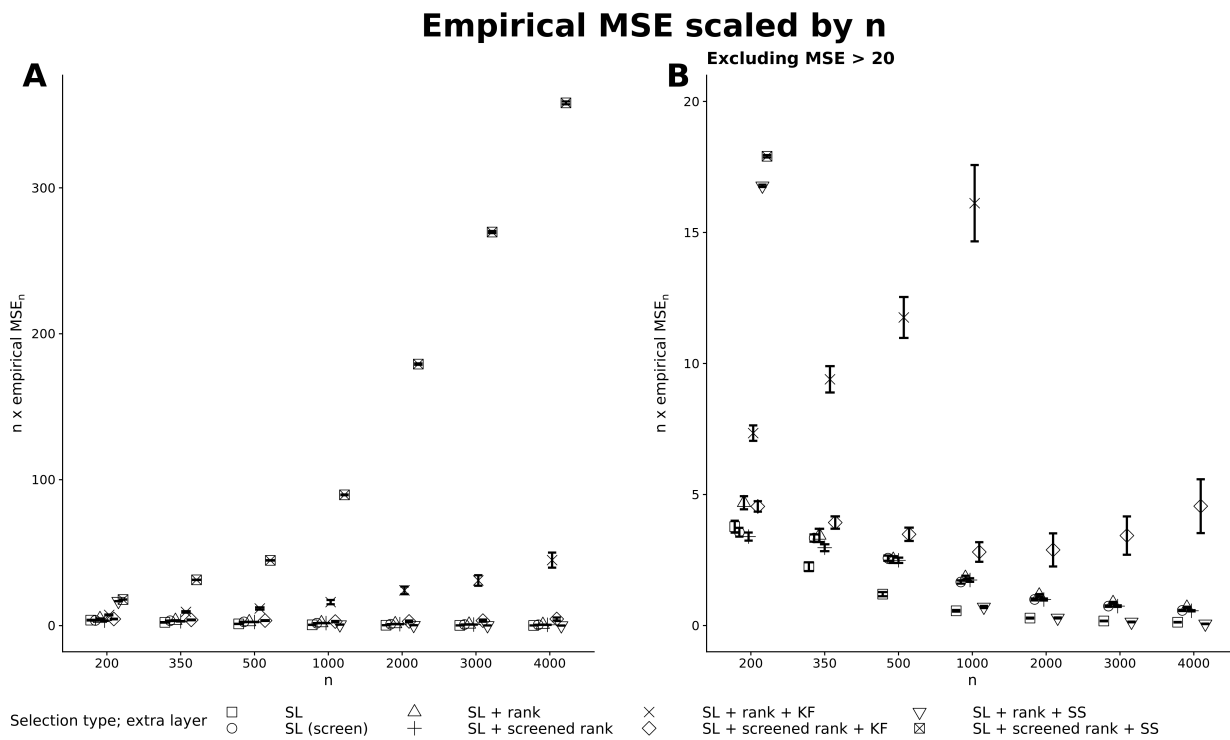


Figure S40: Empirical mean squared error for estimating the test-set AUC scaled by n vs n for each estimator, in setting SC (a weak linear association). The right-hand panel zooms in on MSE < 20. Monte-Carlo error is displayed in vertical bars.

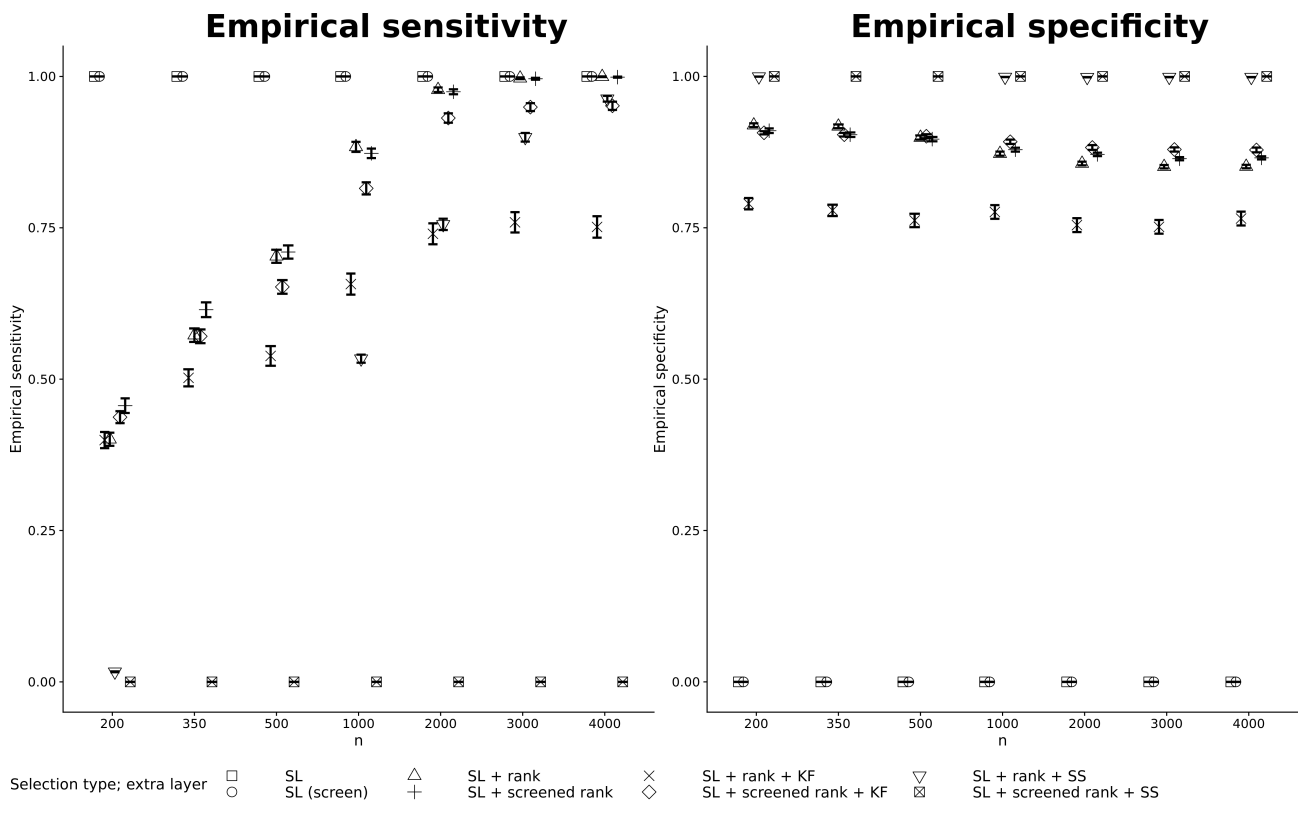


Figure S41: Empirical variable selection sensitivity (left-hand column) and specificity (right-hand column) vs n for each estimator, in setting SC (a weak linear association). Monte-Carlo error is displayed in vertical bars.

9 Additional details for the pancreatic cancer analysis

We had two overall objectives:

1. separate mucinous cysts from non-mucinous cysts, where a mucinous cyst is thought to have some malignant potential; and
2. separate cysts with high malignant potential from cysts with low or no malignant potential.

To meet these objectives, we want to assess both individual biomarkers and panels of biomarkers, both using continuous markers and binary calls.

9.1 Data preprocessing

We performed several preprocessing steps to create analysis data from the raw data. First, we selected the following variables: participant ID, institution, case/control outcome for each objective listed above, maximum specimen volume, and the entire set of continuous biomarkers and binary calls (listed in Table S10), specimen type (endoscopic ultrasound or surgical), age at specimen collection, race/ethnicity, gender, smoking history, history of pancreatitis, type of pancreatitis, diagnosis of diabetes, type of diabetes, presence of cysts, number of cysts, size of cysts, presence of acute pancreatitis, and presence of pancreatic atrophy. After selecting these variables, we remove any variables with proportion of missing data across observations greater than 20%. We further consider pairwise correlations between variables, and remove one variable from each pair with correlation > 0.9 .

9.2 Imputing missing data

Our analyses are all based on multiple imputation via chained equations (MICE, implemented in the R package `mice`; van Buuren, 2007; van Buuren and Groothuis-Oudshoorn, 2010). For $i = 1, \dots, n$ and $j = 1, \dots, r$ (where $n = 321$ is the sample size and $r = 21$ denotes the total number of biomarkers), we denote the i th measurement of biomarker j by X_{ij} , the outcome

Table S10: All biomarkers of interest for the pancreatic cancer analysis.

| Biomarker | Description |
|----------------------------|---|
| CEA | Carcinoembryonic antigen. Serum levels may be elevated in some types of cancer (e.g., colorectal cancer, pancreatic cancer). |
| CEA mucinous call | Binary indicator of whether CEA > 192. |
| ACTB | Actin Beta (Hata et al., 2017) |
| Molecules score | Methylated DNA levels of selected genes (Hata et al., 2017) |
| Molecules neoplasia call | Binary indicator of whether molecules score > 25 |
| Telomerase score | Telomerase activity measured using telomere repeat amplification protocol (Hata et al., 2016) |
| Telomerase neoplasia call | Binary indicator of whether telomerase score > 730 |
| AREG score | Amphiregulin (AREG) overexpression (Tun et al., 2012) |
| AREG mucinous call | Binary indicator of whether AREG score > 112 |
| Glucose score | Glucometer glucose level (Zikos et al., 2015) |
| Glucose mucinous call | Binary indicator of whether glucose score < 50 |
| Combined mucinous call | Binary indicator of whether AREG score > 112 and glucose score < 50 |
| Fluorescence score | Fluorescent protease activity (Ivry et al., 2017) |
| Fluorescence mucinous call | Binary indicator of whether fluorescence score > 1.23 |
| DNA mucinous call | Presence of mutations in a DNA sequencing panel (Singhi et al., 2018) |
| DNA neoplasia call (v1) | Binary indicator of methylated DNA levels of selected genes being above a threshold (Majumder et al., 2019) |
| DNA neoplasia call (v2) | Binary indicator of methylated DNA levels of selected genes being above a threshold (Majumder et al., 2019) |
| MUC3AC score | Expression of protein Mucin 3AC |
| MUC5AC score | Expression of protein Mucin 5AC (Cao et al., 2013) |
| Ab score | Monoclonal antibody reactivity (Das et al., 2014) |
| Ab neoplasia call | Binary indicator of whether Ab score > 0.104 |

of interest by Y_i , and the vector of clinical covariates (removing institution ID) by $W_i := (W_{i1}, \dots, W_{i(q-1)})$. We performed imputation in two steps: first, we imputed missing clinical covariate values; then, based on the imputed covariates, we imputed missing biomarker values. We used the following model to impute the missing covariates:

$$W_{i,j,\text{mis}} \sim Y_i + W_{i,\text{obs}},$$

yielding imputed 10 sets of imputed covariates $\{\tilde{W}_m\}_{m=1}^{10}$. For each of the ten imputed sets of covariates, we used the following model to impute missing biomarker values:

$$X_{i,j,\text{mis}} \sim Y_i + X_{i,j,\text{obs}} + \tilde{W}_{m,i}.$$

These models allow us to relate observed biomarker values, along with total specimen volume, to the unobserved biomarker values, adjusted for other potential risk factors. All imputations were performed using a maximum of 20 iterations and predictive mean matching (PMM; [van Buuren and Groothuis-Oudshoorn, 2010](#)) to create 10 fully-imputed datasets. In some cases, the PMM algorithm failed to converge; in these cases, we used tree-based imputation.

9.3 Variable selection procedures

We use the same variable selection procedures as in the main manuscript: lasso (base, SS, knockoffs) for variable selection, with final predictions made using logistic regression; Super Learner (no selection [denoted SL (benchmark)], extrinsic selection, extrinsic selection with SS); and intrinsic selection designed to control the gFWER, PFP, and FDR, both with and without using Rubin’s Rules via Lemma 2 (denoted SPVIM + {gFWER, PFP, FDR} and SPVIM-RR + {gFWER, PFP, FDR}, respectively).

9.4 Assessing prediction performance

Assessing prediction performance is complicated by both the imputation step and the initial variable selection step. To address this, we performed imputation within cross-fitting within Monte-Carlo sampling; this provides an unbiased assessment of the entire procedure, from imputation to variable selection to prediction. More specifically, for each of 100 replicates and each outcome, we performed the procedures outlined in Algorithms 5 and 6. Algorithm 5 focuses on the performance of a pooled set of variables, while Algorithm 6 focuses instead on the performance of assessing predictiveness within each imputed dataset, then averaging this predictiveness.

Algorithm 5 Imputation and pooled variable selection within cross-fitting and Monte-Carlo sampling

- 1: **for** $b = 1, \dots, 50$ **do**
 - 2: generate a random vector $B_n \in \{1, \dots, 5\}^n$ by sampling uniformly from $\{1, \dots, 5\}$ with replacement, and for each $v \in \{1, \dots, 5\}$, denote by D_v the data with index in $\{i : B_{n,i} = v\}$;
 - 3: **for** $v = 1, \dots, 5$ **do**
 - 4: create 10 imputed datasets $\{Z_{k,-v}\}_{k=1}^{10}$ based on the data in $\cup_{j \neq v} D_j$ using MICE;
 - 5: create 10 imputed datasets $\{Z_{k,v}\}_{k=1}^{10}$ based on the data in D_v using MICE;
 - 6: **for** $k = 1, \dots, 10$ **do**
 - 7: obtain a set of selected variables $S_{k,v}$ by applying the chosen variable selection algorithm to $Z_{k,-v}$;
 - 8: **end for**
 - 9: obtain a final set of selected variables S_v by choosing those variables with index in $\{j \in \{1, \dots, p\} : \sum_{k=1}^K I(j \in S_{k,v}) \geq 0.7\}$;
 - 10: **for** $k = 1, \dots, 10$ **do**
 - 11: train the chosen prediction algorithm on the training data $Z_{k,-v}$ using only variables in S_v ;
 - 12: obtain $\text{AUC}_{k,v}$ and its associated variance $\text{var}(\text{AUC})_{k,v}$ by predicting on the withheld test data $Z_{k,v}$ and measure prediction performance using AUC;
 - 13: **end for**
 - 14: combine the AUCs and associated variance estimators into AUC_v and $\text{var}(\text{AUC})_v$ using Rubin's rules;
 - 15: **end for**
 - 16: compute $\text{CV-AUC}_b = \frac{1}{5} \sum_{v=1}^5 \text{AUC}_v$ and $\text{var}(\text{CV-AUC})_b = \frac{1}{5} \sum_{v=1}^5 \text{var}(\text{AUC})_v$;
 - 17: **end for**
 - 18: compute overall performance by averaging over the Monte-Carlo iterations.
-

Algorithm 6 Imputation and non-pooled variable selection within cross-fitting and Monte-Carlo sampling

- 1: **for** $b = 1, \dots, 50$ **do**
 - 2: generate a random vector $B_n \in \{1, \dots, 5\}^n$ by sampling uniformly from $\{1, \dots, 5\}$ with replacement, and for each $v \in \{1, \dots, 5\}$, denote by D_v the data with index in $\{i : B_{n,i} = v\}$;
 - 3: **for** $v = 1, \dots, 5$ **do**
 - 4: create 10 imputed datasets $\{Z_{k,-v}\}_{k=1}^{10}$ based on the data in $\cup_{j \neq v} D_j$ using MICE;
 - 5: create 10 imputed datasets $\{Z_{k,v}\}_{k=1}^{10}$ based on the data in D_v using MICE;
 - 6: **for** $k = 1, \dots, 10$ **do**
 - 7: obtain a set of selected variables $S_{k,v}$ by applying the chosen variable selection algorithm to $Z_{k,-v}$;
 - 8: train the chosen prediction algorithm on the training data $Z_{k,-v}$ using only variables in $S_{k,v}$;
 - 9: obtain $\text{AUC}_{k,v}$ and its associated variance $\text{var}(\text{AUC})_{k,v}$ by predicting on the withheld test data $Z_{k,v}$ and measure prediction performance using AUC;
 - 10: **end for**
 - 11: combine the AUCs and associated variance estimators into AUC_v and $\text{var}(\text{AUC})_v$ using Rubin's rules;
 - 12: **end for**
 - 13: compute $\text{CV-AUC}_b = \frac{1}{5} \sum_{v=1}^5 \text{AUC}_v$ and $\text{var}(\text{CV-AUC})_b = \frac{1}{5} \sum_{v=1}^5 \text{var}(\text{AUC})_v$;
 - 14: **end for**
 - 15: compute overall performance by averaging over the Monte-Carlo iterations.
-

| Candidate Learner | R Implementation | Tuning Parameter and possible values | Tuning parameter description |
|------------------------|----------------------|--|---|
| Random forests | <code>ranger</code> | <code>max.depth</code> $\in \{1, 10, 20, 30, 100, \infty\}$ | Maximum tree depth |
| Gradient boosted trees | <code>xgboost</code> | <code>max.depth = {4}</code> <code>nrounds</code> $\in \{100, 500, 2000\}$ | Maximum tree depth Number of boosting iterations |
| Elastic net | <code>glmnet</code> | mixing parameter α $\in \{0, \frac{1}{4}, \frac{1}{2}, \frac{3}{4}, 1\}$ | Trade-off between ℓ_1 and ℓ_2 regularization [†] |

Table S11: Candidate learners in the Super Learner ensemble for the pancreatic cyst data analysis along with their R implementation, tuning parameter values, and description of the tuning parameters. All tuning parameters besides those listed here are set to their default values. In particular, the random forests are grown with `mtry` = \sqrt{p}^\dagger , a minimum node size of 5 for continuous outcomes and 1 for binary outcomes, and a subsampling fraction of 1; the boosted trees are grown with shrinkage rate of 0.1 and a minimum of 10 observations per node; and the ℓ_1 tuning parameter for the elastic net is determined via 10-fold cross-validation.

[†]: p denotes the total number of predictors.

9.5 Obtaining a final set of selected biomarkers

We obtain a final set of selected biomarkers by applying the variable selection procedure to the full set of observations for each imputed dataset; our final set for all procedures except SPVIM-RR consists of those metabolites and covariates that were selected in over 70% of the individual imputed datasets.

9.6 Super Learner specification

As in the simulations, we used a different specification for the internal Super Learner in the intrinsic selection procedure (max. depth 4 boosted trees (all tuning parameter values in Table S11) with pre-screening via univariate rank correlation with the outcome) and all other Super Learners (Table S11). In all cases, the final Super Learner fit for prediction performance of the selected set of variables used the candidate learners in Table S11.

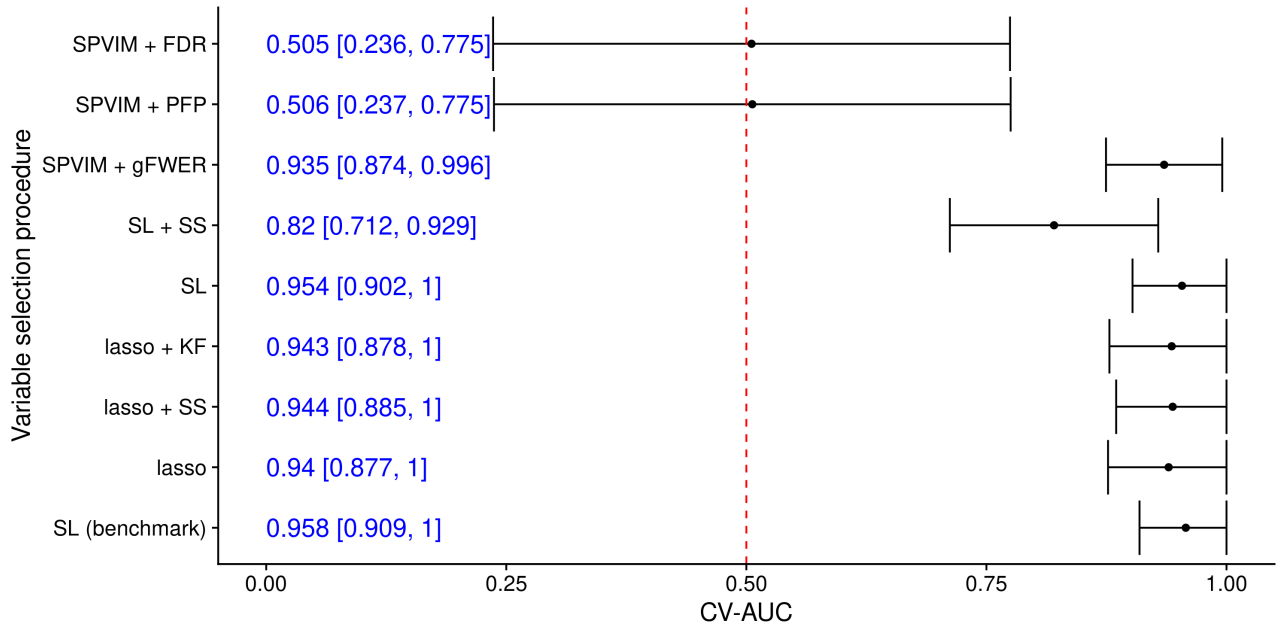


Figure S42: Cross-validated area under the receiver operating characteristic curve (CV-AUC) for predicting whether a cyst is mucinous averaged over 100 replicates of the imputation-within-cross-validated procedure (Algorithm 6) for each variable selection algorithm. Prediction performance for lasso-based methods is based on logistic regression on the selected variables, while performance for Super Learner-based methods is based on a Super Learner. Error bars denote 95% confidence intervals based on the average variance over the 100 replications.

10 Additional results from the pancreatic cyst analysis

In the main manuscript, we performed an analysis with goal of predicting whether a cyst was mucinous, using Algorithm 5 to assess prediction performance. Here, we show results using Algorithm 6 for the mucinous outcome and results from both algorithms for the outcome of whether a cyst has high malignancy potential.

In Figure S42, we present the results of the mucinous analysis under Algorithm 6. Both point and interval estimates of predictiveness are similar to those reported under Algorithm 5 in the main manuscript. This suggests that the approach of pooling variables prior to performance assessment, if done using a sufficiently high threshold for inclusion into the pooled set, may select sufficiently many variables from the individual imputations. We do not present results for SPVIM-RR under Algorithm 6 because the Rubin’s Rules-based procedure is only valid under Algorithm 5.

We present the results of our analysis in Figures S43 and S44 and Table S13. In Figure S43, we see that with the exception of the PFP- and FDR-controlling intrinsic selection procedures, all procedures have moderate predictiveness (as measured by CV-AUC). In all cases, CV-AUC is smaller than for the mucinous outcome. The top-performing algorithms are the Super Learner with no variable selection, the gFWER-controlling intrinsic selection procedure, and the base lasso, with average estimated CV-AUCs of 0.804 (95% confidence interval [CI] of [0.672, 0.936]), 0.78 [0.635, 0.925], and 0.78 [0.639, 0.921], respectively. CV-AUC for other procedures remained above 0.7, but in contrast to the mucinous outcome, the lasso with knockoffs exhibited the lowest CV-AUC of the procedures that selected variables. Similar to the mucinous outcome, neither the PFP- or FDR-controlling intrinsic selection procedures selected any variables on average. We see similar results in Figure S44, again suggesting that both algorithms result in the same variables being considered for predictiveness assessment. In Table S13, we display the final set of biomarkers selected by each procedure. No biomarkers are selected across all seven procedures. However, several biomarkers are selected by five or more procedures: ACTB; molecules and telomerase neoplasia calls (binary variables); a fluorescence mucinous call (a binary variable); and an antibody level score score. Selection across the majority of procedures suggests that these variables are useful for predicting whether a cyst has high malignancy potential. Interestingly, the variables selected by the SPVIM procedure using the stability criterion are a subset of those variables selected by the SPVIM procedure using Rubin’s rules (SPVIM-RR).

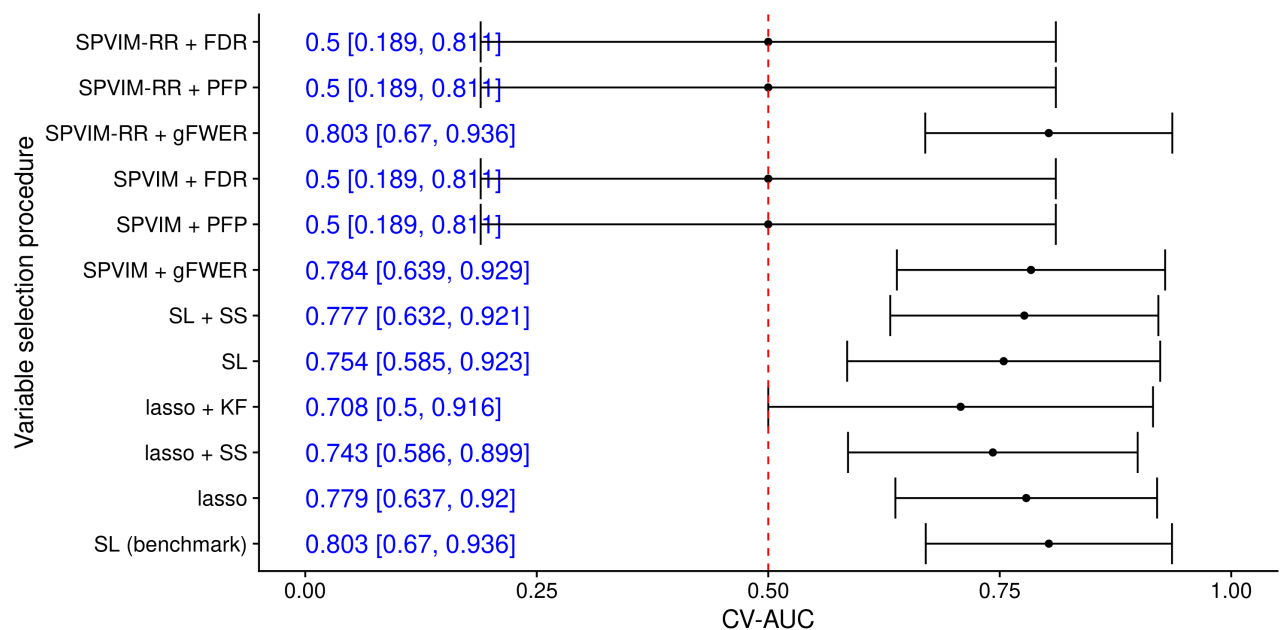


Figure S43: Cross-validated area under the receiver operating characteristic curve (CV-AUC) for predicting whether a cyst has high malignancy potential averaged over 100 replicates of the imputation-within-cross-validated procedure (Algorithm 5) for each variable selection algorithm. Prediction performance for lasso-based methods is based on logistic regression on the selected variables, while performance for Super Learner-based methods is based on a Super Learner. Error bars denote 95% confidence intervals based on the average variance over the 100 replications.

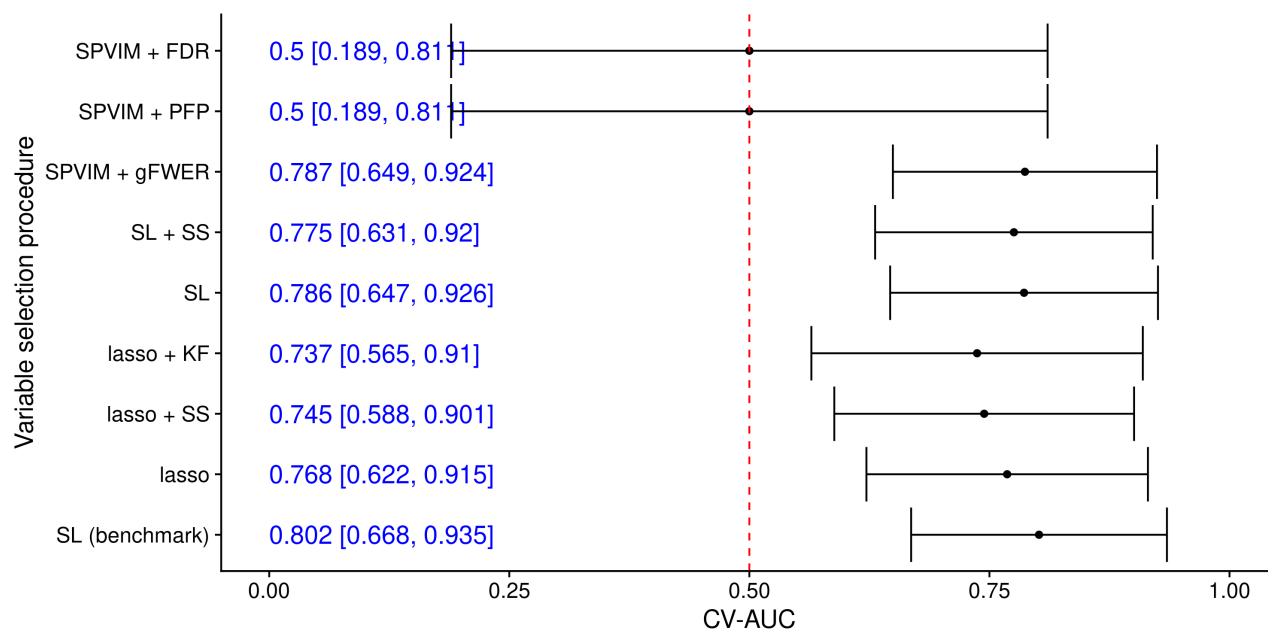


Figure S44: Cross-validated area under the receiver operating characteristic curve (CV-AUC) for predicting whether a cyst has high malignancy potential averaged over 100 replicates of the imputation-within-cross-validated procedure (Algorithm 6) for each variable selection algorithm. Prediction performance for lasso-based methods is based on logistic regression on the selected variables, while performance for Super Learner-based methods is based on a Super Learner. Error bars denote 95% confidence intervals based on the average variance over the 100 replications.

Table S12: Biomarkers selected by each selection procedure for predicting whether a cyst is mucinous on the full imputed dataset. Full definitions of each variable are provided in Table S10.

| Biomarker | lasso | lasso + KF | lasso + SS | SL | SL + SS | SPVIM + gFWER | SPVIM-RR + gFWER | Number of procedures |
|-------------------------|-------|------------|------------|-----|---------|---------------|------------------|----------------------|
| CEA | Yes | No | Yes | No | No | No | No | 2 |
| CEA mucinous call | No | No | Yes | No | No | No | No | 1 |
| ACTB | Yes | No | No | No | Yes | No | No | 2 |
| Molecules (M) score | No | No | Yes | No | Yes | No | No | 2 |
| M neoplasia call | Yes | No | No | Yes | Yes | Yes | Yes | 5 |
| Telomerase (T) score | Yes | No | Yes | No | Yes | No | No | 3 |
| T neoplasia call | Yes | No | No | No | Yes | No | No | 2 |
| AREG (A) score | Yes | Yes | Yes | Yes | No | Yes | Yes | 6 |
| A mucinous call | Yes | No | Yes | No | No | No | No | 2 |
| Glucose (G) score | Yes | No | Yes | No | No | Yes | Yes | 4 |
| G mucinous call | Yes | Yes | Yes | Yes | No | Yes | Yes | 6 |
| A and G mucinous call | Yes | Yes | Yes | Yes | No | Yes | Yes | 6 |
| Fluorescence (F) score | Yes | No | Yes | Yes | Yes | Yes | Yes | 6 |
| F mucinous call | No | No | No | No | Yes | Yes | Yes | 3 |
| DNA neoplasia call (v2) | Yes | No | No | Yes | No | Yes | Yes | 4 |
| MUC3AC score | Yes | Yes | Yes | No | No | Yes | Yes | 5 |
| MUC5AC score | No | No | Yes | No | No | No | No | 1 |
| Ab score | No | No | Yes | No | No | No | No | 1 |
| Ab neoplasia call | No | No | No | No | No | Yes | Yes | 2 |

Table S13: Biomarkers selected by each selection procedure for predicting whether a cyst has high malignancy potential on the full imputed dataset. Full definitions of each variable are provided in Table S10.

| Biomarker | lasso | lasso + KF | lasso + SS | SL | SL + SS | SPVIM + gFWER | SPVIM-RR + gFWER | Number of procedures |
|-------------------------|-------|------------|------------|-----|---------|---------------|------------------|----------------------|
| CEA | Yes | No | Yes | No | No | No | No | 2 |
| CEA mucinous call | Yes | No | Yes | No | No | No | No | 2 |
| ACTB | Yes | No | Yes | Yes | Yes | Yes | Yes | 6 |
| Molecules (M) score | No | No | Yes | No | Yes | No | No | 2 |
| M neoplasia call | Yes | No | Yes | Yes | Yes | Yes | Yes | 6 |
| Telomerase (T) score | No | No | Yes | No | Yes | No | No | 2 |
| T neoplasia call | Yes | Yes | Yes | Yes | Yes | No | No | 5 |
| AREG (A) score | Yes | Yes | Yes | No | No | No | No | 3 |
| A mucinous call | No | No | Yes | No | No | No | No | 1 |
| Glucose (G) score | Yes | No | Yes | No | No | Yes | Yes | 4 |
| G mucinous call | No | No | Yes | No | No | No | No | 1 |
| A and G mucinous call | Yes | No | Yes | No | No | No | Yes | 3 |
| Fluorescence (F) score | Yes | No | Yes | No | Yes | No | Yes | 4 |
| F mucinous call | Yes | No | Yes | No | Yes | Yes | Yes | 5 |
| DNA mucinous call | Yes | No | Yes | Yes | No | No | No | 3 |
| DNA neoplasia call (v1) | No | No | Yes | No | No | No | Yes | 2 |
| DNA neoplasia call (v2) | No | No | Yes | No | No | Yes | Yes | 3 |
| MUC3AC score | Yes | No | Yes | No | No | No | No | 2 |
| MUC5AC score | No | No | Yes | No | No | No | No | 1 |
| Ab score | Yes | Yes | Yes | Yes | No | No | Yes | 5 |
| Ab neoplasia call | Yes | No | Yes | No | No | No | Yes | 3 |